34386

National Library of Canada / Bibliothèque nationale du Canada

CANADIAN THESES ON MICROFICHE / THÈSES CANADIENNES SUR MICROFICHE

NAME OF AUTHOR/*NOM DE L'AUTEUR* RAJESH A. KALIANDASANI

TITLE OF THESIS/*TITRE DE LA THÈSE* BEHAVIOUR OF OPEN WEB STEEL JOISTS

UNIVERSITY/*UNIVERSITÉ* UNIVERSITY OF ALBERTA

DEGREE FOR WHICH THESIS WAS PRESENTED/*GRADE POUR LEQUEL CETTE THÈSE FUT PRÉSENTÉE* M.Sc

YEAR THIS DEGREE CONFERRED/*ANNÉE D'OBTENTION DE CE GRADE* Fall, 1977

NAME OF SUPERVISOR/*NOM DU DIRECTEUR DE THÈSE* DR S.H. SIMMONDS

Permission is hereby granted to the NATIONAL LIBRARY OF CANADA to microfilm this thesis and to lend or sell copies of the film.

The author reserves other publication rights, and neither the thesis nor extensive extracts from it may be printed or otherwise reproduced without the author's written permission.

*L'autorisation est, par la présente, accordée à la BIBLIOTHÈQUE NATIONALE DU CANADA de microfilmer cette thèse et de prêter ou de vendre des exemplaires du film.*

*L'auteur se réserve les autres droits de publication; ni la thèse ni de longs extraits de celle-ci ne doivent être imprimés ou autrement reproduits sans l'autorisation écrite de l'auteur.*

DATED/*DATÉ* July 6, 1977 SIGNED/*SIGNÉ* Rajesh

PERMANENT ADDRESS/*RÉSIDENCE FIXÉ* 228, Dhaula Kuan,
(Army Officers Quarters)
New Delhi - 110010, INDIA.

NL-91 (3-74)

National Library of Canada

Cataloguing Branch
Canadian Theses Division

Ottawa, Canada
K1A 0N4

Bibliothèque nationale du Canada

Direction du catalogage
Division des thèses canadiennes

## NOTICE

The quality of this microfiche is heavily dependent upon the quality of the original thesis submitted for microfilming. Every effort has been made to ensure the highest quality of reproduction possible.

If pages are missing, contact the university which granted the degree.

Some pages may have indistinct print especially if the original pages were typed with a poor typewriter ribbon or if the university sent us a poor photocopy.

Previously copyrighted materials (journal articles, published tests, etc.) are not filmed.

Reproduction in full or in part of this film is governed by the Canadian Copyright Act, R.S.C. 1970, c. C-30. Please read the authorization forms which accompany this thesis.

THIS DISSERTATION
HAS BEEN MICROFILMED
EXACTLY AS RECEIVED

## AVIS

La qualité de cette microfiche dépend grandement de la qualité de la thèse soumise au microfilmage. Nous avons tout fait pour assurer une qualité supérieure de reproduction.

S'il manque des pages, veuillez communiquer avec l'université qui a conféré le grade.

La qualité d'impression de certaines pages peut laisser à désirer, surtout si les pages originales ont été dactylographiées à l'aide d'un ruban usé ou si l'université nous a fait parvenir une photocopie de mauvaise qualité.

Les documents qui font déjà l'objet d'un droit d'auteur (articles de revue, examens publiés, etc.) ne sont pas microfilmés.

La reproduction, même partielle, de ce microfilm est soumise à la Loi canadienne sur le droit d'auteur, SRC 1970, c. C-30. Veuillez prendre connaissance des formules d'autorisation qui accompagnent cette thèse.

LA THÈSE A ÉTÉ
MICROFILMÉE TELLE QUE
NOUS L'AVONS REÇUE

NL-339 (3/77)

THE UNIVERSITY OF ALBERTA

# BEHAVIOUR OF OPEN WEB STEEL JOISTS

by

© Rajesh A. Kaliandasani

A THESIS

SUBMITTED TO THE FACULTY OF GRADUATE STUDIES AND RESEARCH

IN PARTIAL FULFILMENT OF THE REQUIREMENTS FOR THE DEGREE

OF MASTER OF SCIENCE

Department of Civil Engineering

Edmonton, Alberta

Fall, 1977

THE UNIVERSITY OF ALBERTA

FACULTY OF GRADUATE STUDIES AND RESEARCH

The undersigned certify that they have read, and recommend to the Faculty of Graduate Studies and Research, for acceptance, a thesis entitled BEHAVIOUR OF OPEN WEB STEEL JOISTS, submitted by RAJESH A. KALIANDASANI in partial fulfilment of the requirements for the degree of Master of Science.

S.H. Simmonds, Supervisor

D.W. Murray

J.S. Kennedy

Date June 3, 1977

## ABSTRACT

This study investigates the effects of joint eccentricity on the deformations and internal forces in open web steel joists.

The results of an investigation of the effects of joint eccentricity on the deformation, internal stresses and mode of failure of open web steel joists is reported. The study consisted of testing to failure ten joists having variable joint eccentricity, web to chord fabrication detail and chord cross-section. Results of these tests were compared to values obtained from elastic frame analysis. The elastic frame analysis gave a good prediction of deflections and internal stresses up to working load.

The failure mode is dependent on a number of factors of which joint eccentricity is one.

## ACKNOWLEDGEMENTS

The author wishes to express his deep appreciation to Professor S.H. Simmonds for his supervision, patience and support throughout the course of this work. The author also wishes to express his appreciation to Professor D.W. Murray for his invaluable help.

Funding and test specimens have been provided by the Canadian Steel Industries Construction Council.

The author owes special thanks to Alistair Dunbar, Larry Burden, Richard Helfrich and Scotty Rogers who helped in the testing program.

The author thanks Nola Wismer for her expert and speedy typing of the manuscript.

Thanks are also due to the Staff and Graduate Students in the Department of Civil Engineering who helped in numerous ways.

TABLE OF CONTENTS


| | | Page |
|---|---|---|
| Library Release Form | | i |
| Title Page | | ii |
| Signed Approval Page | | iii |
| Abstract | | iv |
| Acknowledgements | | v |
| Table of Contents | | vi |
| List of Tables | | ix |
| List of Figures | | xi |
| CHAPTER 1 - INTRODUCTION | | 1 |
| 1.1 | Open Web Steel Joists | 1 |
| 1.2 | Statement of the Problem | 1 |
| 1.3 | Scope of the Project | 2 |
| 1.4 | Literature Review | 3 |
| CHAPTER 2 - TEST SPECIMENS | | 6 |
| 2.1 | Joist Designation | 6 |
| 2.2 | Joist Selection | 7 |
| 2.3 | Joist Configuration | 7 |
| 2.4 | Geometry | 8 |
| 2.5 | Material Properties | 9 |
| CHAPTER 3 - TEST FACILITY | | 32 |
| 3.1 | Old Test Facility | 32 |

| | | Page |
|---|---|---|
| 3.2 | New Test Facility | 33 |
| 3.3 | Calibration of Jacks | 35 |
| 3.4 | Instrumentation | 36 |
| CHAPTER 4 - TEST PROCEDURE | | 42 |
| 4.1 | Specimen Instrumentation | 42 |
| 4.2 | Initial Adjustments | 43 |
| 4.3 | Loading | 43 |
| 4.4 | Analysis of Test Data | 44 |
| CHAPTER 5 - DISCUSSION OF RESULTS | | 47 |
| 5. | Introduction | 47 |
| 5.2 | Deflections | 47 |
| 5.2.1 | Measured Deflections | 47 |
| 5.2.2 | Comparison of Measured and Calculated Deflections | 50 |
| 5.3 | Axial Force | 51 |
| 5.4 | Bending Moment | 52 |
| 5.5 | Inelastic Behaviour and Failure Mode | 53 |
| 5.6 | Prediction of Ultimate Capacity | 60 |
| CHAPTER 6 - EFFECTS OF JOINT ECCENTRICITY | | 101 |
| 6.1 | Introduction | 101 |
| 6.2 | Deflections | 103 |
| 6.3 | Axial Force | 104 |
| 6.4 | Bending Moments | 105 |
| 6.5 | Discussion of Joint Eccentricity | 106 |

Page

CHAPTER 7 - SUMMARY AND CONCLUSIONS 115

LIST OF REFERENCES 118

APPENDIX A - CALCULATION OF GEOMETRY 119

APPENDIX B - INSTRUMENTATION 120

LIST OF TABLES


| Table | Description | Page |
|---|---|---|
| 2.1 | Geometry of Joist CX01 | 11 |
| 2.2 | Geometry of Joist CX02 | 12 |
| 2.3 | Geometry of Joist CX03 | 13 |
| 2.4 | Geometry of Joist CX04 | 14 |
| 2.5 | Geometry of Joist CX05 | 15 |
| 2.6 | Geometry of Joist CX06 | 16 |
| 2.7 | Geometry of Joist CY01 | 17 |
| 2.8 | Geometry of Joist CY02 | 18 |
| 2.9 | Geometry of Joist CZ01 | 19 |
| 2.10 | Geometry of Joist CZ02 | 20 |
| 2.11 | Material Property of Joists CX01, CX02 and CX03 | 21 |
| 2.12 | Material Property of Joists CX04, CX05 and CX06 | 22 |
| 2.13 | Material Property of Joists CY01 and CY02 | 23 |
| 2.14 | Material Property of Joists CZ01 and CZ02 | 24 |
| 4.1 | Instrumented Members | 46 |
| 5.1 | Comparison of Stresses in Joist CX01, Load 315 Pounds Per Linear Foot | 63 |
| 5.2 | Comparison of Stresses in Joist CX02, Load 315 Pounds Per Linear Foot | 64 |
| 5.3 | Comparison of Stresses in Joist CX03, Load 315 Pounds Per Linear Foot | 65 |
| 5.4 | Comparison of Stresses in Joist CX04, Load 300 Pounds Per Linear Foot | 66 |
| 5.5 | Comparison of Stresses in Joist CX05, Load 300 Pounds Per Linear Foot | 67 |

| | | Page |
|---|---|---|
| 5.6 | Comparison of Stresses in Joist CX06, Load 300 Pounds Per Linear Foot | 68 |
| 5.7 | Comparison of Stresses in Joist CY01, Load 315 Pounds Per Linear Foot | 69 |
| 5.8 | Comparison of Stresses in Joist CY02, Load 315 Pounds Per Linear Foot | 70 |
| 5.9 | Comparison of Stresses in Joist CZ01 at 446 Pounds Per Linear Foot | 71 |
| 5.10 | Summary of Results | 72 |

LIST OF FIGURES


| Figure | Description | Page |
|---|---|---|
| 1.1 | Eccentricity at a Joint | 5 |
| 2.1 | Type 'X' Joint | 25 |
| 2.2 | Type 'Y' Joint | 25 |
| 2.3 | Quantities Measured at a Joint | 26 |
| 2.4 | Quantities Computed at a Joint | 27 |
| 2.5 | Plate Grips on Tension Specimen | 28 |
| 2.6 | Stress-Strain Curve of Top Chord, Joist CX01, CX02, CX03 | 29 |
| 2.7 | Stress-Strain Curve of Top Chord, Joist CX04, CX05, CX06 | 30 |
| 2.8 | Stress-Strain Curve of Top Chord, Joist CY01, CY02 | 31 |
| 3.1 | Joist Specimen in Loading Frame | 37 |
| 3.2 | Pneumatic Jack in Fixed Frame | 37 |
| 3.3 | Calibration of Jack | 38 |
| 3.4 | Load - Calibration Curve | 39 |
| 3.5 | Load - Calibration Curve | 40 |
| 3.6 | Load - Calibration Curve | 41 |
| 5.1 | Load - Deflection Curve, Joist CX01 | 73 |
| 5.2 | Load - Deflection Curve, Joist CX02 | 74 |
| 5.3 | Load - Deflection Curve, Joist CX03 | 75 |
| 5.4 | Load - Deflection Curve, Joist CX04 | 76 |
| 5.5 | Load - Deflection Curve, Joist CX05 | 77 |
| 5.6 | Load - Deflection Curve, Joist CX06 | 78 |
| 5.7 | Load - Deflection Curve, Joist CY01 | 79 |
| 5.8 | Load - Deflection Curve, Joist CY02 | 80 |
| 5.9 | Load - Deflection Curve, Joist CZ01 | 81 |
| 5.10 | Load - Deflection Curve, Joist CZ02 | 82 |

| | | Page |
|---|---|---|
| 5.11 | Failure of Joist CX01 | 83 |
| 5.12 | Failure of Joist CX02 | 83 |
| 5.13 | Failure of Joist CX03 | 84 |
| 5.14 | Yielding at Joint | 84 |
| 5.15 | Failure of Joist CX06 | 85 |
| 5.16 | Failure of Joist CY01 | 85 |
| 5.17 | Yielding of Bottom Chord of Joist CY01 | 86 |
| 5.18 | Yielding of Bottom Chord of Joist CY02 | 86 |
| 5.19 | Yielding of Bottom Chord of Joist CY02 | 87 |
| 5.20 | Yielding of Chord at Spacers, Joist CZ02 | 87 |
| 5.21 | Failure of Joist CZ02 | 88 |
| 5.22 | Failure of Spacers in Joist CZ02 | 88 |
| 5.23 | Section - Deformation of Member 9T(South), Joist CX01 | 89 |
| 5.24 | Section - Deformation of Member 9T(North), Joist CX01 | 90 |
| 5.25 | Section - Deformation of Member 8T(South), Joist CX01 | 91 |
| 5.26 | Section - Deformation of Member 7T(North), Joist CX02 | 92 |
| 5.27 | Section - Deformation of Member 8T(North), Joist CX02 | 93 |
| 5.28 | Section - Deformation of Member 9T(North), Joist CX02 | 94 |
| 5.29 | Section - Deformation of Member 9T(South), Joist CX02 | 95 |
| 5.30 | Section - Deformation of Member 8T(South), Joist CX02 | 96 |
| 5.31 | Section - Deformation of Member 7T(South), Joist CX02 | 97 |
| 5.32 | Predicted and Measured Buckling Axial Load of Joists CX01, CX02, CX03 | 98 |
| 5.33 | Predicted and Measured Buckling Axial Load of Joists CX05, CX06 | 99 |

| | | Page |
|---|---|---|
| 5.34 | Predicted and Measured Buckling Axial Load of Joists CY01, CY02 | 100 |
| 6.1 | Calculation of Eccentricities at Bottom and Top Joints | 110 |
| 6.2 | Variation of Midspan Deflection With Eccentricity | 111 |
| 6.3 | Variation of Top Chord Axial Force With Eccentricity | 112 |
| 6.4 | Variation of Top Chord Moment, at End i, With Eccentricity | 113 |
| 6.5 | Variation of Top Chord Moment, at End j, With Eccentricity | 114 |

# CHAPTER 1

# INTRODUCTION

## 1.1 Open Web Steel Joists

An open web steel joist is a simply supported truss, with parallel or slightly pitched chords and a triangulated web system. Joists are commonly used in roof and floor construction as secondary load carrying members spanning between primary framing members. The top chord is considered to provide continuous support for the floor or roof decking.

Joists are commonly designated as short, intermediate or long span although this designation is somewhat ambiguous. Short span joists are generally produced with continuous bent bar webs which are welded to the chords using either resistance or arc welding. Intermediate span joists generally have web members in a subdivided Warren configuration which are welded to the top chord so as to provide support in the plane of the joist at intervals of two feet. For the long span joist, the process of manufacture is similar to intermediate joists except that the web configuration generally corresponds to a Pratt Truss and the panel spacing may vary. This study is restricted to joists generally designated as intermediate.

## 1.2 Statement of the Problem

The CSA Standard S16.1 (1) Section 16.5.11.4 states that, wherever practical, members of joists meeting at a joint should have their gravity axes intersect at a point, but, the eccentricity can be neglected if the eccentricity does not exceed the greater distance

from the chord neutral axis to the extreme fibres of the chord for continuous web members; or it does not exceed the distance from the neutral axis to the outside face of the chord for non-continuous web members.

If the above requirement is not satisfied, provision should be made for the effects of total eccentricity. This eccentricity is denoted in this report as $e_1$, Figure 1.1. The diameter of structural tubing that is commonly used for web members in steel joists is such that the above requirement is often exceedingly difficult to satisfy.

Unless noted otherwise, the eccentricity, referred to in this study, is the distance along the neutral axis of the chord, between the intersections of the neutral axes of adjacent webs and the neutral axis of the chord. This distance was used because of the ease in measurement and because this length is the equivalent length of the chord used to model joint eccentricity for the elastic frame analysis. This eccentricity is denoted as $e_2$ and the difference between the code eccentricity, $e_1$, and $e_2$ is shown in Figure 1.1.

## 1.3 Scope of the Project

The project was divided into two phases. The first phase consisted of the 'pilot study' by Matiisen (3) in which he investigated the stresses generated in open web steel joists resulting from joint eccentricity. To exaggerate the effects of joint eccentricity the joists tested by Matiisen had low span to depth ratios and unusually high end shears. The second phase, which is the scope of this work is to verify the conclusions for joists with geometry and loading conditions representative of those used in practice and to examine the require-

ments of CSA Standard S16.1 (1).

More specifically this involves determining the effects of joint eccentricity on

(a) the joist deflections at working load;

(b) the degree of secondary moments induced in the chord and web members;

(c) the location of first yielding and the extent of inelastic action;

(d) the mechanism of failure;

(e) means of predicting the above;

(f) means of designing for the above.

The investigation was accomplished by testing joists, and by obtaining stresses in the members by an elastic frame analysis and by measurement of strains.

## 1.4 Literature Review

Although open web steel joists are widely used there is very little published material relating to their behaviour.

Joint eccentricity is referred to in references of Kennedy & Rowan (4) and McDonald (5), but the joists had webs of pre-bent solid rod type, where eccentricities are small. Both references ignored the effect of joint eccentricities while reporting results. Morris, Frovich & Thiensiripipat (6) consider joint eccentricity for truss joints made from HSS sections and reported a considerable decrease in capacity due to joint eccentricity, especially where square tubing was used.

Ohmart & Lenzen (7), and Kennedy & Rowan (4) considered the effects of uniform or mid-point loading on the top chord compared to

panel point loading. Both references reported reduced factors of safety with mid-span loading and the need for more research to determine whether bending stresses could be neglected for certain lengths of panels and joists. Several studies (4,5) were concerned with compression failures of the top chord and, in tests, failure of the top chord was assured by overdesigning the bottom chord.

Yu (8) is the only reference which considers failure of the web members but his investigation was restricted to single and double angle web configurations. The web angles were welded to one side of the chords and the out-of-plane eccentricity was considered rather than the in-plane eccentricity, which is considered in this thesis.

There does not appear to be any work reporting the effect of joint eccentricities on the behaviour of open web steel joists, other than the work done by Matiisen (3). Matiisen found that the effect of joint eccentricity is to increase moments in the members adjacent to the joints. This could be computed closely by an elastic frame analysis of the joist taking into consideration the eccentricity at the joints by including them as members.

Srivastava (9) modified the program PLAST generated by Epstein & Murray (10), whereby he could predict the theoretical buckling load of a joist members. The program used an unsymmetrical I section with a tri-linear stress-strain curve including the strain hardening portion. The program could be applied for different models and boundary conditions.

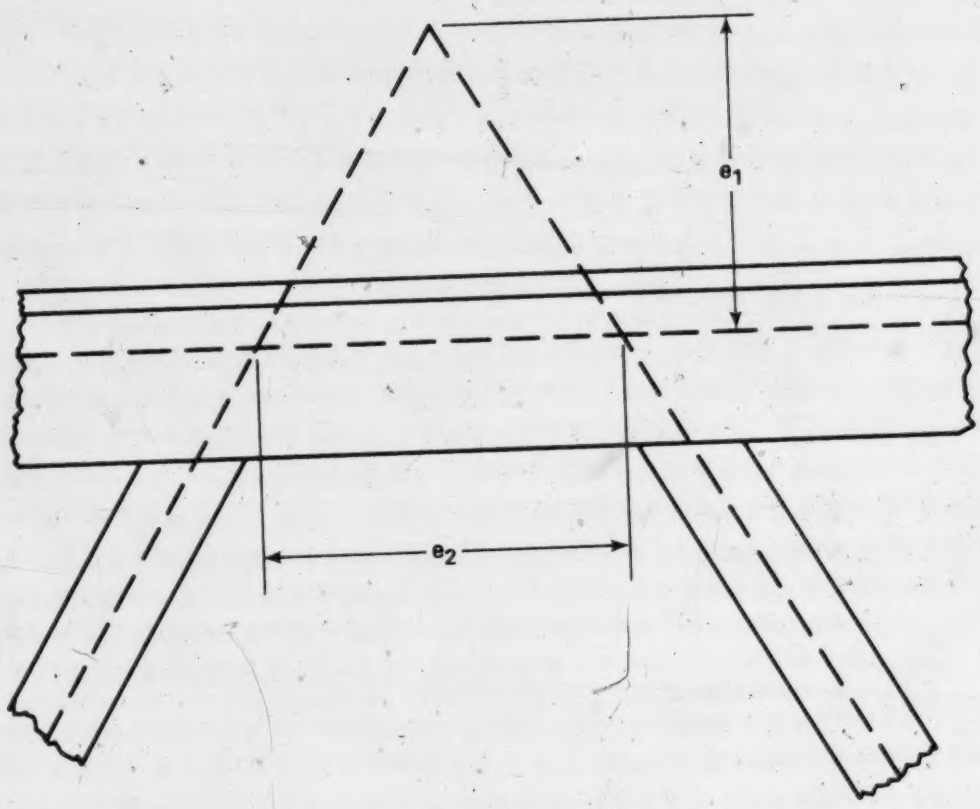


**Figure 1.1 Eccentricity at a Joint.**

# CHAPTER 2

# TEST SPECIMENS

## 2.1 Joist Designation

The study consisted of testing to failure ten open web steel joists. Joists were classified by construction details and identified by character designation. The first letter 'C' denotes the joist is part of the second testing phase. The second letter denotes the joint detail. Joists 'X' and 'Y' denote joists with hat sections for chords and structural tubes for web diagonals. The letter 'X' indicates the joists in which the ends of the web tubing are pinched to form an ellipse so that the major axes of the ends are parallel to the chords as shown in Figure 2.1. The letter 'Y' indicates that the major axes of the pinched ends are perpendicular to the chords as shown in Figure 2.2. The letter 'Z' indicates joists with angle chords and web diagonals.

The testing was broken into four series. The CX(1) series consisted of three joists CX01, CX02 and CX03. The chords of these joists were hot rolled hat sections. The CX(2) series had cold rolled hat sections as chords and were denoted as CX04, CX05 and CX06. The CY series had two joists, CY01 and CY02, which had hot rolled hat sections as chords. The CZ series, CZ01 and CZ02, had hot rolled angle sections as chords.

Joists with similar construction details but different eccentricity combined to form a series. The last two digits give the sequence number of the joist in the series. The eccentricity ($e_2$) at the joint increased as the joist number increased.

## 2.2 Joist Selection

The selection of the test joists was based on observations during the 'pilot study'. To avoid the effects of the end diagonals on the buckling of the top chord it was necessary to have a larger number of panels. Using a panel length on the top chord of two feet the length of joist selected was 38 feet. A depth of two feet was chosen to produce a reasonable span to depth ratio.

A nominal load of 300 pound per linear foot was arbitrarily chosen. When the chords were chosen for the above requirements, the load increased to 315 pounds per linear foot for the CX(1) and CY series.

For the above geometry and two 2 1/2" x 1 1/2" x 1/4" standard angle chord the CZ series was found to have a design load of 446 pounds per linear foot with variable panel lengths.

## 2.3 Joist Configuration

The geometry of each joist was measured prior to a test. The variables considered in a joist were panel lengths, types of chords and webs, and joint eccentricities.

The panel lengths of all joists, except those in the CX(2) and CZ series were two feet. For the CZ series the panel lengths varied from approximately four feet at the ends to two feet at the midspan of the joist. For the CX(2) series the centre panels were one foot. (This was the fabricators standard for a 38 foot length of joist).

The chords of joists in the CX(1), CX(2) and CY series were hat sections. The chords for joists in the CZ series were double angle sections with spacers at approximately sixteen inch centres.

The end diagonals of all joists, except in the CZ series, were

rectangular bars. Those in the CZ series were single angles. The vertical members of joists CX02, CX03, CX04, CX05 and CX06 were hollow tubing; those of CX01 were double rods; and those for the CY01 and CY02 joists were single angles. The verticals for joists in the CZ series were HSS sections.

All other web members of joists in the CX(1), CX(2) and CY series were hollow tubes, while those in the CZ series were double angles.

## 2.4 Geometry

The joint eccentricities for each joist were obtained by measurements made in the laboratory.

Shown in Figure 2.3 is a typical joint of a joist and the quantities to be measured. A vertical line a-a is drawn approximately half way between the web members. A vertical line is dropped a distance w to another line running parallel to the inner edge of the chord. While w is an arbitrary distance, it should be constant for all joints of the joist. This line parallel to the chord should intersect the web members within their unbent portion. The distances D(I,1) and D(I,2) were recorded. The angles between each web member and the chord were measured and recorded.

Figure 2.4 shows the quantities which can be computed by trigonometry. The derivation of the expressions for the computation of the eccentricity is given in Appendix A. In Figure 2.4, the values of y and z are obtained from published information. The line b-b is the true centre of the joint.

The geometry of all joists are given in Tables 2.1 to 2.10.

## 2.5 Material Properties

For the calculation of stresses in any structural member Young's modulus E, the moment of inertia I and the cross sectional area A are required.

The areas for top and bottom chord members were obtained by taking samples of accurately measured lengths (the ends being milled) and weighing them in air and in water. From the loss of weight in water the volume of the specimen can be obtained. Knowing the length of the sample, the area can be calculated. For web members the area was obtained from a plot of load versus strain. The slope of this plot gives a value of EA from which, assuming a value of E, the area could be computed.

Samples of member sections were tested in tension to obtain the value of the axial stiffness EA. These undeformed samples were fifteen to twenty inches long and were cut from the joist after failure in regions in which the stresses were a minimum. To provide a means of gripping the hat and angle sections in the testing machine so that no moments were induced during loading a steel plate was welded to the ends at the centre of gravity of the section as shown in Figure 2.5. For the hollow web tube sections the ends were filled with "Plastic Steel" to a depth of three inches to prevent crushing of the ends during loading.

The strains were measured by electric resistance strain gauges attached to the sample, their number depending on the type of sample (four for double angle sections, three for hat sections, and two for tubes, rods and single angles).

For hat sections strains beyond the elastic region were measured to failure by measuring the extension between two points on the

specimen five to six inches apart. The stress-strain plots are shown in Figures 2.6 to 2.8.

The material and section properties E, I and A are given in Table 2.11 to 2.14. The properties of the chords vary from point to point since they are made from metal scrap and some impurities were encountered at points when the chords were being cut for the estimation of the above properties.

Table 2.1 Geometry of Joist CX01

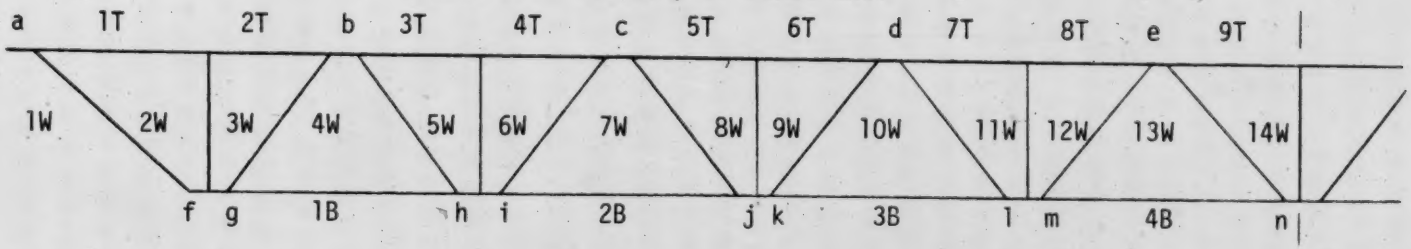


| MEMBER | NORTH | SOUTH | MEMBER | NORTH | SOUTH | MEMBER | NORTH | SOUTH |
|---|---|---|---|---|---|---|---|---|
| a | 3.000 | 3.000 | f | 1.100 | 1.100 | 1W | 39.976 | 39.976 |
| 1T | 33.000 | 33.000 | g | 0.830 | 0.850 | 2W | 22.708 | 22.708 |
| 2T | 23.970 | 23.350 | 1B | 46.350 | 46.960 | 3W | 32.801 | 32.357 |
| b | 1.110 | 1.550 | h | 1.880 | 0.870 | 4W | 31.320 | 31.869 |
| 3T | 23.450 | 23.230 | i | 1.820 | 0.850 | 5W | 22.708 | 22.708 |
| 4T | 22.500 | 22.730 | 2B | 44.440 | 45.940 | 6W | 30.713 | 31.534 |
| C | 0.810 | 1.030 | j | 0.710 | 0.950 | 7W | 31.583 | 31.638 |
| 5T | 22.660 | 22.980 | k | 0.710 | 0.970 | 8W | 22.708 | 22.708 |
| 6T | 23.380 | 22.990 | 3B | 47.260 | 46.570 | 9W | 32.087 | 31.631 |
| d | 0.760 | 0.890 | l | 0.630 | 0.720 | 10W | 32.200 | 32.080 |
| 7T | 23.460 | 23.380 | m | 0.610 | 0.710 | 11W | 22.708 | 22.708 |
| 8T | 23.010 | 23.120 | 4B | 46.450 | 46.700 | 12W | 31.897 | 31.904 |
| e | 0.850 | 0.640 | n | 0.650 | 0.650 | 13W | 31.757 | 32.073 |
| 9T | 22.850 | 23.300 | | | | 14W | 22.708 | |

Table 2.2 Geometry of Joist CX02

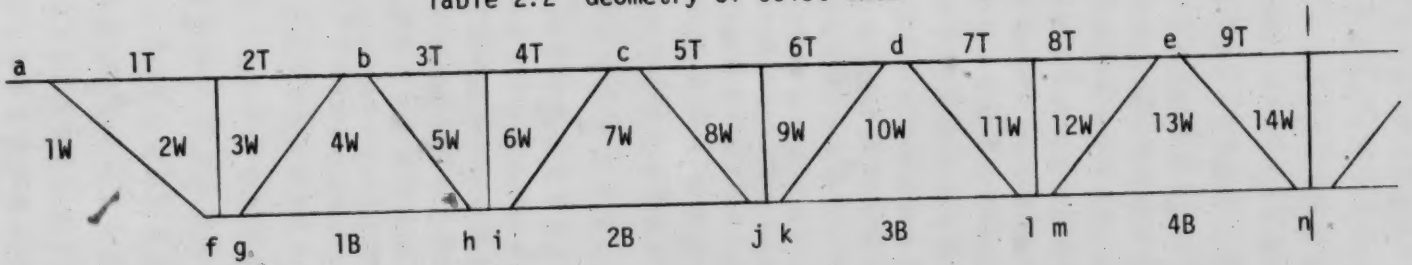


| MEMBER | NORTH | SOUTH | MEMBER | NORTH | SOUTH | MEMBER | NORTH | SOUTH |
|---|---|---|---|---|---|---|---|---|
| a | 3.000 | 3.000 | f | 1.980 | 1.889 | 1W | 40.186 | 40.186 |
| 1T | 33.000 | 33.000 | g | 2.300 | 2.200 | 2W | 23.076 | 23.076 |
| 2T | 24.670 | 22.740 | 1B | 46.110 | 46.270 | 3W | 33.707 | 32.328 |
| b | 2.230 | 1.640 | h | 1.540 | 1.530 | 4W | 30.089 | 31.876 |
| 3T | 20.850 | 23.520 | i | 1.650 | 1.690 | 5W | 23.076 | 23.076 |
| 4T | 23.370 | 23.140 | 2B | 45.150 | 45.120 | 6W | 31.690 | 31.506 |
| c | 1.450 | 1.660 | j | 1.840 | 1.730 | 7W | 31.869 | 31.890 |
| 5T | 23.020 | 23.140 | k | 1.940 | 1.540 | 8W | 23.076 | 23.076 |
| 6T | 23.710 | 23.800 | 3B | 46.115 | 46.040 | 9W | 32.279 | 32.272 |
| d | 0.840 | 0.850 | l | 1.370 | 1.940 | 10W | 32.503 | 32.321 |
| 7T | 24.260 | 23.570 | m | 1.710 | 1.670 | 11W | 23.076 | 23.076 |
| 8T | 23.440 | 23.430 | 4B | 45.988 | 45.990 | 12W | 32.391 | 32.132 |
| e | 0.810 | 0.800 | n | 1.880 | 1.850 | 13W | 32.209 | 32.814 |
| 9T | 23.350 | 24.210 | | | | 14W | 23.076 | |

Table 2.3 Geometry of Joist CX03

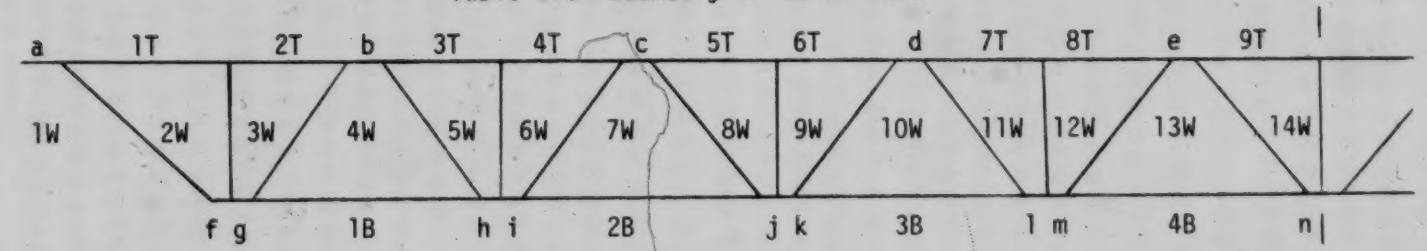


| MEMBER | NORTH | SOUTH | MEMBER | NORTH | SOUTH | MEMBER | NORTH | SOUTH |
|---|---|---|---|---|---|---|---|---|
| a | 3.000 | 3.000 | f | 1.980 | 2.320 | 1W | 39.299 | 39.444 |
| 1T | 33.790 | 33.630 | g | 2.210 | 2.100 | 2W | 23.076 | 23.076 |
| 2T | 21.780 | 22.200 | 1B | 44.430 | 44.180 | 3W | 30.913 | 31.268 |
| b | 1.910 | 2.440 | h | 1.985 | 1.750 | 4W | 31.986 | 30.960 |
| 3T | 24.050 | 22.320 | i | 1.960 | 1.960 | 5W | 23.076 | 23.076 |
| 4T | 22.400 | 22.940 | 2B | 44.710 | 44.950 | 6W | 30.960 | 31.370 |
| c | 2.450 | 2.370 | j | 2.320 | 2.020 | 7W | 31.827 | 32.251 |
| 5T | 23.240 | 23.550 | k | 2.330 | 2.020 | 8W | 23.076 | 23.076 |
| 6T | 22.000 | 23.690 | 3B | 45.170 | 46.070 | 9W | 30.980 | 32.349 |
| d | 2.440 | 2.120 | l | 1.450 | 1.870 | 10W | 32.623 | 32.076 |
| 7T | 24.510 | 23.250 | m | 1.330 | 1.830 | 11W | 23.076 | 23.076 |
| 8T | 22.090 | 22.770 | 4B | 45.660 | 45.490 | 12W | 31.040 | 31.772 |
| e | 2.750 | 2.840 | n | 2.280 | 2.180 | 13W | 33.439 | 32.097 |
| 9T | 25.480 | 24.490 | | | | 14W | 23.076 | |

Table 2.4 Geometry of Joist CX04

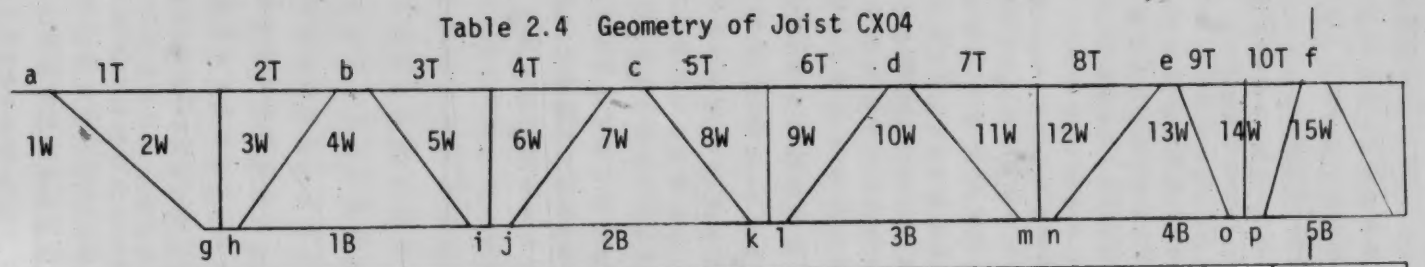


| MEMBER | NORTH | SOUTH | MEMBER | NORTH | SOUTH | MEMBER | NORTH | SOUTH |
|---|---|---|---|---|---|---|---|---|
| a | 2.000 | 2.000 | g | 1.020 | 1.160 | 1W | 31.392 | 32.292 |
| 1T | 23.020 | 23.960 | h | 1.170 | 1.120 | 2W | 22.967 | 22.967 |
| 2T | 23.010 | 24.520 | 1B | 45.570 | 46.250 | 3W | 31.283 | 32.577 |
| b | 0.630 | 0.600 | i | 0.660 | 0.890 | 4W | 32.717 | 31.494 |
| 3T | 23.960 | 22.440 | j | 0.630 | 0.870 | 5W | 22.967 | 22.967 |
| 4T | 21.790 | 22.860 | 2B | 45.930 | 47.370 | 6W | 31.229 | 32.539 |
| c | 0.820 | 0.980 | k | 0.890 | 0.450 | 7W | 33.039 | 32.511 |
| 5T | 24.640 | 24.560 | l | 0.900 | 0.430 | 8W | 22.967 | 22.967 |
| 6T | 24.330 | 24.430 | 3B | 46.210 | 46.330 | 9W | 32.809 | 32.504 |
| d | 0.200 | 0.310 | m | 0.520 | 0.570 | 10W | 32.208 | 31.818 |
| 7T | 23.100 | 22.890 | n | 0.520 | 0.580 | 11W | 22.967 | 22.967 |
| 8T | 22.970 | 23.030 | 4B | 45.940 | 45.440 | 12W | 32.117 | 32.117 |
| e | 0.690 | 0.690 | o | 2.080 | 1.680 | 13W | 32.362 | 31.324 |
| 9T | 24.880 | 23.980 | p | 0.910 | 0.740 | 14W | 22.967 | 22.967 |
| 10T | 10.730 | 11.760 | 5B | 21.470 | | 15W | 24.602 | 25.474 |
| f | 0.630 | | | | | | | |

Table 2.5 Geometry of Joist CX05

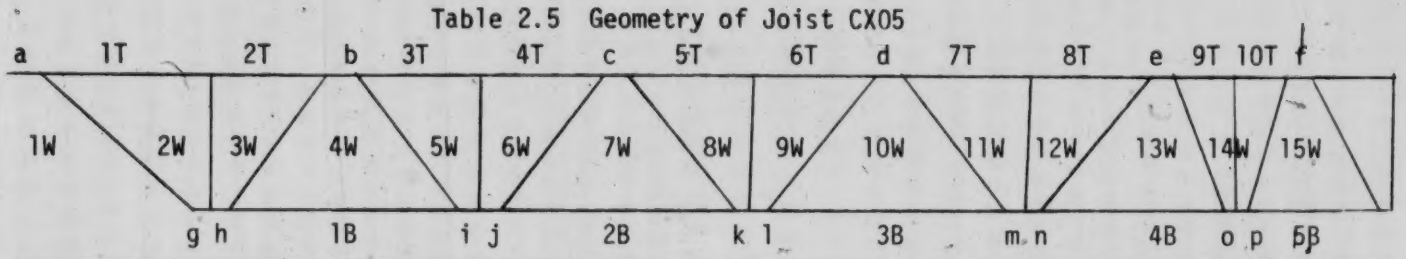


| MEMBER | NORTH | SOUTH | MEMBER | NORTH | SOUTH | MEMBER | NORTH | SOUTH |
|---|---|---|---|---|---|---|---|---|
| a | 2.000 | 2.000 | g | 0.640 | 0.880 | 1W | 31.501 | 32.959 |
| 1T | 22.200 | 23.030 | h | 0.690 | 0.670 | 2W | 22.967 | 22.967 |
| 2T | 23.800 | 24.120 | 1B | 45.700 | 45.500 | 3W | 32.582 | 32.824 |
| b | 1.000 | 0.850 | i | 1.530 | 1.100 | 4W | 32.924 | 32.292 |
| 3T | 24.120 | 23.150 | j | 1.510 | 0.980 | 5W | 22.967 | 22.967 |
| 4T | 22.280 | 23.440 | 2B | 45.940 | 45.400 | 6W | 31.645 | 32.497 |
| c | 1.220 | 1.160 | k | 1.180 | 1.210 | 7W | 33.183 | 32.681 |
| 5T | 24.130 | 23.460 | l | 1.180 | 1.280 | 8W | 22.967 | 22.967 |
| 6T | 24.250 | 23.900 | 3B | 46.020 | 45.300 | 9W | 33.269 | 32.866 |
| d | 1.000 | 0.890 | m | 1.180 | 1.250 | 10W | 32.468 | 31.735 |
| 7T | 23.130 | 22.150 | n | 1.180 | 1.350 | 11W | 22.967 | 22.967 |
| 8T | 22.870 | 24.000 | 4B | 45.690 | 44.500 | 12W | 32.285 | 32.967 |
| e | 0.870 | 1.500 | o | 0.980 | 1.230 | 13W | 32.596 | 31.358 |
| 9T | 24.000 | 21.980 | p | 1.380 | 1.520 | 14W | 22.967 | 22.967 |
| 10T | 10.790 | 12.230 | 5B | 21.600 | | 15W | 25.216 | 26.298 |
| f | 0.580 | | | | | | | |

Table 2.6 Geometry of Joist CX06

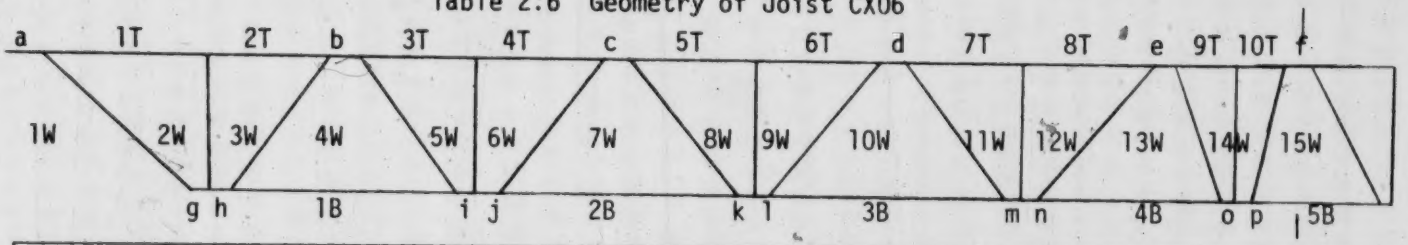


| MEMBER | NORTH | SOUTH | MEMBER | NORTH | SOUTH | MEMBER | NORTH | SOUTH |
|---|---|---|---|---|---|---|---|---|
| a | 2.000 | 2.000 | g | 1.580 | 1.530 | 1W | 30.825 | 30.995 |
| 1T | 22.140 | 22.030 | h | 2.250 | 1.670 | 2W | 22.967 | 22.967 |
| 2T | 23.470 | 23.980 | 1B | 45.700 | 45.000 | 3W | 33.017 | 31.984 |
| b | 1.240 | 1.500 | i | 1.513 | 1.450 | 4W | 32.320 | 32.186 |
| 3T | 23.330 | 23.150 | j | 1.450 | 1.450 | 5W | 22.967 | 22.967 |
| 4T | 22.390 | 22.240 | 2B | 44.940 | 44.400 | 6W | 31.762 | 31.548 |
| c | 2.250 | 2.260 | k | 1.410 | 1.210 | 7W | 31.631 | 31.428 |
| 5T | 23.060 | 23.160 | l | 1.385 | 1.390 | 8W | 22.967 | 22.967 |
| 6T | 23.770 | 22.880 | 3B | 46.020 | 45.300 | 9W | 33.743 | 33.500 |
| d | 1.750 | 1.850 | m | 1.280 | 1.250 | 10W | 32.468 | 31.735 |
| 7T | 23.130 | 22.150 | n | 1.380 | 1.350 | 11W | 22.967 | 22.967 |
| 8T | 22.870 | 23.000 | 4B | 44.690 | 43.800 | 12W | 32.285 | 32.567 |
| e | 1.870 | 1.800 | o | 1.170 | 1.630 | 13W | 32.596 | 32.428 |
| 9T | 24.000 | 22.500 | p | 1.380 | 1.540 | 14W | 22.967 | 22.967 |
| 10T | 11.200 | 12.100 | 5B | 21.428 | | 15W | 25.216 | 26.228 |
| f | 0.780 | | | | | | | |

Table 2.7 Geometry of Joist CY01

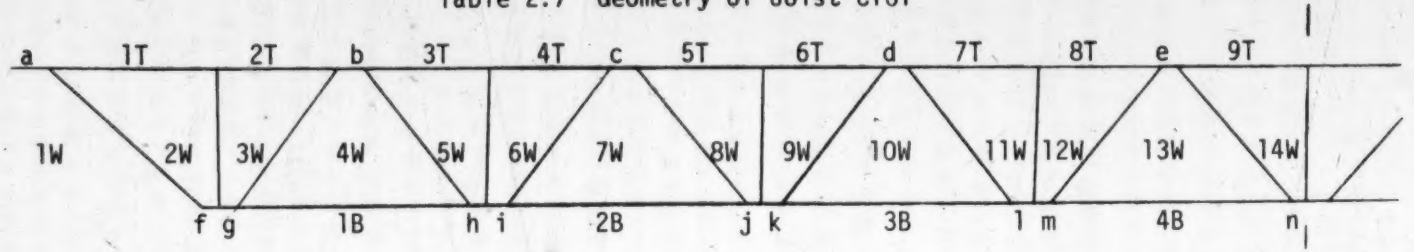


| MEMBER | NORTH | SOUTH | MEMBER | NORTH | SOUTH | MEMBER | NORTH | SOUTH |
|---|---|---|---|---|---|---|---|---|
| a | 2.000 | 2.500 | f | 0.640 | 1.150 | 1W | 41.985 | 41.326 |
| 1T | 35.780 | 35.500 | g | 0.410 | 0.780 | 2W | 22.977 | 22.977 |
| 2T | 23.660 | 24.290 | 1B | 46.990 | 46.890 | 3W | 32.688 | 32.741 |
| b | -0.250 | -0.190 | h | 0.560 | 0.520 | 4W | 32.859 | 32.648 |
| 3T | 24.050 | 23.900 | i | 0.570 | 0.530 | 5W | 22.977 | 22.977 |
| 4T | 23.820 | 24.640 | 2B | 46.400 | 47.680 | 6W | 32.424 | 33.167 |
| c | -0.377 | -0.201 | j | 0.300 | 0.330 | 7W | 32.352 | 32.776 |
| 5T | 23.450 | 23.900 | k | 0.300 | 0.320 | 8W | 22.977 | 22.977 |
| 6T | 24.450 | 24.090 | 3B | 47.710 | 47.260 | 9W | 33.084 | 32.965 |
| d | -0.364 | -0.137 | l | 0.330 | 0.250 | 10W | 32.656 | 32.763 |
| 7T | 23.890 | 23.740 | m | 0.320 | 0.240 | 11W | 22.977 | 22.977 |
| 8T | 24.000 | 24.140 | 4B | 47.960 | 47.520 | 12W | 32.764 | 32.978 |
| e | -0.336 | -0.254 | n | 0.060 | 0.060 | 13W | 33.200 | 32.776 |
| 9T | 24.340 | 23.680 | | | | 14W | 22.977 | |

Table 2.8 Geometry of Joist CY02

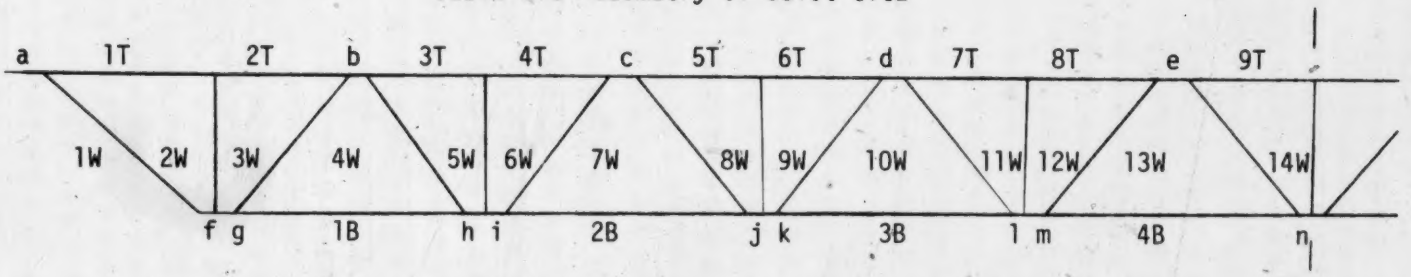


| MEMBER | NORTH | SOUTH | MEMBER | NORTH | SOUTH | MEMBER | NORTH | SOUTH |
|---|---|---|---|---|---|---|---|---|
| a | 2.100 | 2.000 | f | 0.670 | 0.580 | 1W | 41.809 | 42.960 |
| 1T | 35.780 | 35.570 | g | 0.510 | 0.590 | 2W | 22.700 | 22.700 |
| 2T | 24.070 | 23.660 | 1B | 47.200 | 46.500 | 3W | 32.716 | 32.680 |
| b | 0.540 | 0.450 | h | 0.520 | 0.450 | 4W | 32.387 | 31.955 |
| 3T | 23.220 | 22.940 | i | 0.560 | 0.460 | 5W | 22.700 | 22.700 |
| 4T | 24.040 | 24.630 | 2B | 47.730 | 47.510 | 6W | 32.977 | 33.158 |
| c | 0.579 | 0.490 | j | 0.490 | 0.560 | 7W | 32.417 | 32.209 |
| 5T | 23.730 | 22.970 | k | 0.500 | 0.620 | 8W | 22.700 | 22.700 |
| 6T | 23.920 | 23.940 | 3B | 47.620 | 47.120 | 9W | 32.616 | 33.195 |
| d | 0.630 | 0.590 | l | 0.350 | 0.580 | 10W | 32.724 | 31.933 |
| 7T | 23.920 | 23.040 | m | 0.330 | 0.570 | 11W | 22.700 | 22.700 |
| 8T | 23.540 | 24.530 | 4B | 47.060 | 47.150 | 12W | 32.465 | 33.224 |
| e | 0.560 | 0.480 | n | 0.400 | 0.390 | 13W | 32.523 | 32.110 |
| 9T | 23.690 | 23.100 | | | | 14W | 22.700 | |

Table 2.9 Geometry of Joist CZ01

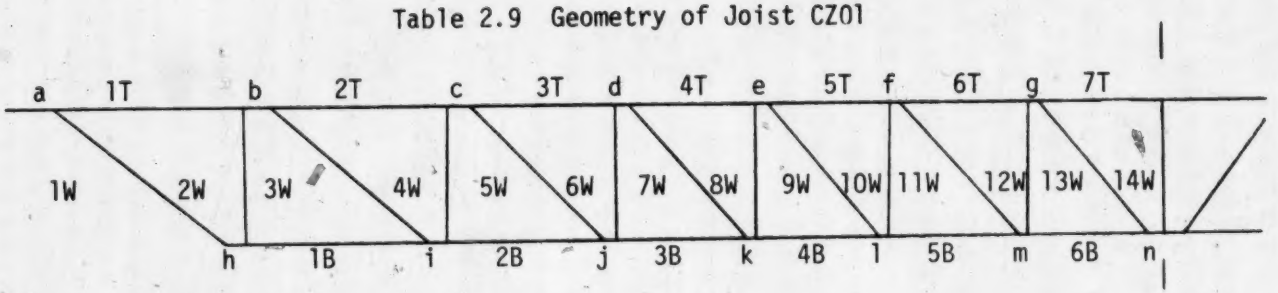


| MEMBER | NORTH | SOUTH | MEMBER | NORTH | SOUTH | MEMBER | NORTH | SOUTH |
|---|---|---|---|---|---|---|---|---|
| a | 1.500 | 1.500 | h | 0.360 | 0.860 | 1W | 53.533 | 53.079 |
| 1T | 49.000 | 49.000 | 1B | 45.900 | 45.850 | 2W | 22.360 | 22.360 |
| b | 0.870 | 1.300 | i | 0.100 | 0.550 | 3W | 50.276 | 49.846 |
| 2T | 45.130 | 45.100 | 2B | 39.680 | 39.010 | 4W | 22.360 | 22.360 |
| c | 1.280 | 0.510 | j | 0.070 | 0.790 | 5W | 44.436 | 44.522 |
| 3T | 38.470 | 39.290 | 3B | 25.450 | 25.290 | 6W | 22.360 | 22.360 |
| d | 0.200 | 0.350 | k | 0.550 | 0.710 | 7W | 33.727 | 33.496 |
| 4T | 25.800 | 25.650 | 4B | 25.950 | 25.140 | 8W | 22.360 | 22.360 |
| e | 0.790 | 0.500 | l | 0.050 | 0.860 | 9W | 33.660 | 33.273 |
| 5T | 25.210 | 25.500 | 5B | 20.530 | 21.100 | 10W | 22.360 | 22.360 |
| f | 0.550 | 0.210 | m | 0.470 | 0.150 | 11W | 29.986 | 30.600 |
| 6T | 20.450 | 21.040 | 6B | 20.530 | 20.530 | 12W | 22.360 | 22.360 |
| g | 0.050 | 0.330 | n | 0.470 | 0.470 | 13W | 30.322 | 30.133 |
| 7T | 20.950 | 20.670 | | | | 14W | 22.360 | |

Table 2.10 Geometry of Joist CZ02

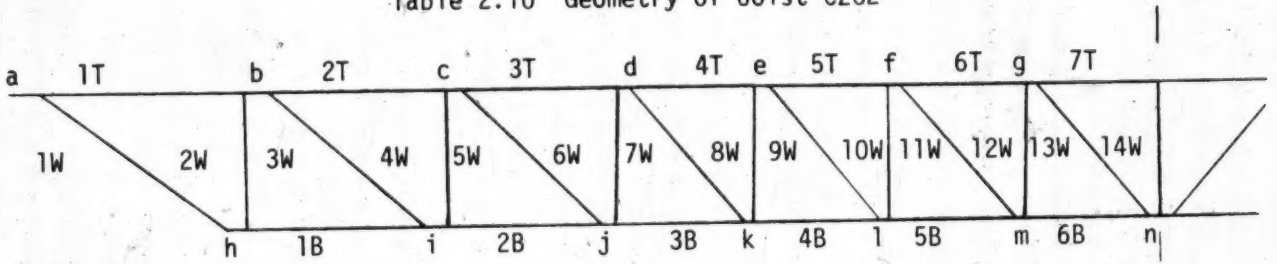


| MEMBER | NORTH | SOUTH | MEMBER | NORTH | SOUTH | MEMBER | NORTH | SOUTH |
|---|---|---|---|---|---|---|---|---|
| a | 1.500 | 1.500 | h | 0.360 | 0.610 | 1W | 53.761 | 54.197 |
| 1T | 49.250 | 48.980 | 1B | 44.560 | 45.000 | 2W | 22.360 | 22.360 |
| b | 0.880 | 0.670 | i | 1.440 | 1.000 | 3W | 49.784 | 50.007 |
| 2T | 45.920 | 45.430 | 2B | 39.150 | 38.910 | 4W | 22.360 | 22.360 |
| c | 0.150 | 0.250 | j | 0.850 | 1.090 | 5W | 44.955 | 44.790 |
| 3T | 39.850 | 38.900 | 3B | 25.490 | 25.310 | 6W | 22.360 | 22.360 |
| d | 1.250 | 1.100 | k | 0.760 | 0.690 | 7W | 33.720 | 33.697 |
| 4T | 25.210 | 24.900 | 4B | 25.900 | 24.910 | 8W | 22.360 | 22.360 |
| e | 0.820 | 1.100 | l | 0.100 | 1.090 | 9W | 34.050 | 33.399 |
| 5T | 25.180 | 25.176 | 5B | 20.870 | 20.750 | 10W | 22.360 | 22.360 |
| f | 1.100 | 0.890 | m | 0.130 | 0.250 | 11W | 30.518 | 30.443 |
| 6T | 20.500 | 20.610 | 6B | 19.930 | 19.930 | 12W | 22.360 | 22.360 |
| g | 0.830 | 0.780 | n | 1.070 | 1.070 | 13W | 29.867 | 29.767 |
| 7T | 19.870 | 20.010 | | | | 14W | 22.360 | |

Table 2.11 Material Property of Joists CX01, CX02 & CX03

| MEMBER | E | I | A | SKETCH |
|---|---|---|---|---|
| TOP CHORD | 29450 | 0.215 | 1.110 | |
| BOTTOM CHORD | 29800 | 0.184 | 0.922 | |
| END DIAGONALS | 29600 | 0.005 | 0.333 | |
| VERTICALS (CX01) | 29600 | 1.393 | 0.400 | |
| 3W, 4W, 6W | 29600 | 0.075 | 0.385 | |
| ALL OTHER WEBS | 29600 | 0.038 | 0.340 | |
| VERTICALS (CX02,3) | 29600 | 0.008 | 0.310 | |

Table 2.12 Material Property of Joists CX04, CX05 & CX06

| MEMBER | E | I | A | SKETCH |
|---|---|---|---|---|
| TOP CHORD | 29500 | 0.125 | 0.922 | |
| BOTTOM CHORD | 29600 | 0.160 | 0.803 | |
| END DIAGONALS | 29600 | 0.008 | 0.600 | |
| VERTICALS | 29600 | 0.017 | 0.130 | |
| 3W, 4W, 6W | 29600 | 0.049 | 0.288 | |
| ALL OTHER WEBS | 29600 | 0.017 | 0.130 | |

Table 2.13 Material Property of Joists CY01 & CY02

| MEMBER | E | I | A | SKETCH |
|---|---|---|---|---|
| TOP CHORD | 29700 | 0.202 | 1.104 | |
| BOTTOM CHORD | 29800 | 0.141 | 0.820 | |
| END DIAGONALS | 29600 | 0.031 | 0.483 | |
| VERTICALS | 29600 | 0.022 | 0.230 |  |
| 3W, 4W, 6W | 29600 | 0.104 | 0.420 | |
| ALL OTHER WEBS | 29600 | 0.048 | 0.280 | |

Table 2.14 Material Property of Joists CZ01 & CZ02

| MEMBER | E | I | A | SKETCH |
|---|---|---|---|---|
| TOP CHORD | 29600 | 1.180 | 1.880 | ⊓ |
| BOTTOM CHORD | 29600 | 1.020 | 1.620 | ⊔ |
| END DIAGONALS | 29600 | 0.180 | 1.360 | ⌐ |
| VERTICALS | 29600 | 0.084 | 0.531 | ▭ |
| 3W | 29600 | 0.088 | 0.600 | ⊓ |
| ALL OTHER WEBS | 29600 | 0.044 | 0.460 | ⊓ |

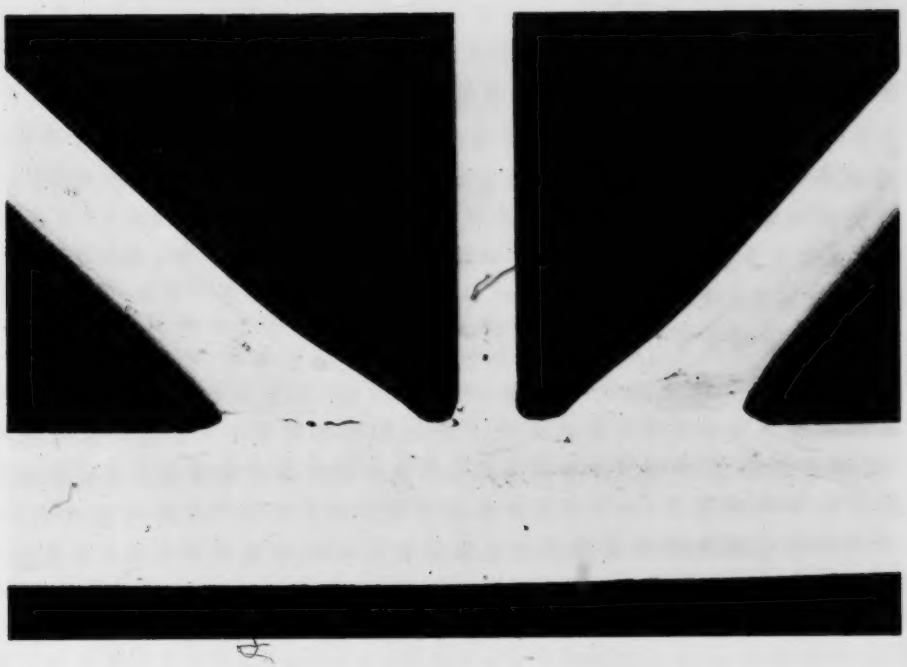

Figure 2.1 Type 'X' joint

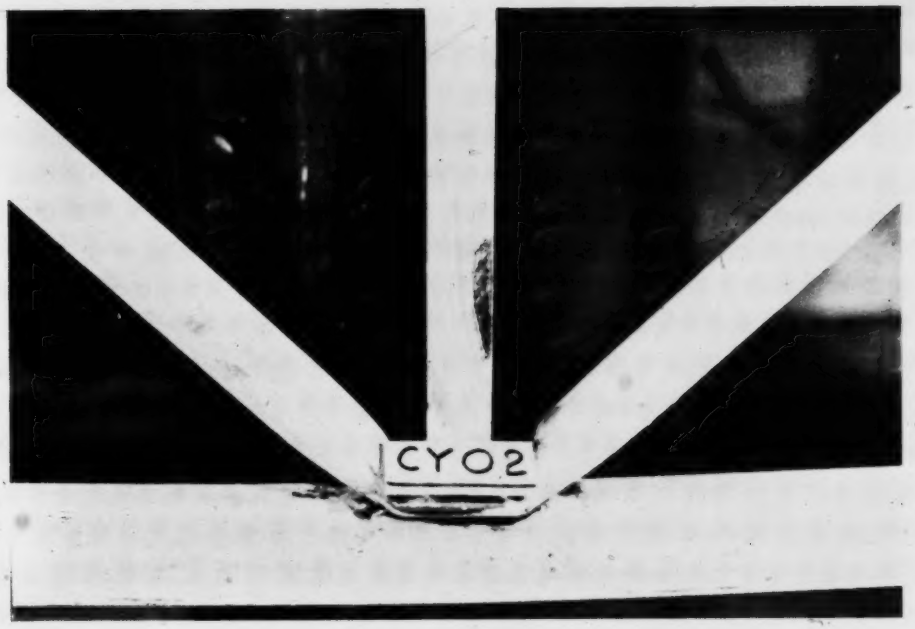


Figure 2.2 Type 'Y' joint

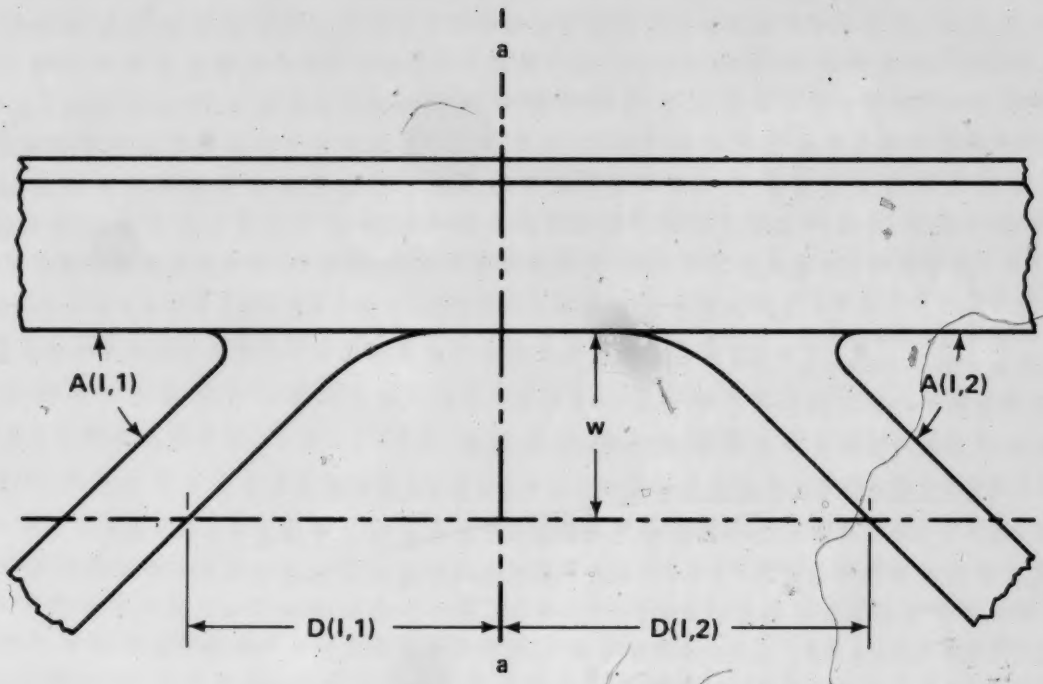


**Figure 2.3 Quantities measured at a Joint.**

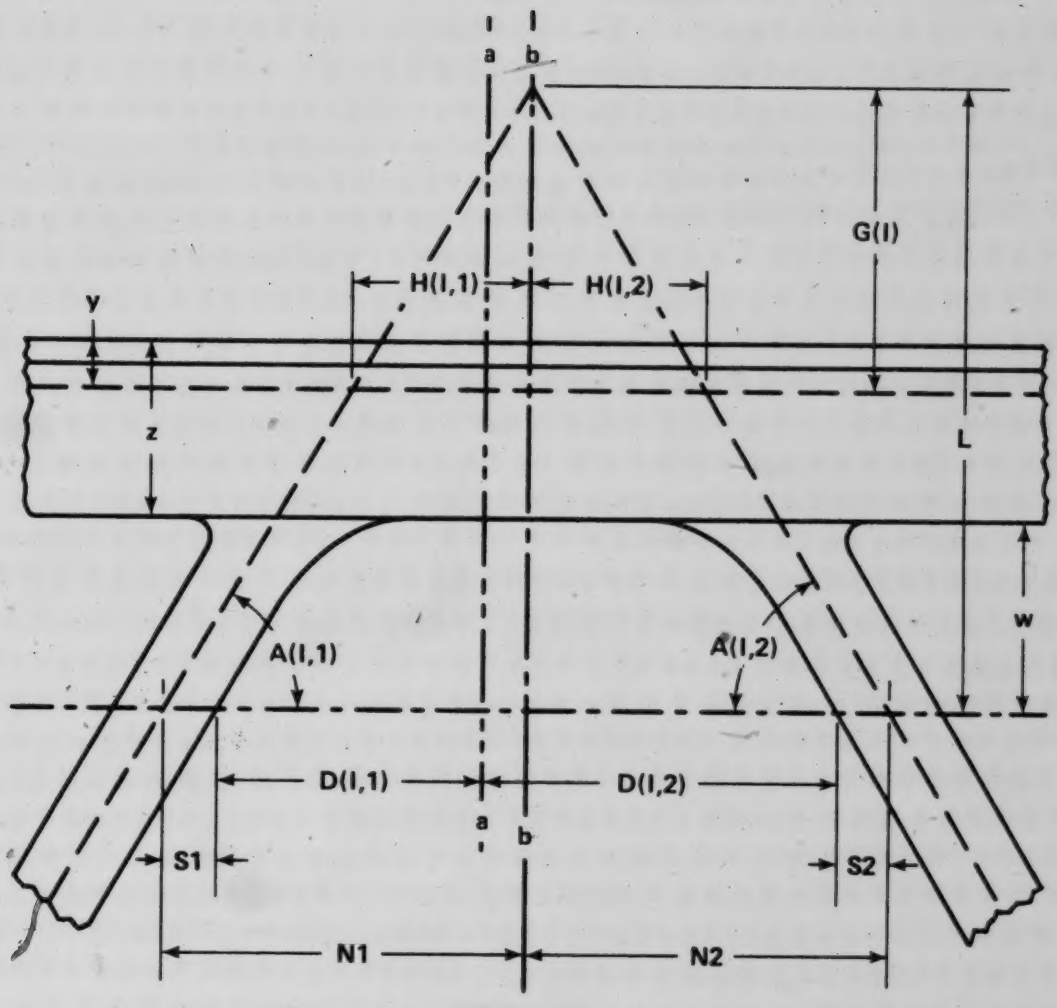


**Figure 2.4 Quantities computed at a joint.**

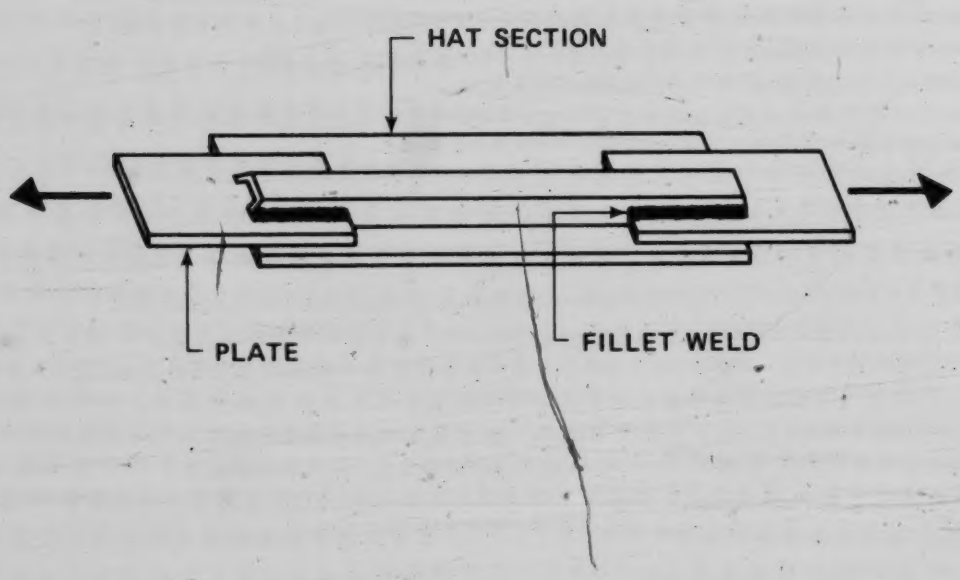


Figure 2.5 Plate grips on tension specimen

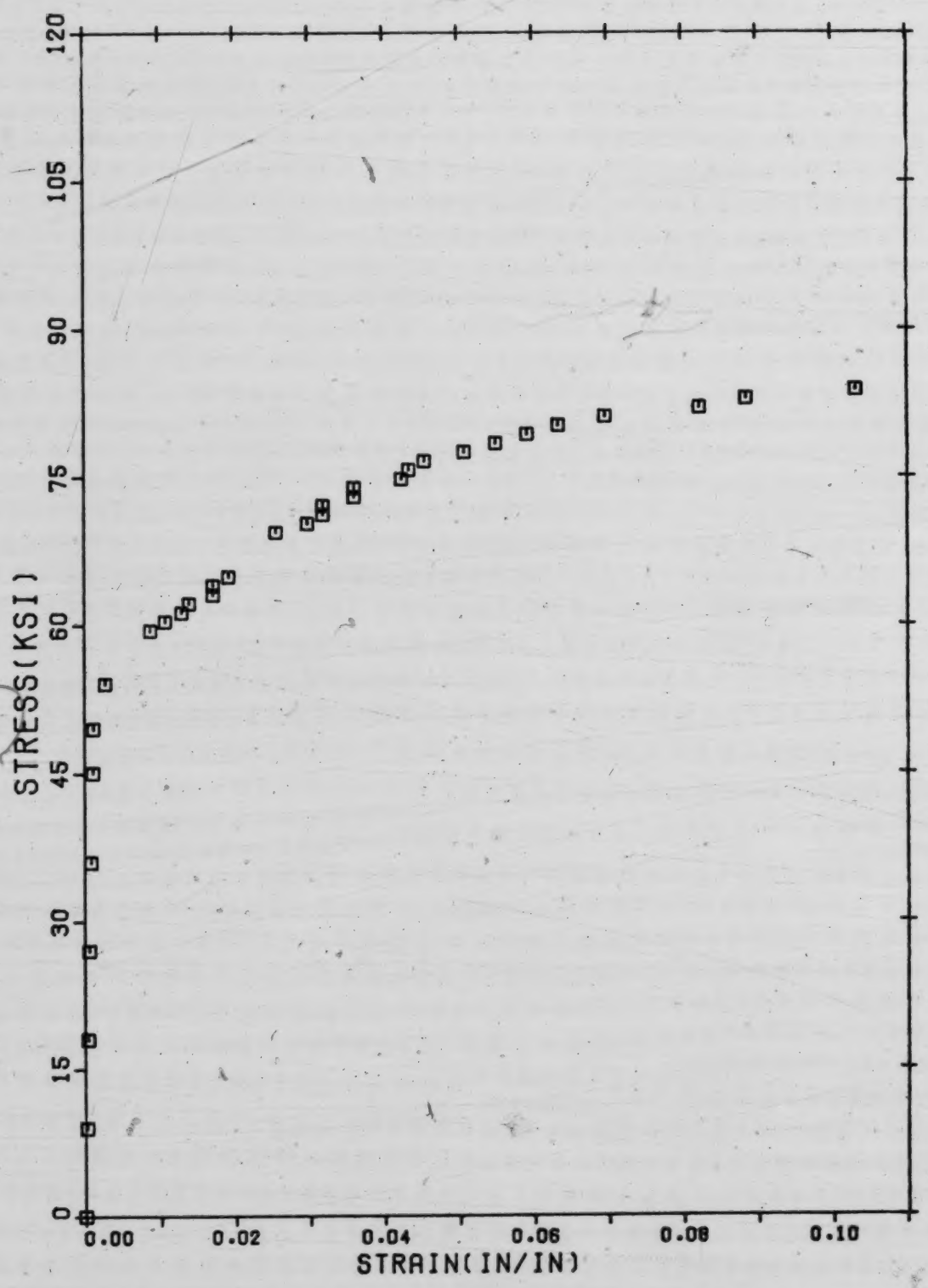


Figure 2.6 Stress-Strain Curve of Top Chord, joist CX01, CX02, CX03

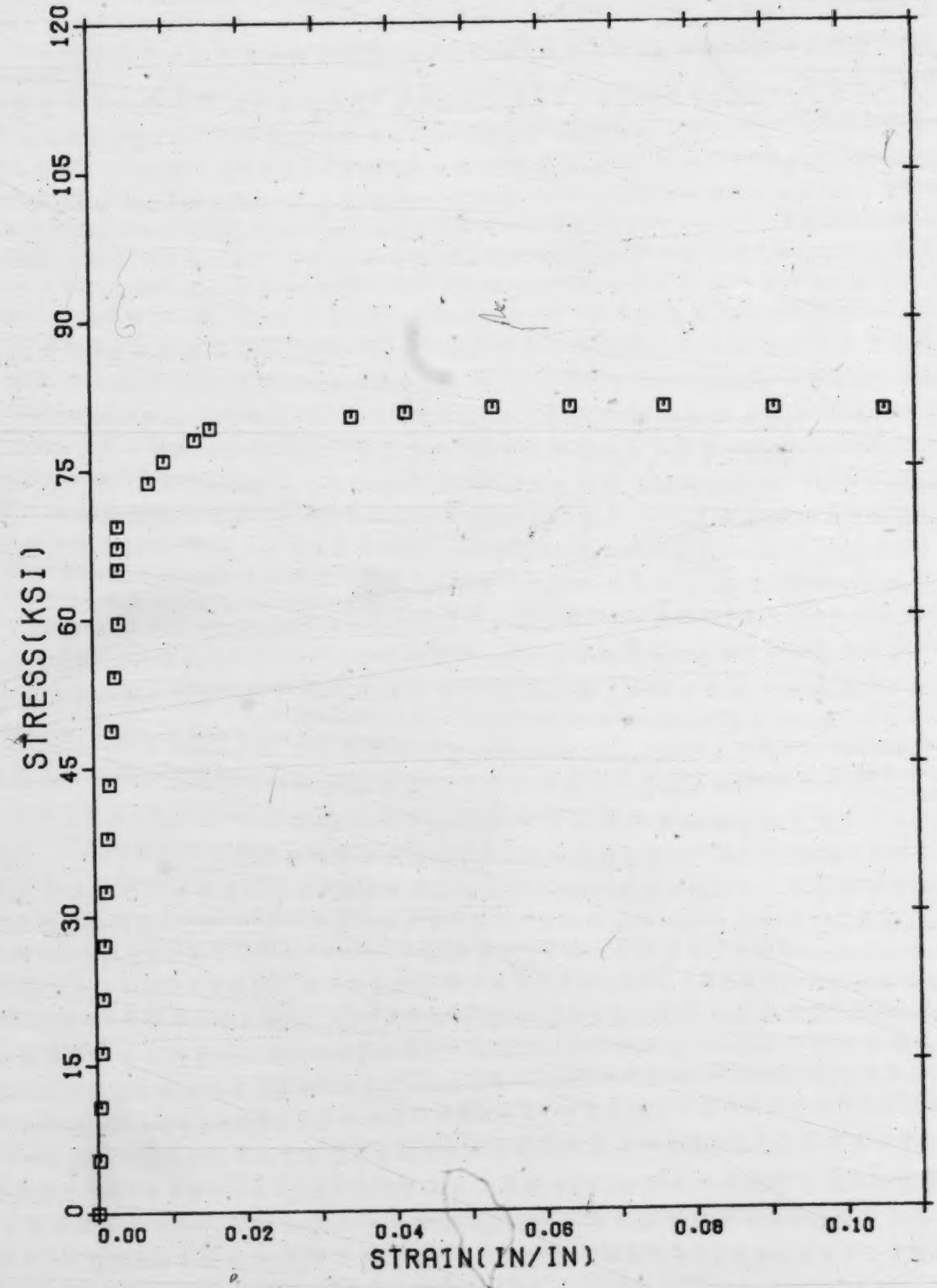


Figure 2.7 Stress-Strain Curve of Top Chord, joist CX04, CX05, CX06

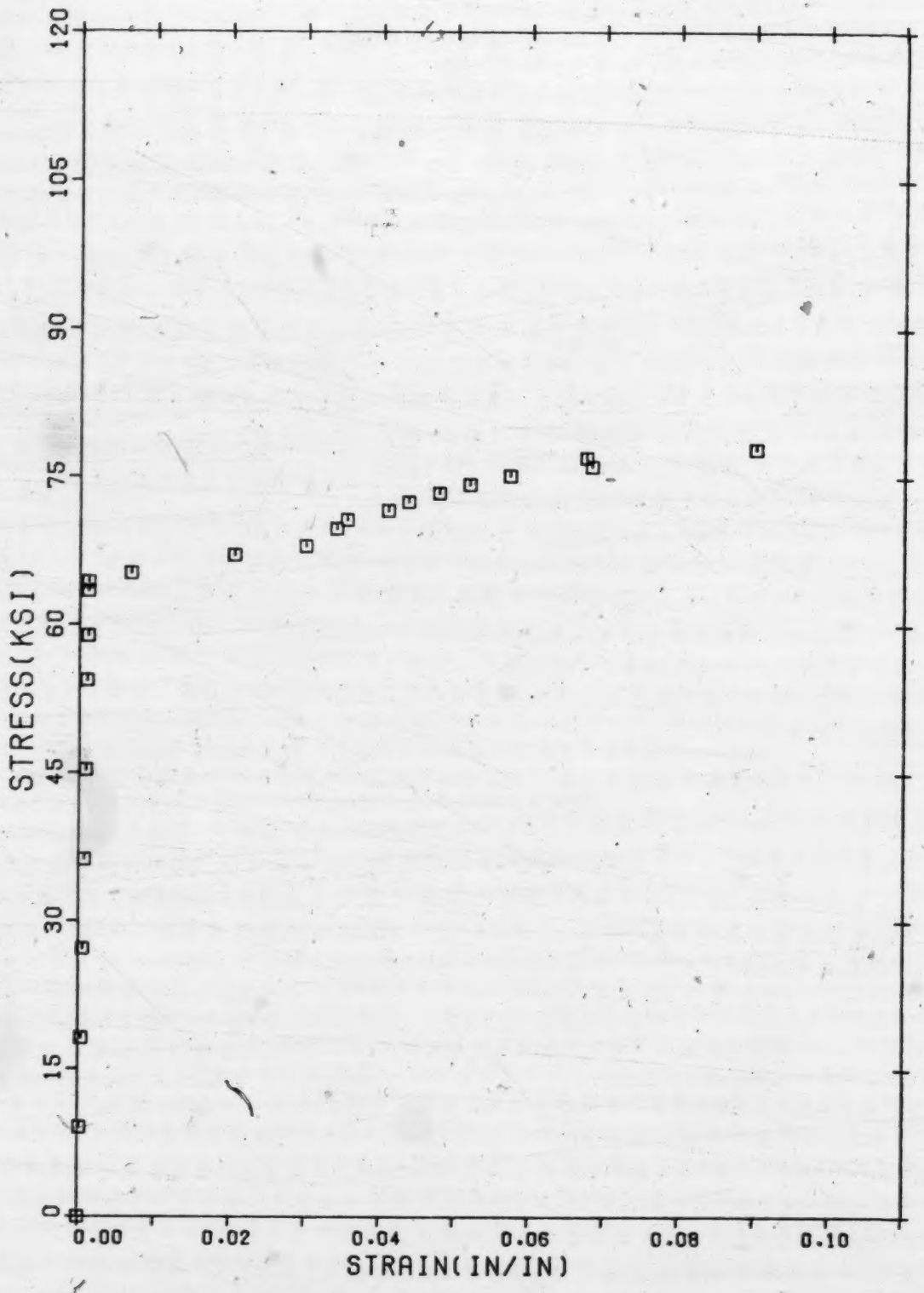


Figure 2.8 Stress-Strain Curve of Top Chord, joist CY01, CY02

# CHAPTER 3

# TEST FACILITY

## 3.1 Old Test Facility

The first series of joist tested by Matiisen (3) had a large depth to span ratio to accentuate the effect of joint eccentricity. The result was a much heavier design load for the type of chord used than would normally occur in practice. The joists were loaded with hydraulic jacks of ten ton capacity which were located under the floor of the test bed and transmitted the load through tension rods which passed through the test bed on either side of the joist. With this procedure the weight of the loading cradle, consisting of the top cross arm, rods, bottom cross arm and jack, was 156 pounds. Thus before any load was applied from the hydraulic jack to the joist this load was already acting at each panel point. While this surcharge was known and taken into account while reducing the data it amounted to approximately 10% of the total load applied to the joist.

An additional problem with this loading arrangement was that if the joists were completely unloaded during the test it was possible for the load cells to be misaligned and the yokes to become twisted. Thus a minimum of one-tenth of design load applied by the jacks was maintained on the unloading part of the curve. Also it was possible to load the joists at two feet intervals only, because of the spacing of the sleeves in the load bed, which restricts the geometry of the joists that would be tested.

For joists with smaller depth to span ratios the surcharge for the loading yokes would be a substantial amount of the capacity of the

joist. For the CX(1) series the working load is 315 pounds per linear foot, this surcharge would be approximately 25% of the working load. Assuming the capacity of the joist to be 1.7 times working load or 1071 pounds per panel point, the load applied by the jacks at failure would be 915 pounds, or less than 5% of their capacity. The problems associated with operating accurately the loading pattern with hydraulic jacks within 5% of their capacity are insurmountable especially when the differences in jack friction can vary by 1% to 2% of their capacity.

The strain and deflection data were recorded on a Digitec strain recorder which punched the readings on a paper tape. This process took approximately two minutes for a set of readings. This data could not be interpreted until after the test. It was also found that when the paper tape was taken to the computer centre for processing there would be characters which were misread due to slight misalignment of punching. Therefore the tape had to be further proof read and errors edited manually.

Thus the problems encountered with the old test facility required a new loading system for the joist tests of the second phase. The strain recording system was modified to take advantage of the acquisition of a Nova 2/10 minicomputer and associated data recording devices. This improved the accuracy and ease in monitoring the strains and deflections.

## 3.2 New Test Facility

The new loading arrangement permits up to twenty taskmaster pneumatic rams to be fed from a single manifold connected to a single pressure point. These jacks are suspended and react against a W10x21

beam which is located directly above the test joist and is supported by four columns (Figure 3.1). Hence there is no surcharge load from the loading arrangements. The jacks can be positioned at any spacing along the reaction beam. This arrangement removes the difficulties inherent in the old test facility.

To determine the load applied by the jacks during the test, an identical jack was pressured from the same manifold as those acting on the specimen and placed in a fixed frame as shown in Figure 3.2. The load exerted by this jack was measured by a load cell and the assumption that this load corresponded to the load exerted by each jack on the joist was made. This was later modified as discussed in Section 3.3.

Strain gauges were located on certain members and transducers were used to monitor deflections at alternate bottom panel points. The voltage impulse in the gauges, transducers and the load cell were measured by a digital voltmeter and the raw data fed to the Nova 2/10 minicomputer. This raw data was stored on disk files and simultaneously reduced to strains or deflections which could be simultaneously displayed on the control terminal. A dial gauge was also used to check the deflections at the centre line of the joist.

Lateral bracing of the top chord was provided so that the (KL/r) in-plane was greater than the (KL/r) out-of-plane to ensure in-plane buckling. This bracing was kept horizontal during the test by means of a screw thread arrangement. In some joists additional rods were used at the ends of the joist without the above freedom of vertical movement. Similar lateral bracing was provided at five points on the bottom chords.

## 3.3 Calibration of Jacks

Initially the jack and the load cell were calibrated against a proving ring in an arrangement which consisted of the jack, load cell and the proving ring in a fixed frame. The loading and unloading followed the same straight line on a plot of load cell load versus proving ring load.

It was concluded from the above that the friction in the jacks was negligible. When the data of the first joists was being processed it was suspected that friction may have played a role in the loading and unloading of the joists. This suspicion was confirmed when a load cell was placed to monitor the reaction at one end of the joist. There was a discrepancy between the load computed by monitoring the jack in the fixed frame and the end reaction, the variation being from 0% to 10%, the lower percentage being that for lower loads. This was further confirmed when both reactions were monitored by load cells.

A load cell was placed under a jack on the joist as shown in Figure 3.3 and a plot of load by the jack which moved and one where it did not move is shown in Figures 3.4 to 3.6. The friction is in one direction when the jacks are being loaded and in the opposite direction on the unloading part as seen by the horizontal part of the curve at maximum applied load. The curve for the loading zone follows nearly the same path no matter how many times it is loaded and is independent of the maximum load and rate of loading. This loading part can be approximated by a straight line from which the loads on the joist can be calculated by monitoring the load given by the load cell on the fixed frame. For the unloading portion of the curve this could not be generalized since for a different rate of loading and the maximum load attained a

new unloading path was generated.

## 3.4 Instrumentation

Most of the data generated by the joist tests was collected, recorded and partially processed automatically. The measuring devices (strain gauges, load cells, and linear displacement voltage transducers) were excited by a common six volt power supply and produced outputs in the range of $\pm$6 volts. These analog signals were converted to digital form by a digital voltmeter controlled by a program in the Nova.

An interactive Fortran program written for the Nova provided the capability to monitor load and midspan deflection during load application, and to request an output of a set of readings, which were further recorded on a 1.2 million word disk. The processing and recording of data at a particular level of load application was completed in five seconds.

The method of processing the voltages to give deflections, strains and loads is given in Appendix B.

After completion of the test the data was printed on a hard copy terminal, saved on a digital casette tape, and transmitted to the Amdahl 470 computer for further processing. This included the calculation of member forces and moments, and a linear regression analysis of the strain data in the elastic range to check the reliability of the gauges.

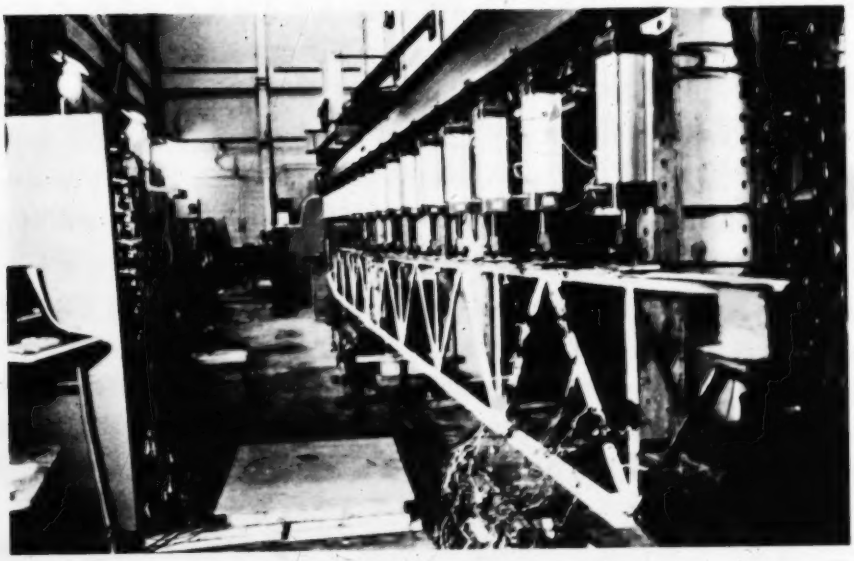

Figure 3.1 Joist specimen in loading frame

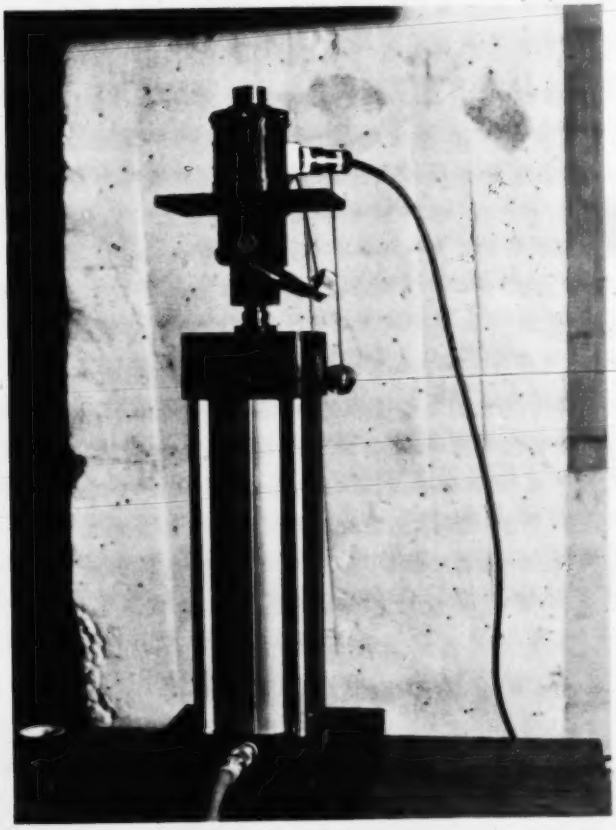

Figure 3.2 Pneumatic jack in fixed frame

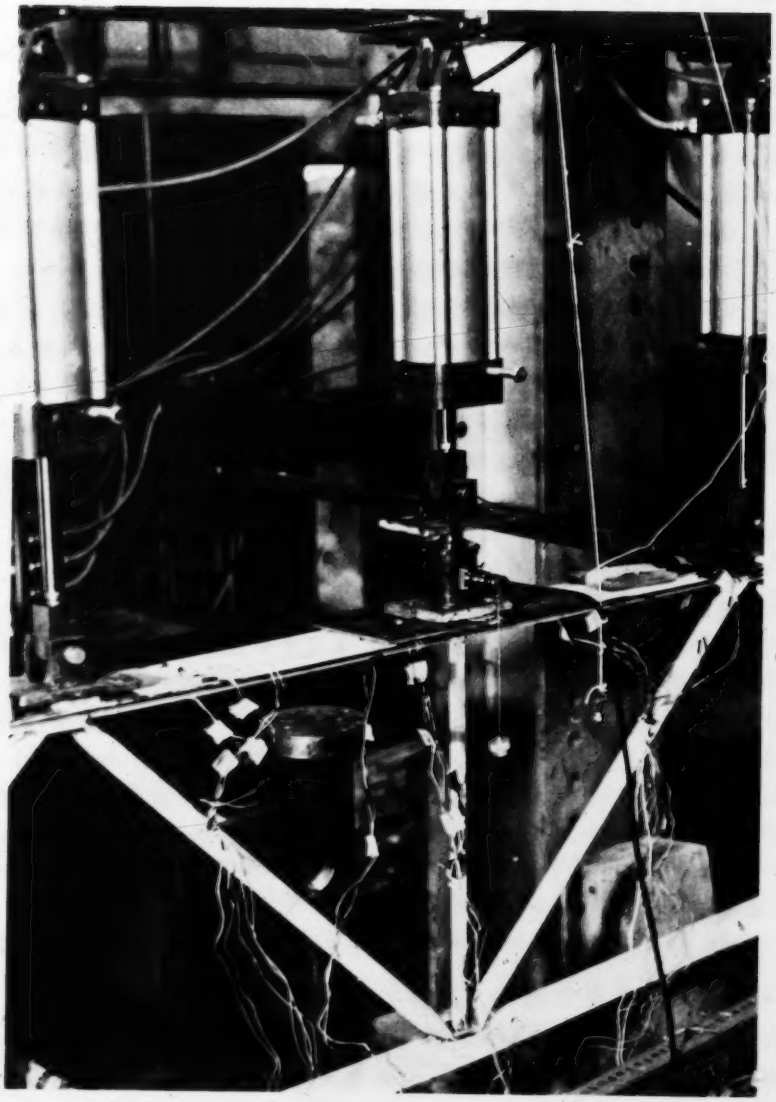

Figure 3.3 Calibration of jack

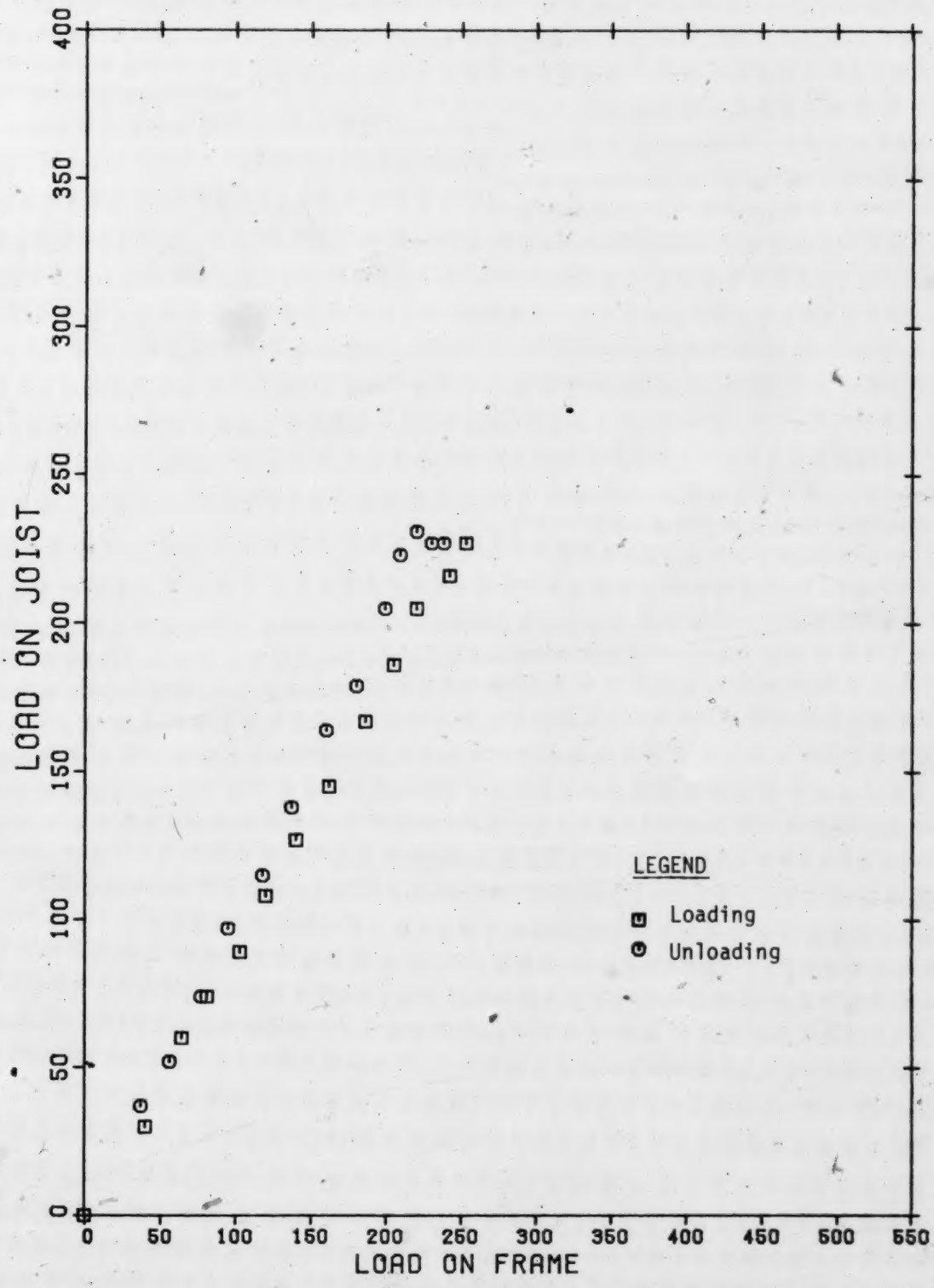


Figure 3.4 Load-Calibration Curve

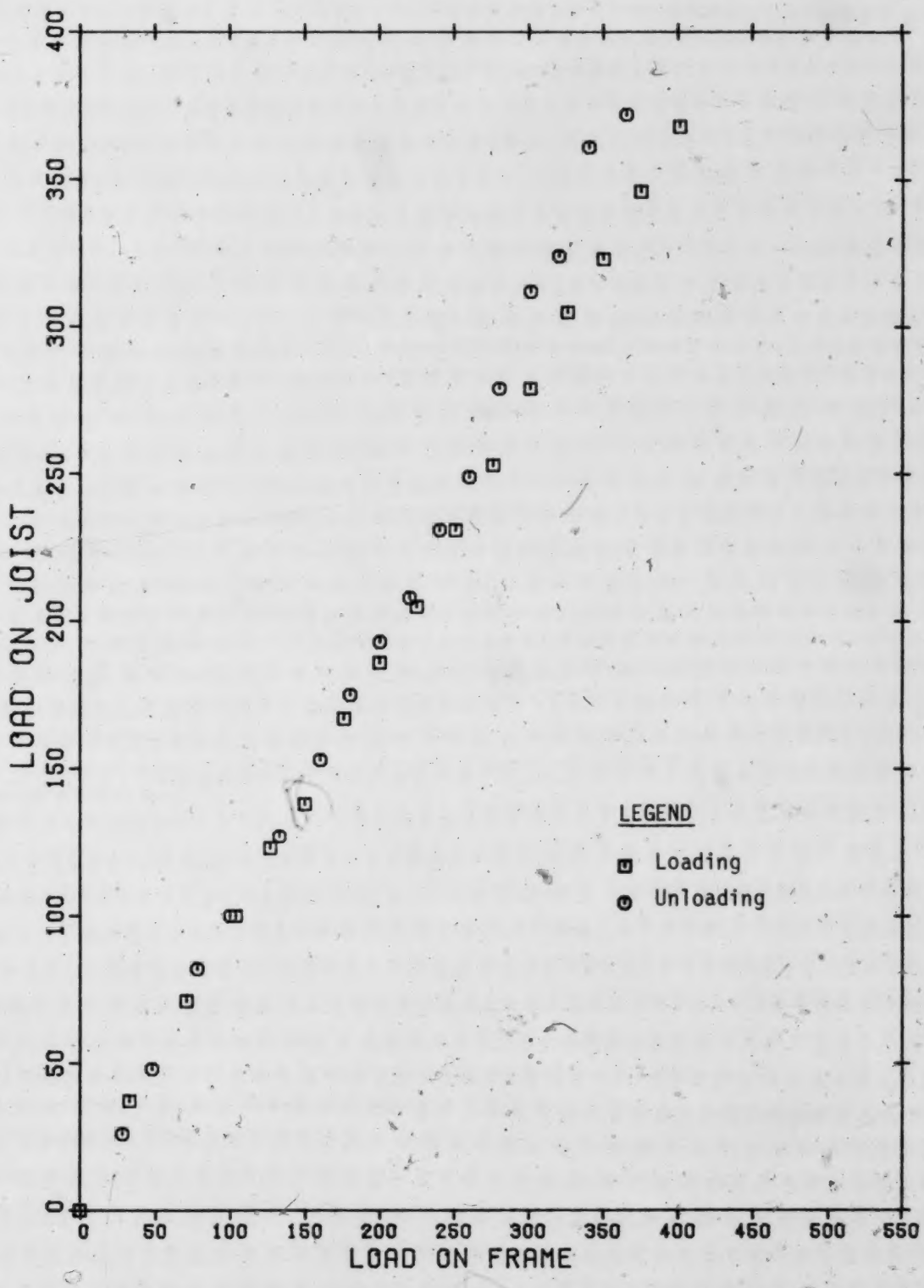


Figure 3.5 Load-Calibration Curve

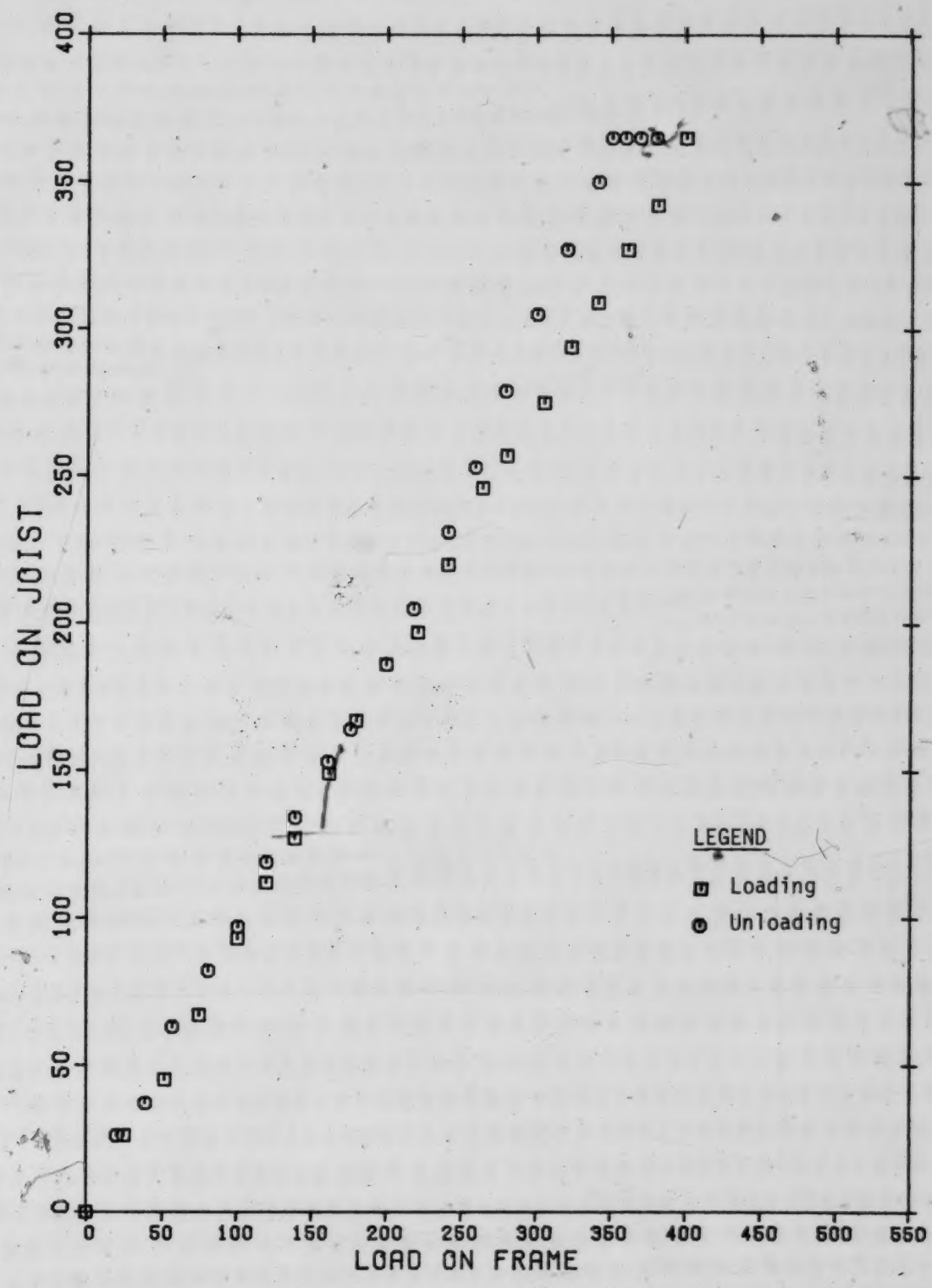


Figure 3.6 Load-Calibration Curve

# CHAPTER 4

# TEST PROCEDURE

## 4.1 Specimen Instrumentation

Gauges were located on selected members which were found to be critical in the pilot study. In general these members were adjacent to the joint at the end of the bottom chord in case a joint mechanism was formed at the end of a joist and in the top chord near mid-span of the joist where buckling was expected.

Due to the variation in joist configuration different members were gauged in different joist series and the actual members instrumented are given in Table 4.1.

Transducers were used to measure deflections at alternate panel points on the bottom chord. A dial gauge was used to check the deflection through the test at the centre line of the joist.

The joist was supported on a roller at one end and a hinge at the other. The joist was plumbed and laterally braced to ensure in-plane buckling.

The load from the jacks was transmitted onto the specimen through bearing plates 5" x 1-1/2" x 1/4" which were levelled by plaster of Paris.

A test run was made prior to the actual test. The specimen was loaded to approximately 0.7 times working load. The test run was used to check the gauges, seat the jacks and compare the test run results with those from the elastic frame analysis.

## 4.2 Initial Adjustements

The strain gauge outputs were initially balanced before each test at approximately zero volts and initial readings were taken.

The joist was loaded to ten pounds to seat the jacks on the specimen. This load was taken off prior to the acquisition of the first set of readings at zero load.

## 4.3 Loading

The joist was loaded at the panel points on the top chord by jacks fed from the central manifold. The joist was loaded to approximately 1.60 times working load in steps of approximately 60 pounds. The readings of strains, vertical deflection and applied load were taken at every increment.

The value 1.60 times working load was selected as the proof load as given by the CSA Standard S136 (2) Section 8.2.6(b). After final calibration of the jacks it was found that 1.60 times working load was never achieved but that only a value of 1.40 working load was achieved. The joist was then unloaded completely in steps of 100 pounds to obtain a residual midspan vertical deflection. Readings were taken at every decrement.

For joists with hot rolled top chords, loading was carried to failure. Initially this loading was in approximately 100 pound increments until significant inelastic behaviour was observed, after which the loads were regulated by increments of 0.5 inch midspan deflection. Readings of strains, loads and deflections were taken at every increment. While readings were being obtained the load was kept constant by means of a pressure regulator.

For joists with cold rolled top chords the joists were reloaded to failure except for joist CX05 which was loaded again to 1.60 times working load, unloaded and then reloaded to failure, for reasons given in Chapter 5.

## 4.4 Analysis of Test Data

The raw voltage readings recorded on the Nova 2/10 minicomputer were further processed to give stresses in the members on which strain gauges were located.

A program took the raw voltage readings subtracted them from the original voltages and converted them to strains and deflections. These were stored in different files containing applied loads and strains, and applied loads and deflections.

For each gauge a file relating applied load and strain was created. A linear regression analysis was run on the data and a correlation coefficient obtained. If the correlation coefficient was between 0.8 to 1.0, the gauge was accepted otherwise it was ignored.

Another two files were generated, one contains the geometry of a joist including material properties and the other contains the location of the strain gauges on the joist.

A second program, which derives input from the files of strain values, location of the gauges and the geometry of the joist, was used to compute bar forces, moments, and stresses at gauge locations and member joints.

For each increment of applied load the axial force and moments were obtained from the strain readings. Two consecutive loadings were extrapolated to give member moments and axial forces at working load.

The mean, standard deviation and the coefficient of variation were obtained at this load.

Table 4.1 Instrumented Members

| JOIST | MEMBERS INSTRUMENTED |
|---|---|
| CX01 | 8T(N), 9T(N), 1B(N), 1W(N), 3W(N) |
| CX02 | 8T(N), 9T(N), 1B(N), 1W(N), 3W(N) |
| CX03 | 8T(N), 9T(N), 1B(N), 1W(N), 3W(N) |
| CX04 | 9T(N), 10T(N), 10T(S), 2T(N), 3T(N), 1B(N), 5B(N), 1W(N), 3W(N), 4W(N) |
| CX05 | 9T(N), 10T(N), 10T(S), 2T(N), 3T(N), 1B(N), 5B(N), 1W(N), 3W(N), 4W(N) |
| CX06 | 9T(N), 10T(N), 10T(S), 3T(N), 1B(N), 1W(N), 3W(N), 4W(N) |
| CY01 | 2T(N), 3T(N), 8T(N), 9T(N), 9T(S), 1B(N), 1W(N), 3W(N), 4W(N) |
| CY02 | 2T(N), 3T(N), 8T(N), 9T(N), 9T(S), 1B(N), 1W(N), 3W(N), 4W(N) |
| CZ01 | 2T(N), 3T(N), 7T(S), 6T(S), 5T(S), 1B(N), 1W(N), 3W(N), 4W(N) |
| CZ02 | 2T(N), 3T(N), 7T(S), 6T(S), 5T(S), 1B(N), 1W(N), 3W(N), 4W(N) |

Note: (North) is abbreviated as (N)
(South) is abbreviated as (S)

# CHAPTER 5

# DISCUSSION OF RESULTS

## 5.1 Introduction

Each test joist was analysed using a frame analysis computer program. This program utilizes the elastic stiffness matrix procedure and is described by Matiisen (3). The joist geometry and material properties required as input were obtained by measurement in the laboratory. Output consists of the joint displacements and the axial forces, bending moments and shear forces at each end of the members. Joint eccentricity is modelled as the insertion of short chord members having a length of $e_2$ and properties of the chord.

Certain joint displacements and member forces were obtained empirically. A discussion of these values and a comparison with predicted values are contained in the following sections.

## 5.2 Deflections

### 5.2.1 Measured Deflections

The load-deflection plots for all test joists are given in Figure 5.1 to 5.10. In general each joist was loaded in increments to a load corresponding to 1.60 WL (1.60 times working load) and then unloaded in decrements to zero load. The joists were then reloaded in increments to failure. Due to problems associated with calibration of the jacks as described in Chapter 3, the actual load applied before unloading was less than proposed and some scatter in the unloading branch occurred. For clarity, only the loading portions of the load-deflection

curves are plotted.

Prior to final testing an initial test run to approximately 0.7 WL was made to check the gauges. The load-deflection response in all cases was linear and is not presented with the final test values. Since the load-deflection response was linear for all joists to loads greater than those applied during this initial loading it is concluded that these initial loadings to check the gauges did not influence the joist behaviour in the subsequent testing.

Joist CX01, CX02 and CX03 were initially loaded to 1.46 WL. For each joist the initial portion of the load-deflection plot is linear. This linear response applied to loads of 1.2 WL for joists CX01 and CX02 and to 1.0 WL for CX03, above which the deflection increased at a greater rate than the load. On reloading, the load-deflection response was linear in all three joists up to the point of previous unloading and this slope was parallel to the initial slope. For greater loads the curve is an extension of the curve obtained prior to unloading.

Joists CX04, CX05 and CX06 were loaded to a value of 1.42 WL, 1.39 WL and 1.41 WL, respectively, before unloading. The behaviour of these joists was similar to the previous set of joists and the initial response was linear to loads corresponding to 1.2 WL for all joists.

The chords for joists CX04, CX05 and CX06 consisted of hat sections formed by cold rolling of steel plate. In CSA Standard S136(2), for light gauge steel structural members, there is a provision in Section 8.2.5 which stipulates that as a measure of quality control the second application of the proof load of 1.60 WL shall not increase the residual deflection caused by the first application of this load by more than 3%, and the deflection recovery, upon removal of the second

application of the proof load, shall be at least 90% of the total deflection. Joist CX05 was tested according to these provisions. The joist was found to be satisfactory, in fact, the residual deflection between successive loadings was negligible and after the second application of the proof load the recovery was 92%.

For joist CX05, when loading was resumed to failure it was observed that the joist was failing by lateral buckling at a load corresponding to 1.66 WL. The joist was then unloaded and the lateral bracing reinforced. Load was then applied until the top chord buckled in the plane of the joist at 1.72 WL. A discussion of chord buckling is given in Section 5.5. The load-deflection response for this last loading to failure is given in Figure 5.5 as plus signs. It should be noted that the deflection gauges were reset to zero and are so plotted. It should also be noted that the slope of the curve is linear to the previous maximum load.

Joists CZ01 and CZ02 were loaded initially to the same load as the previous joists. Due to an initial misunderstanding that the design load for these joists was 446 pounds per linear foot rather than the nominal 300 pounds per linear foot for the other joists, this amounted to 1.10 WL. The behaviour was similar to the other joists and the initial response was linear to 0.73 WL.

For joists CZ01 the air pressure in the compressor was not sufficient to fail the joist. The maximum load that could be applied corresponded to 1.30 WL. An air pressure bottle which permitted the use of higher air pressures was fitted to the jack manifold and the joist reloaded to failure at a load of 1.55 WL. The path of this loading was linear up to 1.30 WL which corresponds to the previous load value.

### 5.2.2 Comparison of Measured and Calculated Deflections

A method of computing deflections for open web steel joists is contained in Section 16.5.14.2 of CSA Standard S16.1(1). This method computes the deflection of the joist as a simply supported beam having a moment of inertia obtained by considering only the effects of the two chords. This deflection is increased by 10% to account for axial deformations in the web members. No allowance is made for effects of joint eccentricity. This method was used in addition to the elastic frame analysis to predict the mid-span deflection of each test joist.

The elastic frame analysis gives an excellent prediction of joist deflection in the initial linear range. Also for all subsequent loadings the joist behaved elastically in the initial range.

For joist CX01 the deflection given by the CSA method and the actual deflection coincide exactly. For CX02 and CX03 the deflection calculated by the frame analysis are 4.0% and 5% greater than the CSA method, which reflects the effects of joint eccentricity.

For CX04, CX05 and CX06, the deflection calculated by the frame analysis are 3.5%, 4.0% and 6.0%, respectively, greater than that given by the CSA method. For joists CY01 and CY02 the frame analysis gives deflection 4% and 7% greater than by the CSA method. For joists CZ01 and CZ02 the frame analysis predicts the behaviour to be 2% and 4% greater, respectively.

From the above plots it can be generalized that the slope of the initial load-deflection response decreases as the eccentricity of the joist increases in otherwise similar joists. This decrease in slopes is very small and, in the range of eccentricities used in practice, can be neglected. In the case of the CY series the decrease in slope

is negligible because each had, approximately, the same value of eccentricity, the CY01 had a negative eccentricity ($e_2$) of 0.30 while CY02 had a positive eccentricity of 0.50.

## 5.3 Axial Force

The axial force is computed from strain measurements obtained at specific locations on the joist as described in Chapter 4. The increment of axial force is computed for each increment of loading and then extrapolated to give the axial force at design load. The mean and coefficient of variation of these extrapolated values is given in Tables 5.1 to 5.9.

The axial force is also obtained for an elastic frame analysis design load. A comparison of the measured and calculated axial force is also tabulated in Tables 5.1 to 5.9. For the top and bottom chords the end i is the North end of the member, while for the webs, end i is the end framing into the top chord.

The difference in measured axial forces at the two ends of a given member is within 2%. The difference in measured and calculated axial force, for axial force above 20,000 pounds, is generally around 4% but not greater than 7%, the measured axial force being higher in most cases.

The numerical difference in the measured and calculated axial force, for axial forces less than 20,000 is very small numerically, but as a percentage is generally around 7% but not greater than 11% depending upon the magnitude of the force.

The elastic frame analysis is found to predict the axial force in a member accurately. The numerical difference between the predicted

and measured values is attributed to the difficulty in determining the applied load precisely.

## 5.4 Bending Moment

The bending moments are computed from strains obtained at the instrumented locations. The increment of bending moments was computed for each increment of loading and then extrapolated to give the bending moment at working load. The mean of these extrapolated values was then obtained. Since the strain gauges were located at a distance of six inches from the ends of a member the value of the moment at the gauge location was linearly extrapolated to the end of the member to facilitate comparisons with predicted values.

The bending moment was also obtained for an elastic frame analysis at design load. A comparison of the measured and calculated bending moment as a ratio of the yield moment for the particular member is given in Tables 5.1 to 5.9.

The moments, both measured and calculated are small. Although the comparison between these moments appears at first glance to be poor there is a definite correlation between them in that the moments have the same direction and when the calculated moment is larger the measured moment followed the same tendency.

The measured moments are sensitive to the value of the strain in that a small error in strains will result in a larger error in the computed moments. These errors will be exaggerated when the moments are extrapolated to give the moments at the ends of the member.

The elastic frame analysis is found to predict the tendency and the value of the bending moments at the measured ends. The agree-

ment is better as the magnitude of the moments is increased. Due to the sensitivity of the measured moments to small errors in measured values of strains it is concluded that the computed moments from the frame analysis are more reliable than the measured moments.

## 5.5 Inelastic Behaviour and Failure Mode

An examination of those joists in the pilot study that had failed by buckling of the top chord hat sections indicated that, in the region of the buckle, there was a significant flattening of the cross section. Since no measurements of distortion of the cross section were made during the testing it was not possible to determine whether any of this distortion had taken place prior to the buckling of the chord and so had influenced the location where buckling occurred. To investigate this possibility sets of Demic points were glued to the outer flanges of the top chord in the panels near midspan. Each set was located on a line perpendicular to the axis of the joist with one point on each side flange of the hat section at an initial spacing of two inches, such that a change in this spacing as measured by a Demic gauge would give a qualitative measure of the amount of distortion of the hat section as the joist is loaded.

To facilitate visual observation of inelastic behaviour due to localized yielding of the material, each joist was given a coat of white wash immediately prior to loading.

There was a considerable difference in the behaviour of the joists when loaded beyond the elastic range and in the mode of failure. For this reason these two items are discussed separately for each joist. For convenience a summary of the failure load and mode of failure for

each joist is given in Table 5.10.

A phenomena was observed with the CX(1) series of joists that was not duplicated with the other series. Shortly after the application of the load equal to 1.2 WL, a localized flaking of the white wash along the sides of the top and bottom chords about midheight and in the region of the joints was observed. This flaking is shown in Figure 5.14 and although the flaking increased in intensity it did not appear to increase in extent as further load was applied. This flaking was attributed to local yielding of the chord in the web of the hat section in this region.

The hat section used in the chords of the CX(1) series is a hot rolled section such that the web portion is approximately 60% of the thickness of the flanges. It would appear that the joint detail is such that when the forces are applied through welding to the centre portion of the inner flange there is a tendency to deform the cross section. Since the web portions are thinner and unreinforced local yielding takes place in the web. This local yielding was observed for all three joists in the CX(1) series although there was variation from small to large joint eccentricities. Since there did not appear to be a visibly distinguishable difference in this local yielding with an increase in joint eccentricity, it is concluded that this phenomena is due primarily to the type of joint connection and chord section rather than due to joint eccentricity.

This is further demonstrated by the fact that this local yielding was not observed in the CX(2) series even though these joists had significant joint eccentricities. In this case, although the joint details are the same as for series CX(1), the chord hat section is

formed by cold rolling of steel plate, hence, the web and flange thicknesses are equal. Thus the distortion is not emphasized in the web. On the other hand with the CY series the chord hat section was similar to the section for the CX(1) series, but because the web is bent such that it spans across the inner flanges of the chord and the welding further stiffens the section, no flaking of the white wash on the side of the hat section as described for the CX(1) series was observed.

That the cross section of the CX(1) series deformed more that with the other joist series was confirmed by the Demic gauge readings. If there were no deformation of the cross section the measured lateral increase in the distance between the outer flanges of the compressive chord could be computed due to the Poisson's Ratio effect. The measured lateral movement at midspan for several panels near midspan for joists CX01 and CX02 are given in Figures 5.23 to 5.31. It can be seen that the lateral movement is generally in excess of 100 times that attributable to Poisson's Ratio and in member 9T(South) for joist CX02 is 320 times larger. This is contrasted with measured lateral displacements for the CX(2) series which were generally less than 12 times larger and for the CY series which were only two times larger than those computed from the Poisson's Ratio effect.

From an examination of Figure 5.23 to 5.25 there seems little doubt that the location of the top chord failure for joist CX01 was influenced by the distortion of the cross section. This joist failed by in-plane buckling of the top chord in panel 8T(North), Figure 5.11. This panel is not the panel with the maximum axial force but, being adjacent to the midspan panel, has an axial force that is approximately 95% of the maximum value. Unfortunately there were no Demic points at

the middle of this panel but there were on the three panels located immediately south. From the distortions of these panels a failure pattern is postulated.

The lateral bracing was welded to the top chord to one side only so as not to act as a stiffner across the two sides of the outer flange of the chord. The load from the jacks were applied to the top chord at the panel points through one inch flats that spanned across the top flange and which were set in plaster of Paris to provide an even bearing. As load was applied there is a tendency for the section to open, that is a spreading of the two halves of the outer flange. The load plates provide some restraint so that this spreading is more pronounced in alternate panels. Immediately prior to failure by buckling there was a distinct tendency for members 8T(South) and 9T(North) to suddenly reverse and for the section to close whereas the panel between had a rapid increase in the amount of opening. This tendency was so pronounced that member 9T(north) actually closed by approximately 0.08 inch from the unloaded position. From this wave motion it is certain that the adjacent panel, member 8T(North) must have opened at least as much as member 9T(South) and may have flattened even more resulting in a reduction of the moment of inertia such that buckling occurred in this panel. Again it is emphasized that this involved a certain amount of extrapolation of observation since member 8T(North) was not instrumented.

To verify this conclusion, Demic points were placed at the middle of all six top chord members near midspan of joist CX02. The results of these readings are presented in Figure 5.26 to 5.31. Again the tendency for the top chord to open is clearly observable

with the opening much more pronounced in alternate panels. It is noted that for none of these members was there observed the rapid reversal or increase in the transverse measurement across the chord although the spread in member 9T(South), Figure 5.29 is very large. This joist did not fail by top chord buckling which could likely be inferred from the absence of sudden rapid distortion of the chord. It could be speculated that from the Demic readings, had failure not occurred in the compression diagonal but due to in-plane buckling of the top chord, that this buckling would have occurred in member 9T(South).

Joist CX04 failed by lateral buckling of the top chord. The lateral bracing system used for this joist corresponded to that used for the CX(1) series. Using K = 0.9 for in-plane calculations at k = 1.0 for out-of-plane calculations this gave an effective slenderness ratio, (KL/r), for in-plane buckling of 50 and for out-of-plane buckling of 43. However for the cold-formed chords of the CX(2) series this bracing spacing resulted in values of 48 and 52, respectively. This might have been sufficient to prevent out-of-plane buckling except that one of the braces at midspan was not properly welded to the top chord. Hence the effective length for out-of-plane buckling was much greater than for in-plane buckling, which resulted in the observed failure mode.

To prevent such failures in joists CX05 and CX06 the lateral bracing spacing was altered to give effective slenderness ratios for in-plane and out-of-plane buckling of 48 and 38, respectively. Joist CX05 failed by in-plane buckling of the top chord in panel 9T(North) and CX06 by buckling of the end compression diagonal, member 3W(South) Figure 5.15.

Both joists in the CY series behaved in a similar manner. A certain amount of localized yielding around the joint between the top chord and vertical was observed at loads of 1.3 WL. Since the overall stresses were substantially below the yield point and there seemed to be a large amount of weld material in this region, this inelastic behaviour may be due to residual stresses from the welding.

Both CY01 and CY02 failed by a general yielding of the bottom chord in the panels adjacent to midspan. Yielding began near the joints as shown in Figure 5.17 and 5.18 and proceeded across the panel until yielding was general as shown in Figure 5.19. This yielding of the bottom chord resulted in large midspan deflections and the test was stopped when the midspan deflection approached eleven inches, the limit of travel for the jacks.

The chords of the CZ series of joists consisted of two angles separated by a clear space of two inches. These two angles were connected by the vertical members which were a 2 x 1 inch tube. In addition flat spacers were welded across the square at approximately twelve inch centres as shown in Figure 5.20.

Beginning with loads as low as 0.5 WL localized yielding of the chords in the region of spacers was observed. The extent of yielding at working load is shown in Figure 5.20. It was also observed, but not measured, that there was a tendency of the two chords to move relative to one another in the direction along the axis of the joist.

Joist CZ02 having the larger joint eccentricities was tested first. Since the chords were different a different lateral bracing pattern was used. Using the same number of braces as used for the CX(1) and CY series resulted in effective slenderness ratios of the

top chord using K=0.9 for in-plane bending and K=1.0 for out-of-plane bending of 24 and 29 respectively. Joist CZ02 failed by lateral buckling of the top chord at a load of only 1.26 WL.

For loads just above the working load there was a slight bowing or sweep observed in the joist. This seemed to correspond with the different longitudinal shortening of the two angles of the chord.

To prevent a similar failure for joist CZ01 which had essentially zero joist eccentricity the lateral bracing was doubled such that the effective slenderness ratio out-of-plane was only 60% of in-plane effective slenderness ratio. Again for loads just above the design working load there was a noticeable difference in the shortening of the two angles of the top chord and the force in the lateral bracing as judged by hand vibrating them was significantly larger than for comparable loads for joists in the other series. As the load increased a noticeable sweep, inspite of the bracing, developed and the yielding in the vicinity of the spacers increased. At a load of 1.55 WL yielding of the middle panel of the bottom chord began which resulted in the sharp increase in the load-deflection plot, Figure 5.9. Simultaneous to this yielding there was a definite out-of-plane bowing of the top chord at midspan between the braces which increased as the joist deflected, the load remaining essentially constant. Failure occurred by this bowing increasing to form a sharp lateral buckle between the braces.

The phenomena of differential shortening or differential longitudinal movement between the two angles of the top chord was observed for both joists CZ01 and CZ02. No explanation of this observation is given. Since it appeared in joist CZ01 which has as close to

zero eccentricity as could be fabiracted it would not appear to be the result of joint eccentricity.

Since the joists of the CZ series differed in many respects from the joists in the other series and since the behaviour and failure mode appeared to be influenced to a great extent by the differential longitudinal movement of the angles of the top chord resulting in a out-of-plane sweep of the chord for which no explanation could be found, these joists are not discussed further.

## 5.6 Prediction of Ultimate Capacity

The behaviour of an open web steel joist up to working load can be predicted from an elastic frame analysis. An attempt to predict the failure load was made by examining the different modes of failure.

A joist can fail by excessive deflection caused by yielding of the bottom chord. This type of failure occurred for the joists in the CY series. The failure load for this type of failure can be predicted by computing the load corresponding to the axial force in the bottom chord from a simple truss analysis that is equal to the chord area times the yield stress. For the joists in the CY series this procedure predicted the failure load to within 2% which is within the accuracy of being able to determine the applied load. With the exception of joist CX04 which failed by lateral buckling all joists in the CX series failed by either in-plane buckling of the top chord or out-of-plane buckling of the end compression member. To predict which type would occur first resulted in attempts to predict the buckling loads.

Joists CX05 and CX06 were identical except that joist CX06 had

larger joint eccentricities which induced much larger end moments in the end compression diagonal. Joist CX06 failed by buckling of this diagonal whereas joist CX05 failed by buckling of the top chord at midspan. On the other hand joists CX02 and CX03 were identical except for joint eccentricity but it was joist CX02 with the smaller joint eccentricity and end moments that buckled in the web diagonal. An examination of axial forces and plastic moment capacities at the ends of the members did not appear to explain why the different buckling locations occurred.

To predict the buckling load of the top chord the computer program described by Srivastava (9) was used. This program assumes that normal sections remain plane and that the material response can be represented by a tri-linear relationship. By integrating the curvatures corresponding to the moments required for equilibrium from a given initial displacement the axial load at which the lateral displacement becomes unbounded is obtained. The results of these analyses are shown in Figures 5.32 to 5.34.

The plotted points are the predicted load-deflection curves from the top chord panels adjacent to midspan. The horizontal lines are the axial forces measured in these members at the time of failure. For those joists which failed by in-plane buckling of the top chord these lines are shown as solid lines whereas for those joists that failed by other modes are shown as dotted lines.

The program overestimates the buckling load of the top chord in all cases. It must be remembered that this is expected for those joists shown as dashed lines since presumably the buckling load of the top load had not been reached prior to failure by some other means. For those joists that did fail by buckling of the top chord the best agree-

ment is with joist CX05 which did not buckle in the panel predicted but in the panel adjacent.

Since the program did not take into account local distortions of the cross-section, initial out-of-straightness of the chord, residual stresses and variations from true panel point loading, all items which would tend to reduce the buckling load it is not too surprising that the program overestimates the buckling load but unfortunately not by a consistent amount. From the attempts made in this study no procedure was found that would reliably predict the buckling load of compression members in a joist.

Table 5.1 Comparison of Stresses in Joist CX01,
Load 315 Pounds Per Linear Foot

| Member | Calc. Axial Force | Meas. Axial Force at End I | | Meas. Axial Force at End J | | Calc. Mi/My | Meas. Mi/My | Calc. Mj/My | Meas. Mj/My |
|---|---|---|---|---|---|---|---|---|---|
| | | Mean | Cov | Mean | Cov | | | | |
| 8T | 28626 | 30362 | 8.0 | 29715 | 7.6 | -0.011 | -0.029 | | |
| 9T | 30052 | 31166 | 7.4 | 31552 | 7.3 | | | 0.011 | 0.027 |
| 1B | -13695 | -11959 | 9.8 | -14104 | 7.3 | -0.011 | -0.110 | | |
| 1W | -10693 | -10172 | 7.9 | -10274 | 9.9 | -0.330 | -0.367 | -0.150 | -0.400 |
| 3W | 7453 | 6954 | 8.9 | 7675 | 6.8 | | | -0.14 | -0.497 |

Note: A positive Axial Force signifies compression.
Anticlockwise Moment is positive.

Table 5.2 Comparison of Stresses in Joist CX02, Load 315 Pounds Per Linear Foot

| Member | Calc. Axial Force | Meas. Axial Force at End I | | Meas. Axial Force at End J | | Calc. Mi/My | Meas. Mi/My | Calc. Mj/My | Meas. Mj/My |
|---|---|---|---|---|---|---|---|---|---|
| | | Mean | Cov | Mean | Cov | | | | |
| 8T | 28249 | 29468 | 3.5 | 28638 | 2.8 | -0.016 | -0.025 | | |
| 9T | 29573 | | | 30612 | 2.3 | | | | |
| 1B | -13709 | -17417 | 3.2 | -16750 | 4.6 | -0.036 | -0.089 | 0.025 | 0.149 |
| 1W | -10459 | - 9830 | 3.0 | -10022 | 3.0 | -0.300 | -0.196 | -0.125 | -0.399 |
| 3W | 7036 | 7581 | 3.5 | 7414 | 5.4 | -0.370 | -0.560 | -0.110 | -0.082 |

Note: A positive Axial Force signifies compression.
Anticlockwise Moment is positive.

Table 5.3 Comparison of Stresses in Joist CX03,
Load 315 Pounds Per Linear Foot

| Member | Calc. Axial Force | Meas. Axial Force at End I | | Meas. Axial Force at End J | | Calc. Mi/My | Meas. Mi/My | Calc. Mj/My | Meas. Mj/My |
|---|---|---|---|---|---|---|---|---|---|
| | | Mean | Cov | Mean | Cov | | | | |
| 8T | 28066 | 28122 | 2.2 | 27805 | 6.8 | | | | |
| 9T | 29638 | | | 29220 | 3.3 | | | 0.013 | 0.016 |
| 1B | -13236 | | | -14552 | 2.4 | | | 0.290 | 0.162 |
| 1W | -10177 | - 9507 | 3.5 | - 9553 | 3.7 | -0.515 | -0.188 | -0.502 | -0.346 |
| 3W | 6828 | 7480 | 2.1 | 7102 | 7.2 | -0.770 | -0.711 | | |

Note: A positive Axial Force signifies compression.
Anticlockwise Moment is positive.

Table 5.4 Comparison of Stresses in Joist CX04, Load 300 Pounds Per Linear Foot

| Member | Calc. Axial Force | Meas. Axial Force at End I | | Meas. Axial Force at End J | | Calc. Mi/My | Meas. Mi/My | Calc. Mj/My | Meas. Mj/My |
|---|---|---|---|---|---|---|---|---|---|
| | | Mean | Cov | Mean | Cov | | | | |
| 9T | 28238 | 29404 | 5.4 | 28778 | 5.4 | -0.035 | -0.008 | 0.093 | 0.0392 |
| 10T | 28246 | 30787 | 3.5 | 28889 | 5.9 | -0.090 | -0.092 | 0.003 | 0.010 |
| 11T | 28288 | 28193 | 5.6 | | | -0.019 | -0.021 | | |
| 2T | 5513 | | | 5470 | 2.5 | | | 0.025 | 0.071 |
| 3T | 15159 | 15052 | 5.8 | | | -0.099 | -0.058 | | |
| 1B | -10979 | | | -12005 | 2.5 | | | 0.030 | 0.022 |
| 5B | -28290 | -29604 | 2.5 | -28659 | 5.9 | -0.039 | -0.030 | | |
| 1W | - 7785 | | | - 7289 | 5.4 | | | | |
| 3W | 4053 | - 4399 | 2.5 | | | | | | |
| 4W | - 4597 | - 4907 | 3.9 | - 4897 | 3.8 | -0.390 | -0.097 | 0.450 | 0.310 |

Note: A positive Axial Force signifies compression.
Anticlockwise Moment is positive.

Table 5.5 Comparison of Stresses in Joist CX05, Load 300 Pounds Per Linear Foot

| Member | Calc. Axial Force | Meas. Axial Force at End I | | Meas. Axial Force at End J | | Calc. Mi/My | Meas. Mi/My | Calc. Mj/My | Meas. Mj/My |
|---|---|---|---|---|---|---|---|---|---|
| | | Mean | Cov | Mean | Cov | | | | |
| 9T | 28245 | | | 27340 | 2.5 | | | 0.041 | 0.039 |
| 10T | 28249 | 28740 | 4.7 | | | 0.040 | 0.008 | | |
| 11T | 28292 | | | 28596 | 5.1 | | | 0.041 | 0.059 |
| 2T | 5439 | | | 5579 | 2.2 | | | -0.036 | -0.330 |
| 3T | 15135 | 15882 | 5.1 | | | 0.092 | 0.110 | | |
| 1B | -10599 | [illegible] | 2.4 | | | | | 0.0094 | 0.015 |
| 5B | -28295 | | | -29358 | 5.6 | | | | |
| 1W | - 7837 | | | - 7584 | 12.9 | | | 0.015 | 0.026 |
| 3W | 3697 | 4061 | 2.4 | 3975 | 6.3 | -1.220 | -1.300 | -1.800 | -0.500 |
| 4W | - 5367 | - 4831 | 6.3 | - 4838 | 5.7 | -0.710 | -0.360 | 0.530 | 0.890 |

Note: A positive Axial Force signifies compression.
Anticlockwise Moment is positive.

Table 5.6 Comparison of Stresses in Joist CX06, Load 300 Pounds Per Linear Foot

| Member | Calc. Axial Force | Meas. Axial Force at End I | | Meas. Axial Force at End J | | Calc. Mi/My | Meas. Mi/My | Calc. Mj/My | Meas. Mj/My |
|---|---|---|---|---|---|---|---|---|---|
| | | Mean | Cov | Mean | Cov | | | | |
| 9T | 28305 | 28350 | 2.0 | 28608 | 1.6 | -0.043 | -0.005 | 0.040 | 0.010 |
| 10T | 28308 | 29653 | 2.5 | | | -0.040 | -0.054 | | |
| 11T | 28347 | | | 29582 | | | | 0.036 | 0.030 |
| 3T | 15142 | 14972 | 5.4 | | | -0.107 | -0.066 | | |
| 1B | -10707 | | | -11575 | 2.2 | | | -0.071 | -0.028 |
| 1W | - 8035 | | | - 7793 | 4.7 | | | -0.285 | -0.018 |
| 3W | 5706 | 6025 | 2.2 | 6604 | 2.2 | -0.750 | -0.290 | -0.180 | -0.060 |
| 4W | - 4858 | - 5104 | 1.6 | - 5139 | 1.7 | -0.780 | -0.580 | | |

Note: A positive Axial Force signifies compression.
Anticlockwise Moment is positive.

Table 5.7 Comparison of Stresses in Joist CY01, Load 315 Pounds Per Linear Foot

| Member | Calc. Axial Force | Meas. Axial Force at End I | | Meas. Axial Force at End J | | Calc. Mi/My | Meas. Mi/My | Calc. Mj/My | Meas. Mj/My |
|---|---|---|---|---|---|---|---|---|---|
| | | Mean | Cov | Mean | Cov | | | | |
| 2T | 8871 | 8650 | 2.5 | | | 0.150 | | | |
| 3T | 18072 | 18044 | 3.4 | | | -0.034 | -0.092 | | |
| 8T | 28591 | 28791 | 2.7 | 29060 | 3.1 | | | | |
| 9T | 29938 | | | 30028 | 2.4 | | | | |
| 10T | 29938 | 29295 | 2.4 | 30752 | 4.9 | -0.035 | -0.051 | 0.032 | 0.052 |
| 1B | -13701 | | | -12048 | 2.5 | -0.135 | -0.052 | 0.081 | 0.031 |
| 1W | -10529 | -10886 | 5.6 | -10929 | 2.6 | | | | |
| 3W | 6698 | 7612 | 12.9 | 7557 | 2.9 | | | 0.299 | 0.100 |
| 4W | - 6060 | - 6726 | 3.5 | | | -0.110 | -0.073 | | |

Note: A positive Axial Force signifies compression.
Anticlockwise Moment is positive.

Table 5.8 Comparison of Stresses in Joist CY02, Load 315 Pounds Per Linear Foot

| Member | Calc. Axial Force | Meas. Axial Force at End I | | Meas. Axial Force at End J | | Calc. Mi/My | Meas. Mi/My | Calc. Mj/My | Meas. Mj/My |
|---|---|---|---|---|---|---|---|---|---|
| | | Mean | Cov | Mean | Cov | | | | |
| 2T | 9193 | | | 8855 | 2.7 | | | 0.555 | 0.038 |
| 3T | 18595 | 21979 | 3.6 | | | | | | |
| 8T | 29561 | 29490 | 2.4 | 29786 | 2.5 | 0.021 | 0.027 | | |
| 9T | 30901 | 30881 | 1.7 | 30606 | 2.4 | | | | |
| 10T | 30901 | 30417 | 2.1 | 30381 | 3.5 | -0.025 | -0.045 | | |
| 1B | -14233 | -14963 | 2.7 | -14368 | 2.7 | -0.013 | -0.281 | 0.024 | 0.120 |
| 1W | -10814 | -10873 | 4.5 | -10624 | 3.1 | | | 0.850 | 0.725 |
| 3W | 6930 | | | 7493 | 2.4 | | | -0.315 | -0.265 |
| 4W | - 6093 | - 7075 | 2.8 | | | -0.007 | -0.0995 | | |

Note: A positive Axial Force signifies compression.
Anticlockwise Moment is positive.

Table 5.9 Comparison of Stresses in Joist CZ01, Load 446 Pounds Per Linear Foot

| Member | Calc. Axial Force | Meas. Axial Force at End I | | Meas. Axial Force at End J | | Calc. Mi/My | Meas. Mi/My | Calc. Mj/My | Meas. Mj/My |
|---|---|---|---|---|---|---|---|---|---|
| | | Mean | Cov | Mean | Cov | | | | |
| 6T | 43321 | 44581 | 5.4 | 41526 | 2.5 | -0.051 | -0.033 | 0.051 | 0.028 |
| 7T | 43613 | 44038 | 5.6 | 42397 | 1.5 | -0.046 | -0.011 | | |
| 8T | 43612 | 40492 | 4.7 | | | -0.045 | -0.030 | | |
| 1T | 17229 | 15695 | 5.9 | 15429 | 2.9 | -0.114 | -0.010 | -0.049 | -0.030 |
| 2T | 29249 | 27479 | 5.4 | | | -0.023 | -0.015 | | |
| 1B | -17359 | -13895 | 3.8 | | | -0.010 | -0.036 | | |
| 6B | -43330 | -41871 | 2.5 | -40923 | -2.6 | -0.049 | -0.017 | 0.041 | 0.028 |
| 1W | -28999 | -26659 | 3.5 | -27161 | 3.4 | -0.068 | -0.010 | -0.043 | -0.013 |
| 2W | 7891 | 7176 | 1.5 | 7375 | 1.4 | -0.540 | -0.038 | -0.580 | -0.05 |
| 3W | -13279 | -12589 | 4.5 | | | | | | |

Note: A positive Axial Force signifies compression.
Anticlockwise Moment is positive.

Table 5.10 Summary of Results

| JOIST | DESIGN LOAD lbs/ft | FAILURE LOAD lbs/ft | LOAD FACTOR =FL/DL | AVE $e_2$(in) | AVE $e_1$ | CODE $e_1$ | CHORD YIELD STRESS KSI | ORDER OF TEST | TOP CHORD CONFIGURATION | MODE OF FAILURE |
|---|---|---|---|---|---|---|---|---|---|---|
| CX01 | 315 | 542.7 | 1.72 | 0.9 | 0.45 | 0.42 | 55.9 | 1 | Hot Rolled | Top Chord 8T (North) |
| CX02 | 315 | 538.2 | 1.71 | 1.3 | 0.65 | 0.42 | 55.9 | 2 | Hot Rolled | Web 3W (South) |
| CX03 | 315 | 494.8 | 1.57 | 2.4 | 1.20 | 0.42 | 55.9 | 3 | Hot Rolled | Top Chord 9T (South) |
| CX04 | 300 | 482.5 | 1.61 | 0.6 | 0.30 | 0.52 | 78.9 | 8 | Cold Rolled | Lateral Buckling |
| CX05 | 300 | 516.0 | 1.72 | 1.1 | 0.55 | 0.52 | 78.9 | 9 | Cold Rolled | Top Chord 9T (North) |
| CX06 | 300 | 507.4 | 1.69 | 1.7 | 0.85 | 0.52 | 78.9 | 10 | Cold Rolled | Web 3W (South) |
| CY01 | 315 | 497.4 | 1.58 | -0.3 | -0.15 | 0.82 | 64.5 | 4 | Hot Rolled | Chord Yielding |
| CY02 | 315 | 496.5 | 1.58 | 0.5 | 0.25 | 0.82 | 64.5 | 5 | Hot Rolled | Chord Yielding |
| CZ01 | 446 | 692.5 | 1.55 | 0.6 | - | - | - | 7 | Std Angles | Lateral Buckling |
| CZ02 | 446 | 560.5 | 1.26 | 0.8 | - | - | - | 6 | Std Angles | Lateral Buckling |

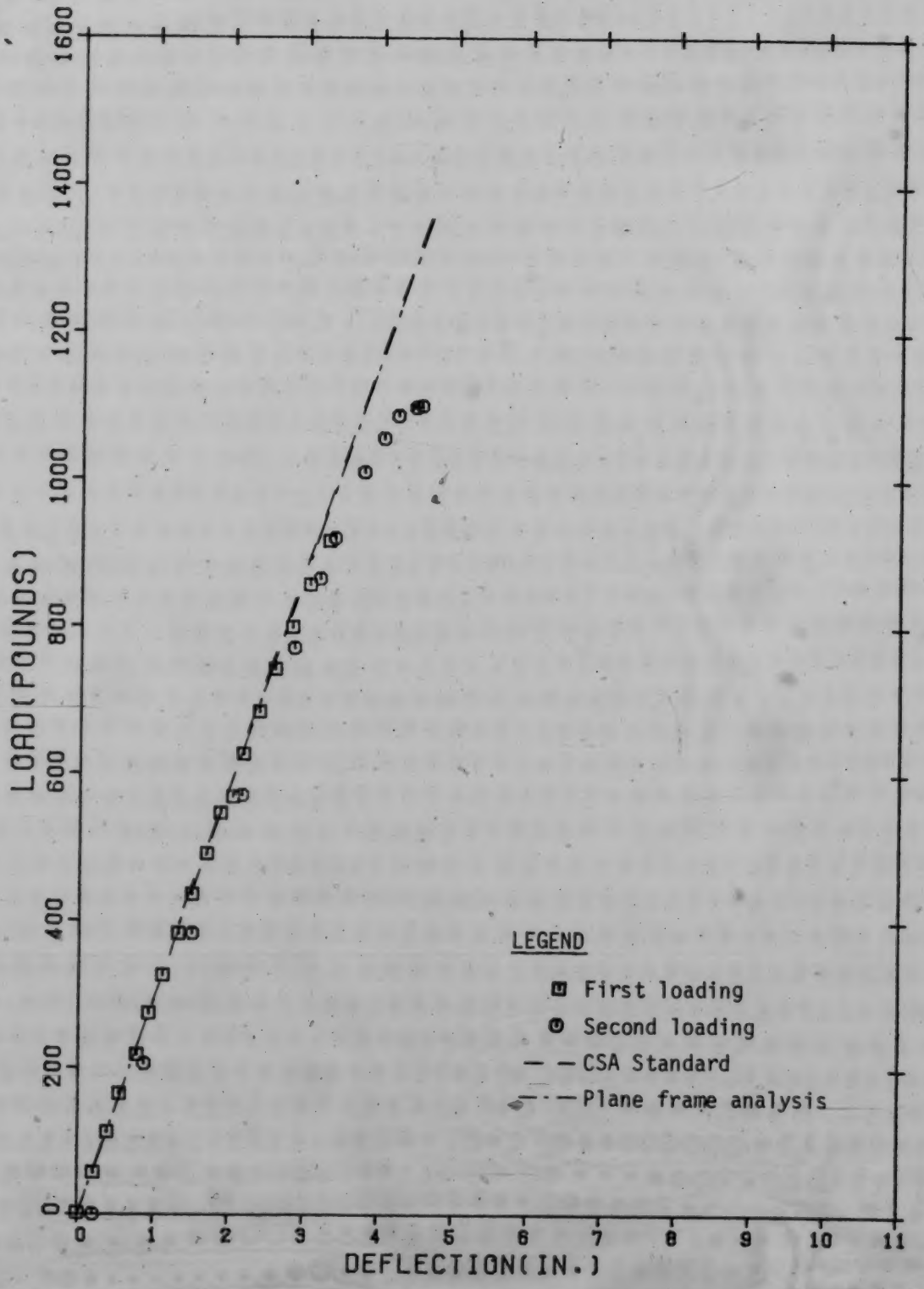


Figure 5.1 Load-deflection curve, joist CX01

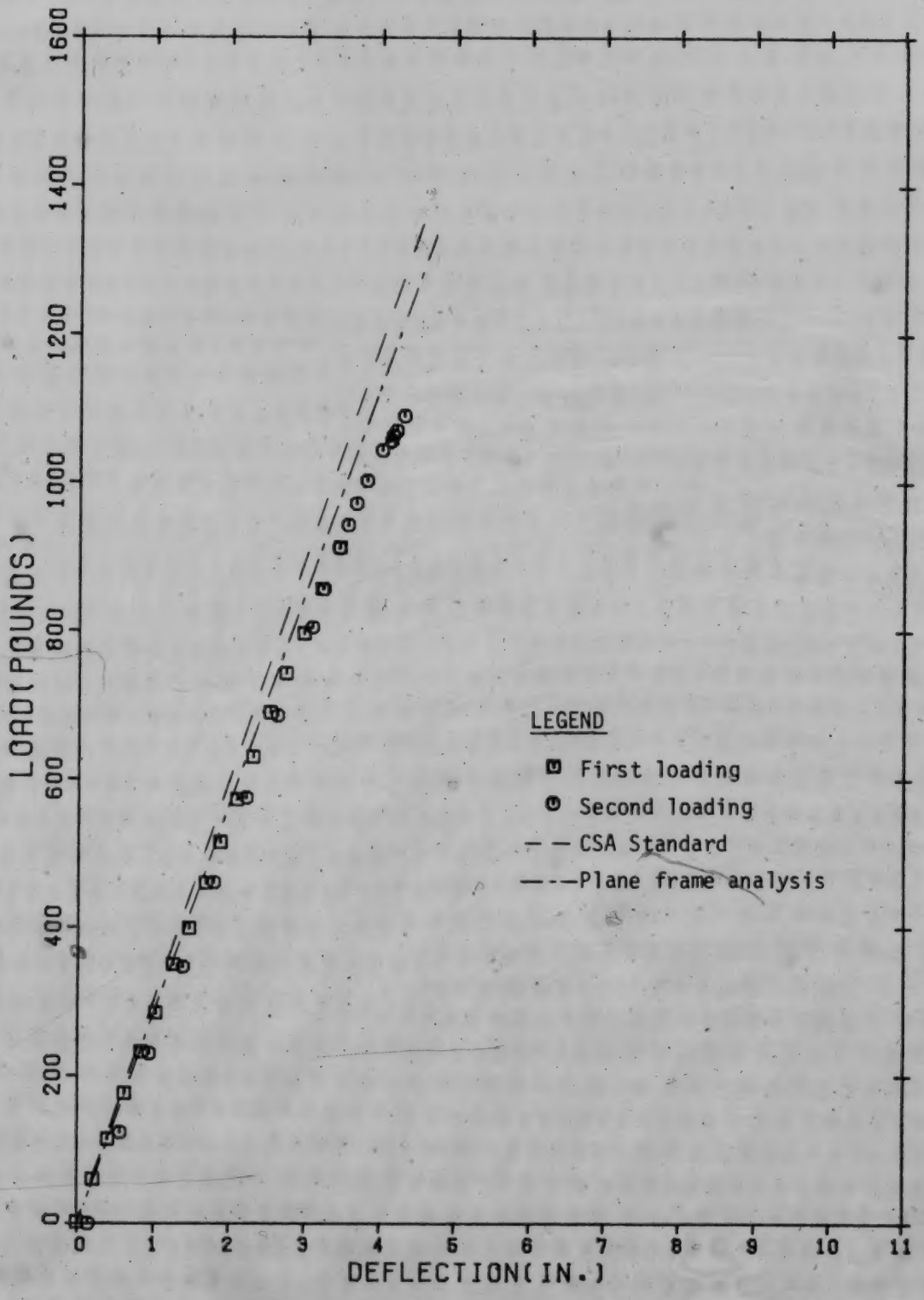


Figure 5.2 Load-Deflection Curve, joist CX02

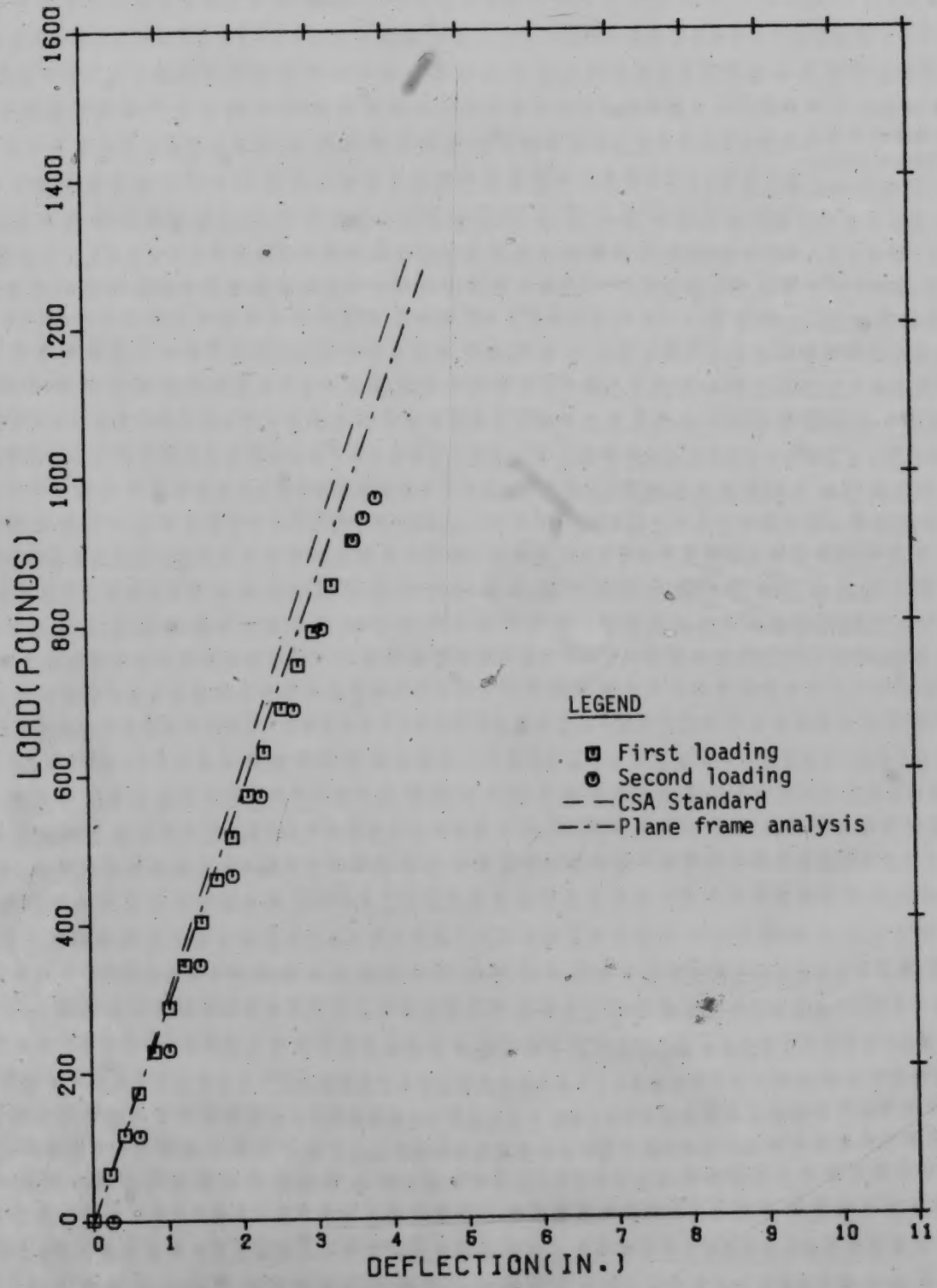


Figure 5.3 Load-Deflection Curve, joist CX03

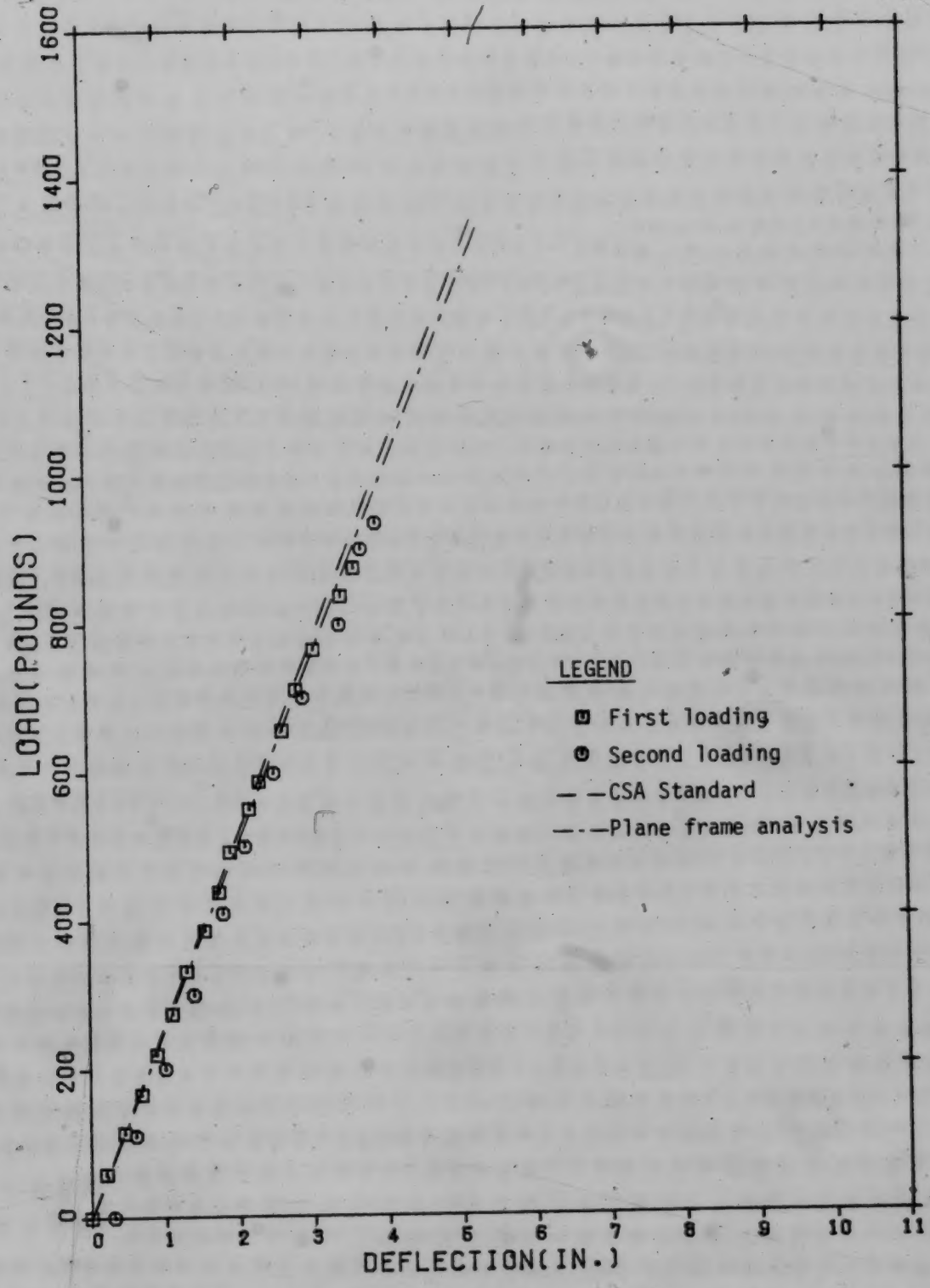


Figure 5.4 Load-Deflection Curve, joist CX04

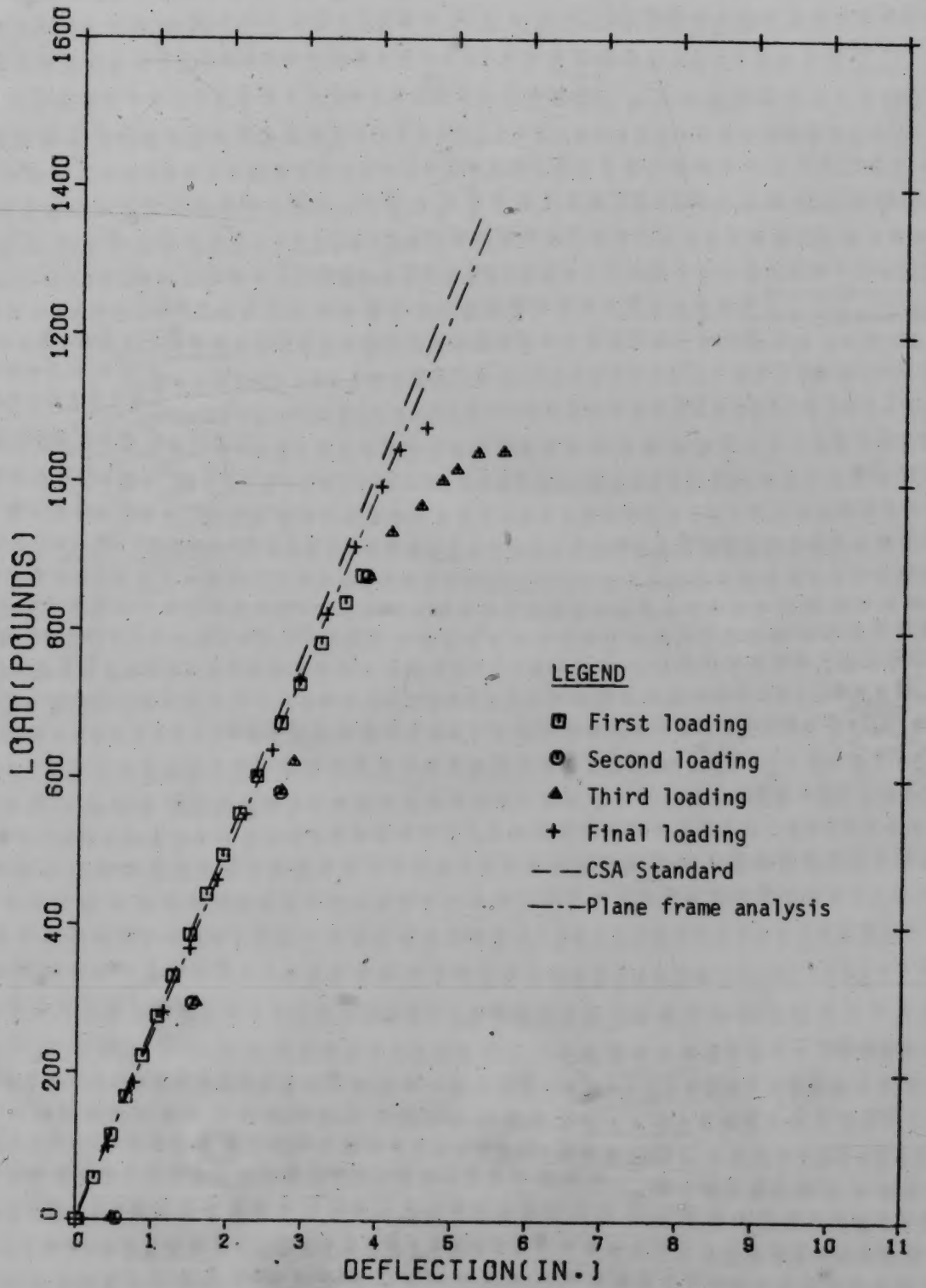


Figure 5.5 Load-Deflection Curve, joist CX05

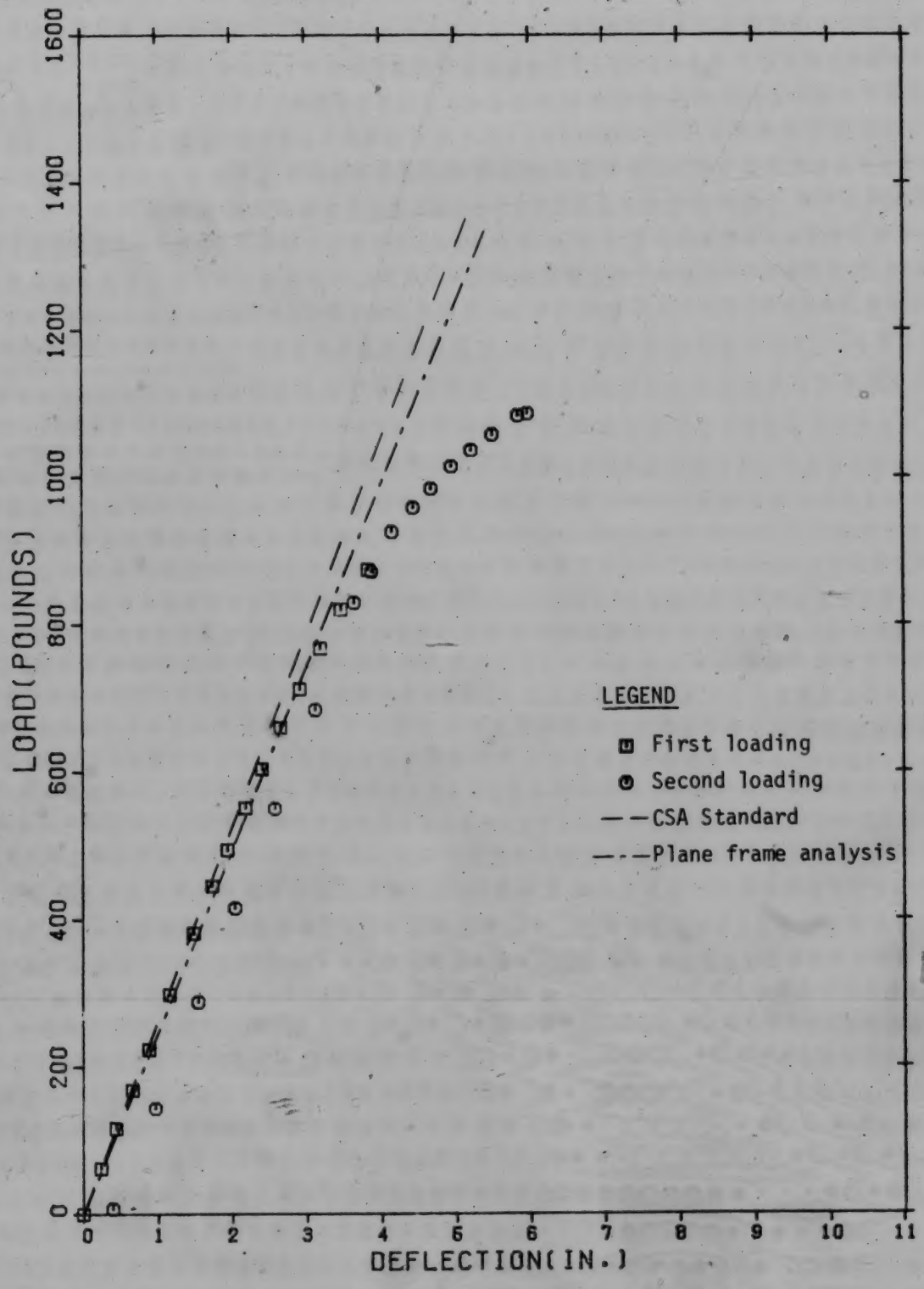


Figure 5.6 Load-Deflection Curve, joist CX06

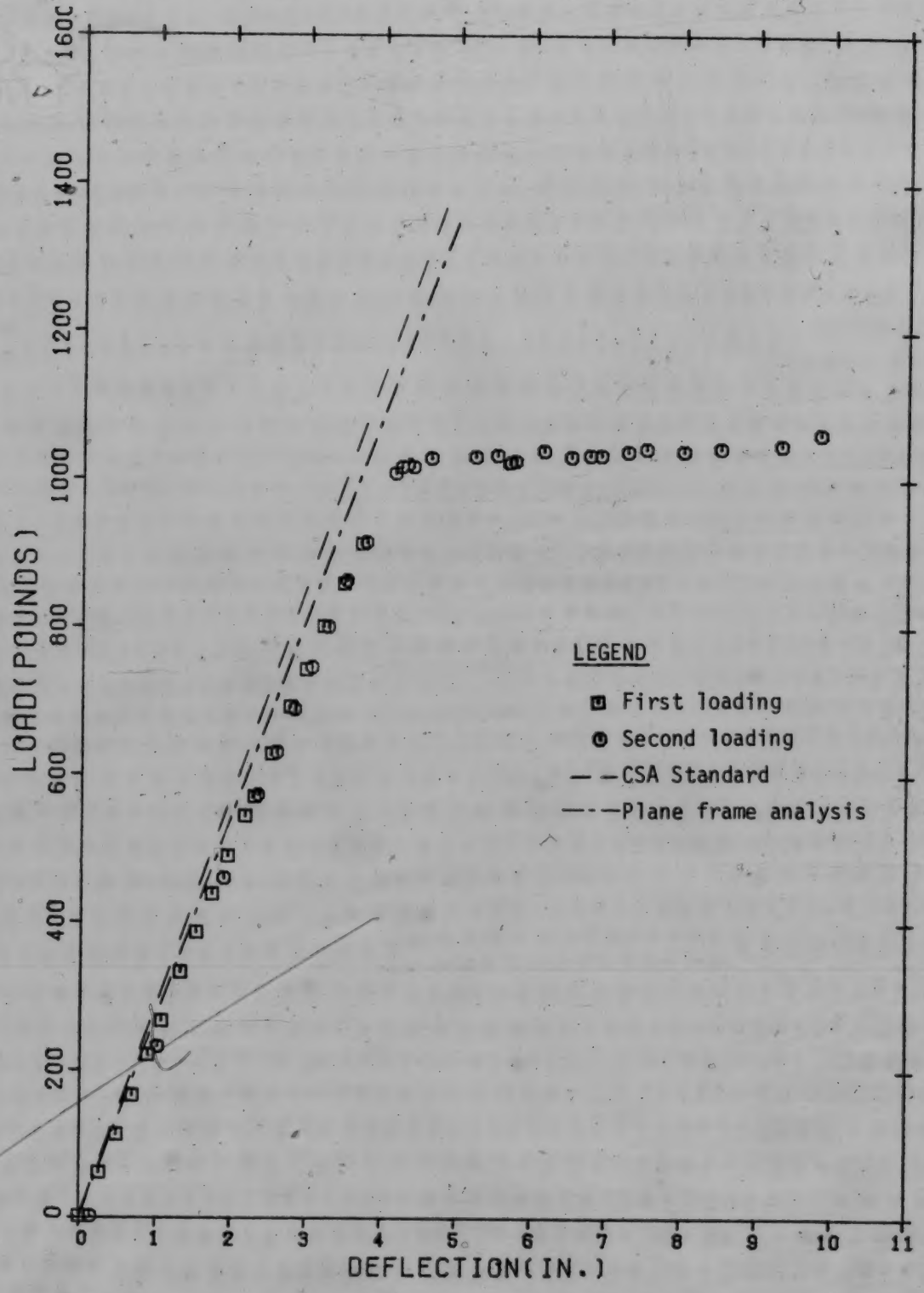


Figure 5.7 Load-Deflection Curve, joist CY01

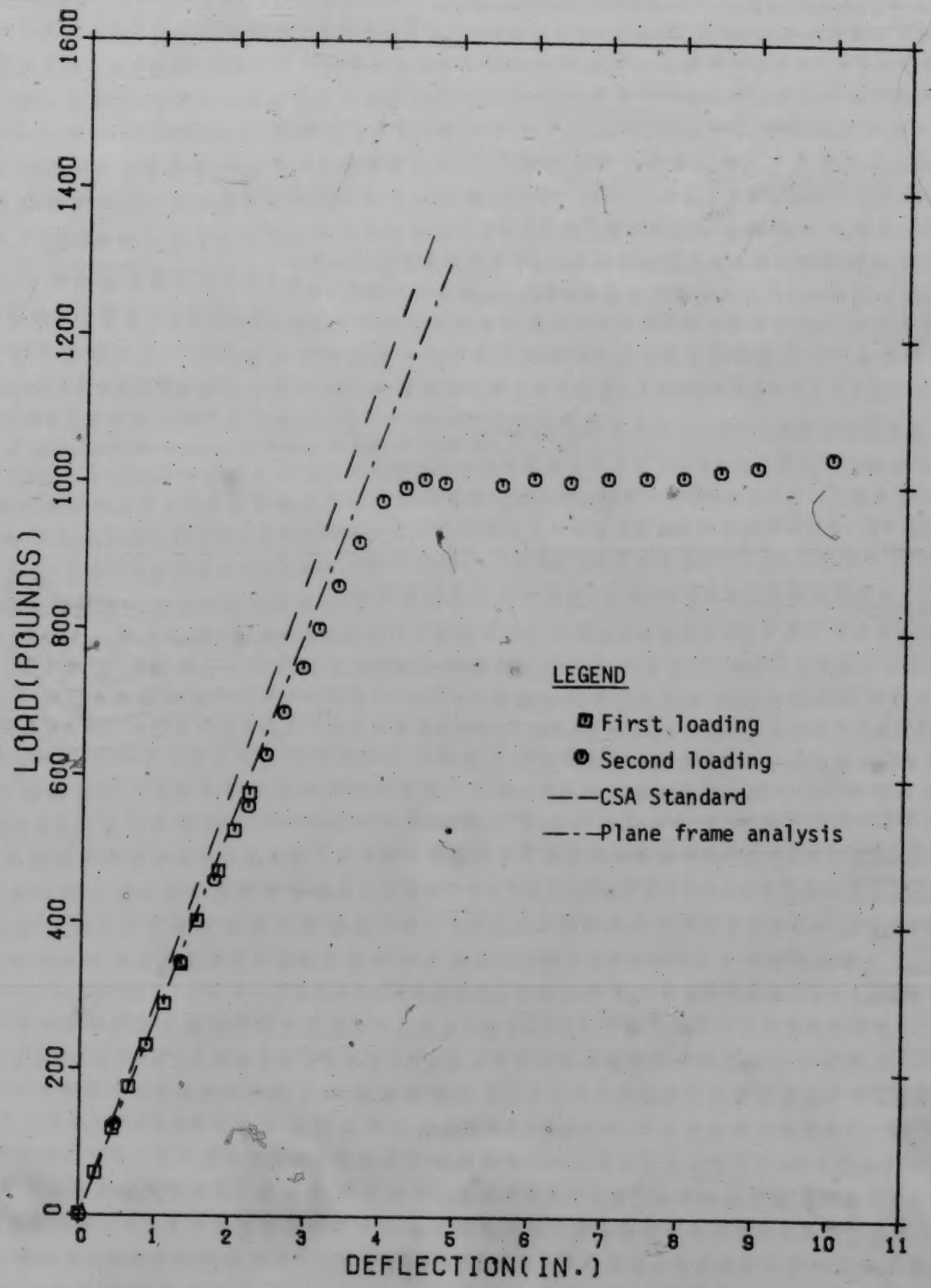


Figure 5.8 Load-Deflection Curve, joist CY02

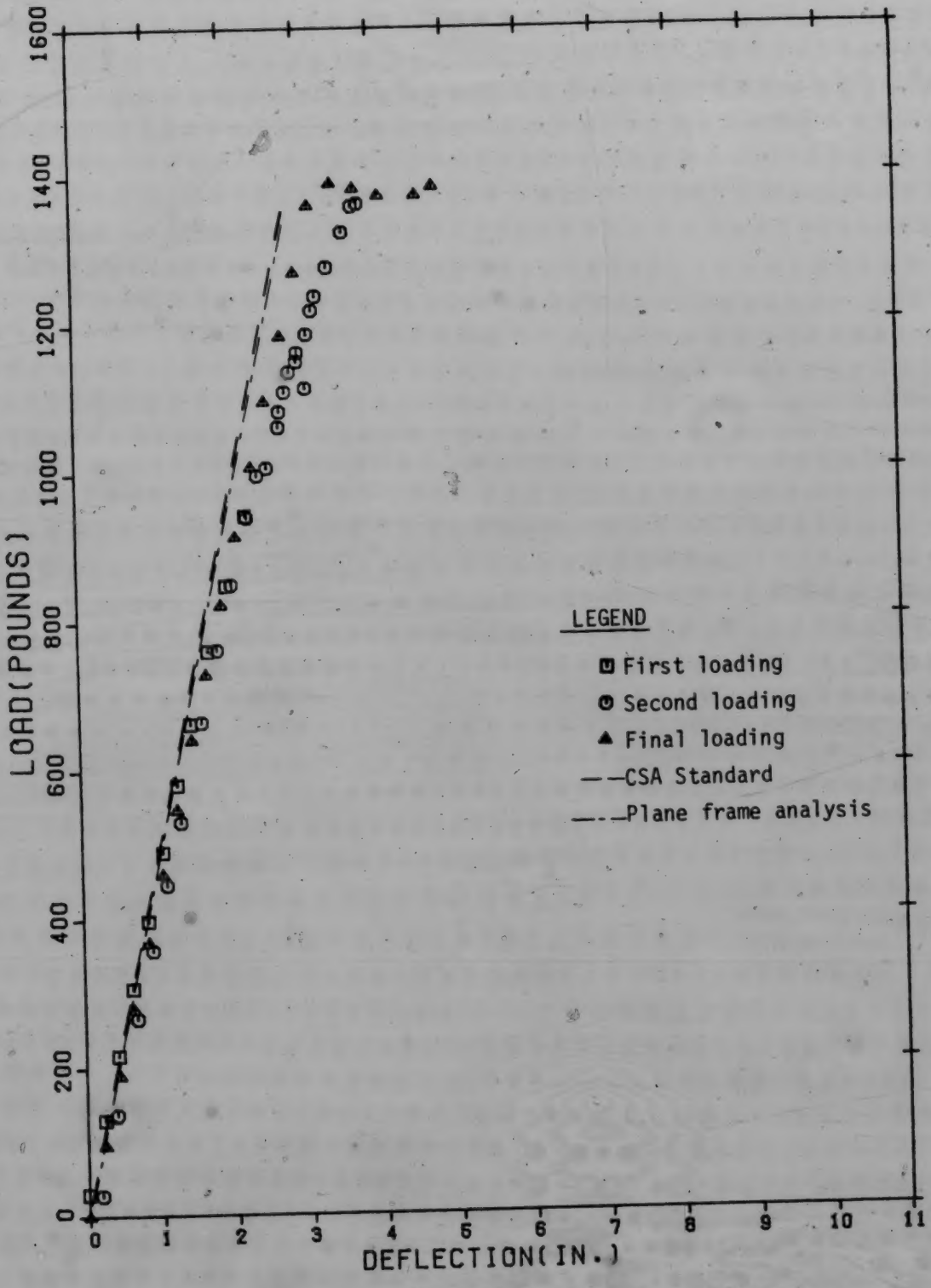


Figure 5.9 Load-Deflection Curve, joist CZ01

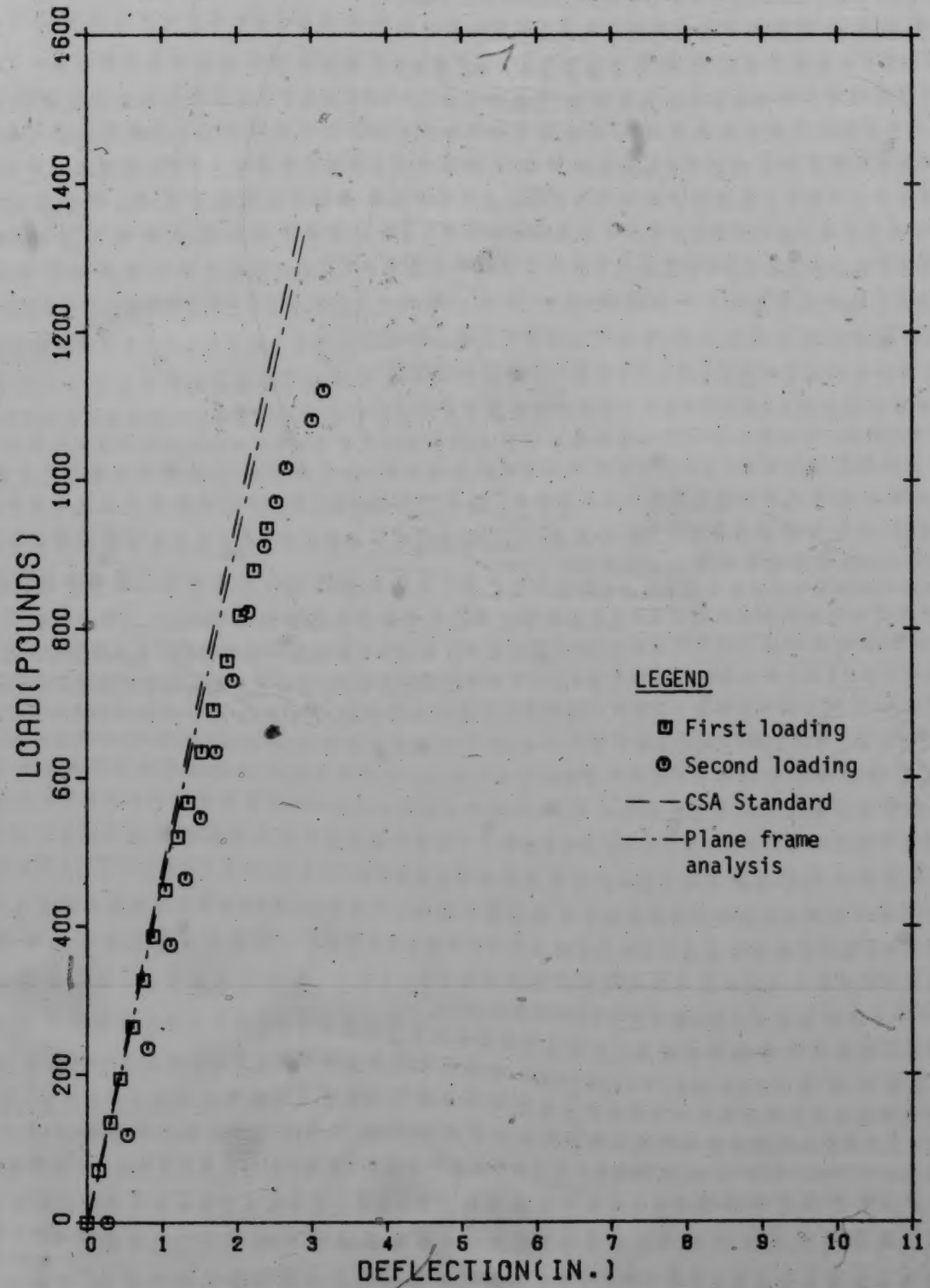


Figure 5.10 Load-Deflection Curve, joist CZ02

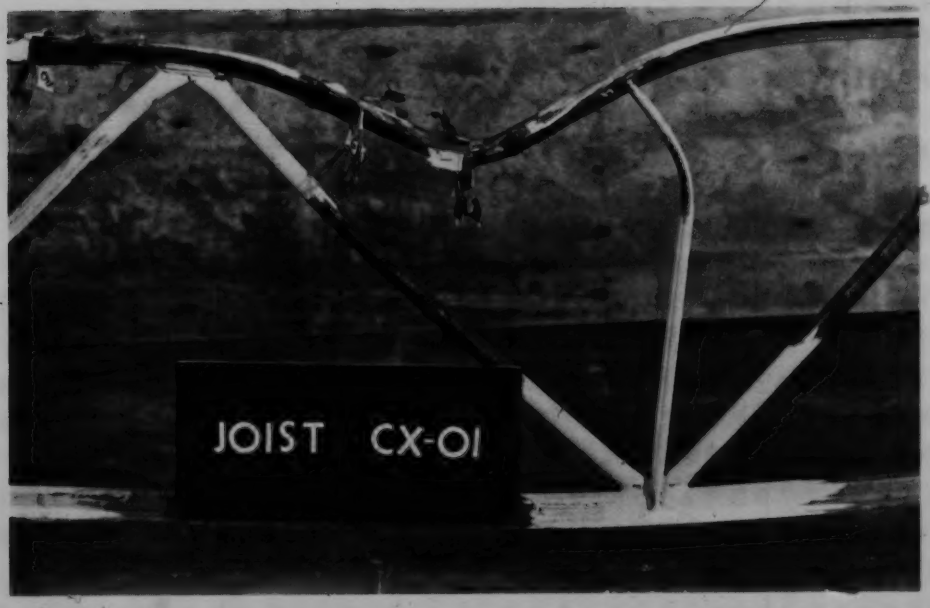


Figure 5.11 Failure of joist CX01

Figure 5.12 Failure of joist CX02

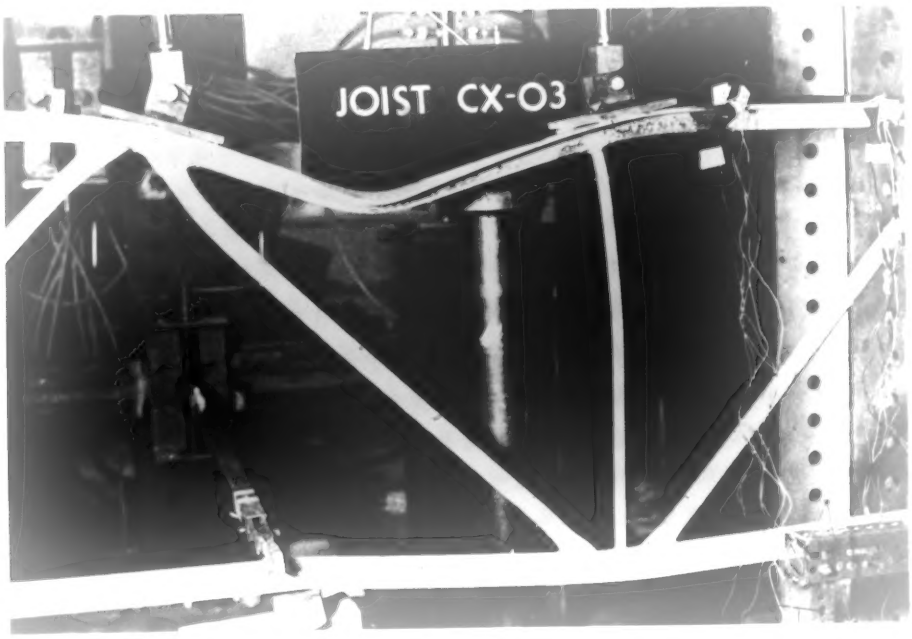


Figure 5.13 Failure of joist CX03

Figure 5.14 Yielding at joint

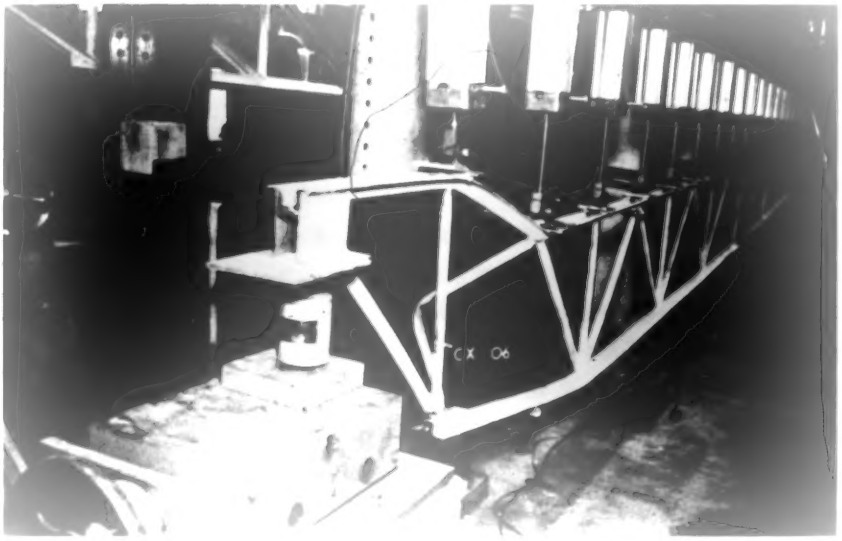


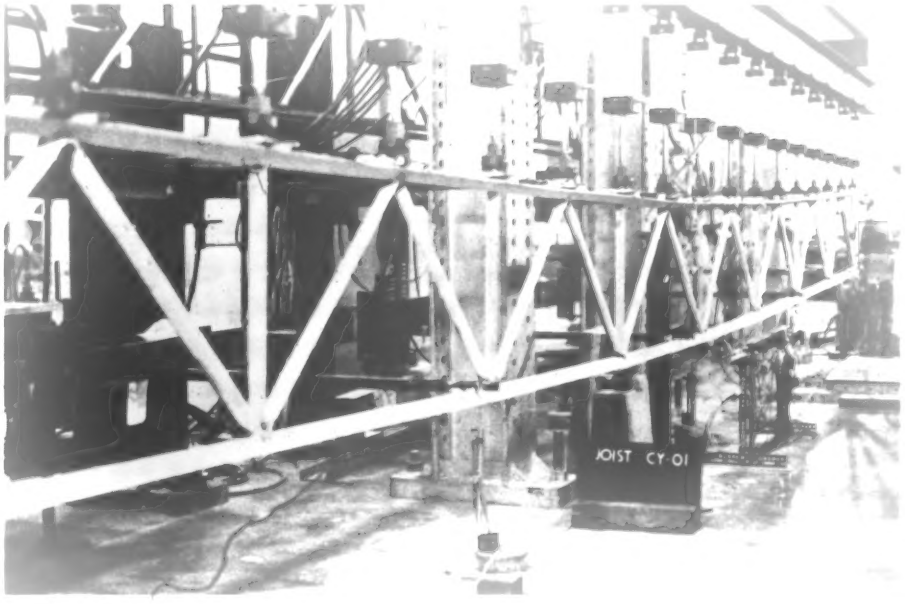


Figure

Figure 5.17 Yielding of bottom chord of joist CY01

Figure 5.18 Yielding of bottom chord of joist CY02

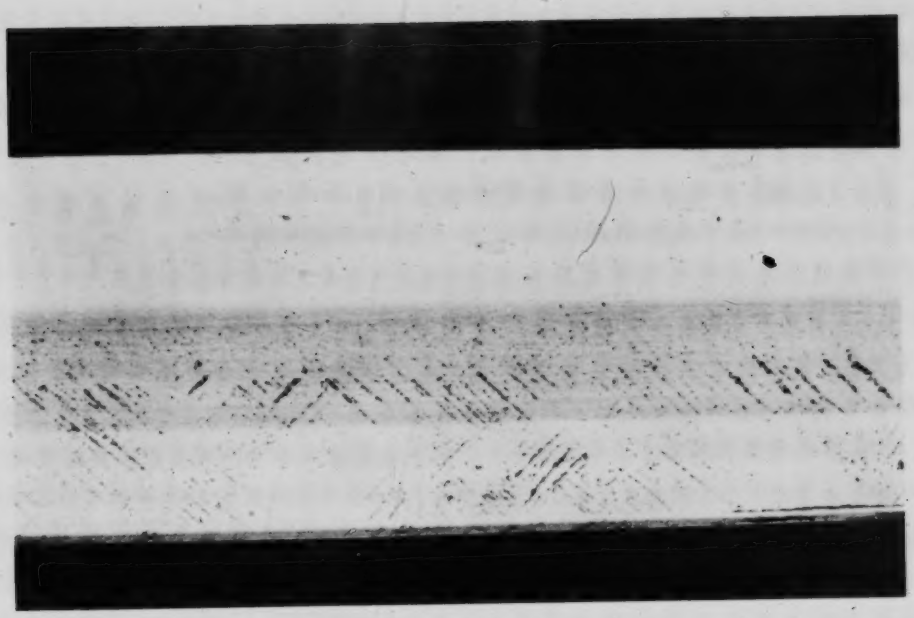

Figure 5.19 Yielding of bottom chord of joist CY02

Figure 5.20 Yielding of chord at spacers, joist CZ02

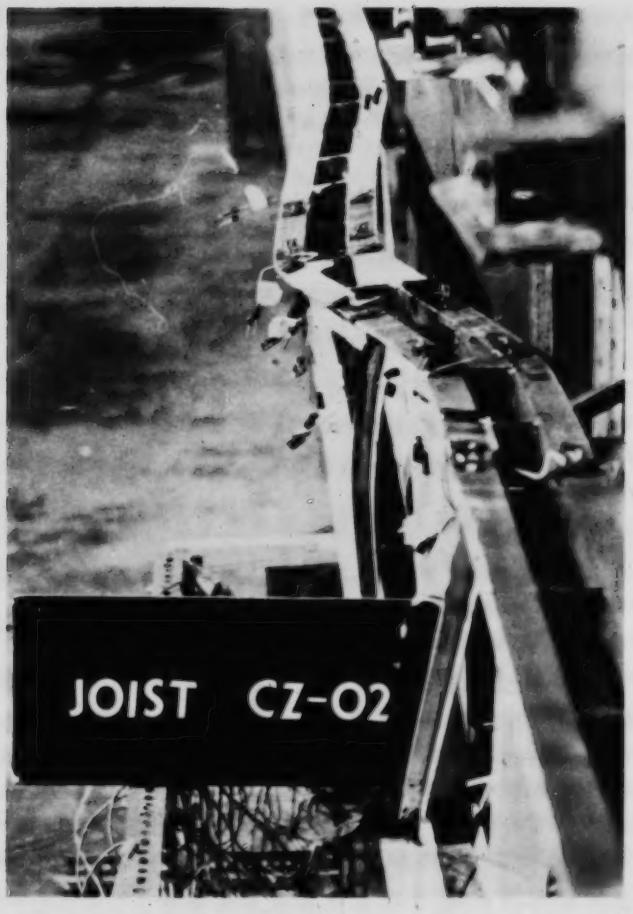


Figure 5.21 Failure of joist CZ02

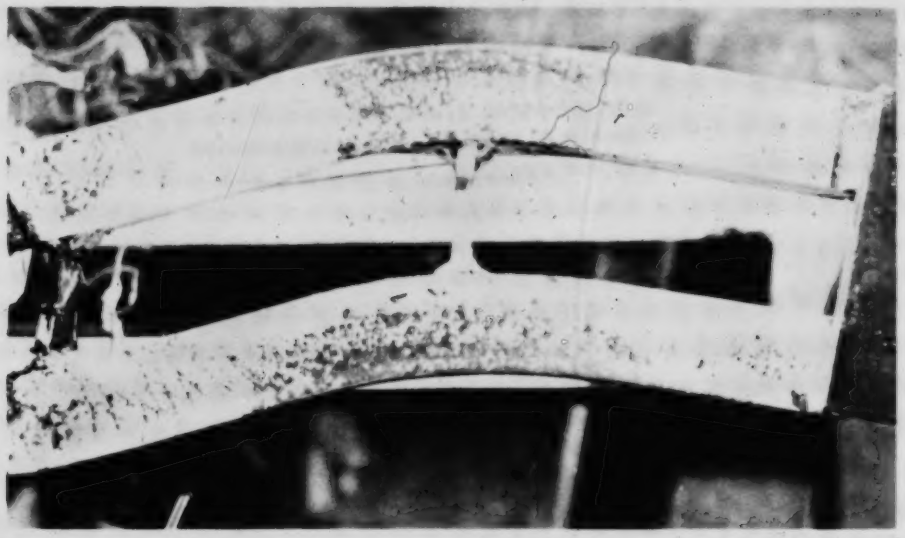

Figure 5.22 Failure of spacers in joist CZ02

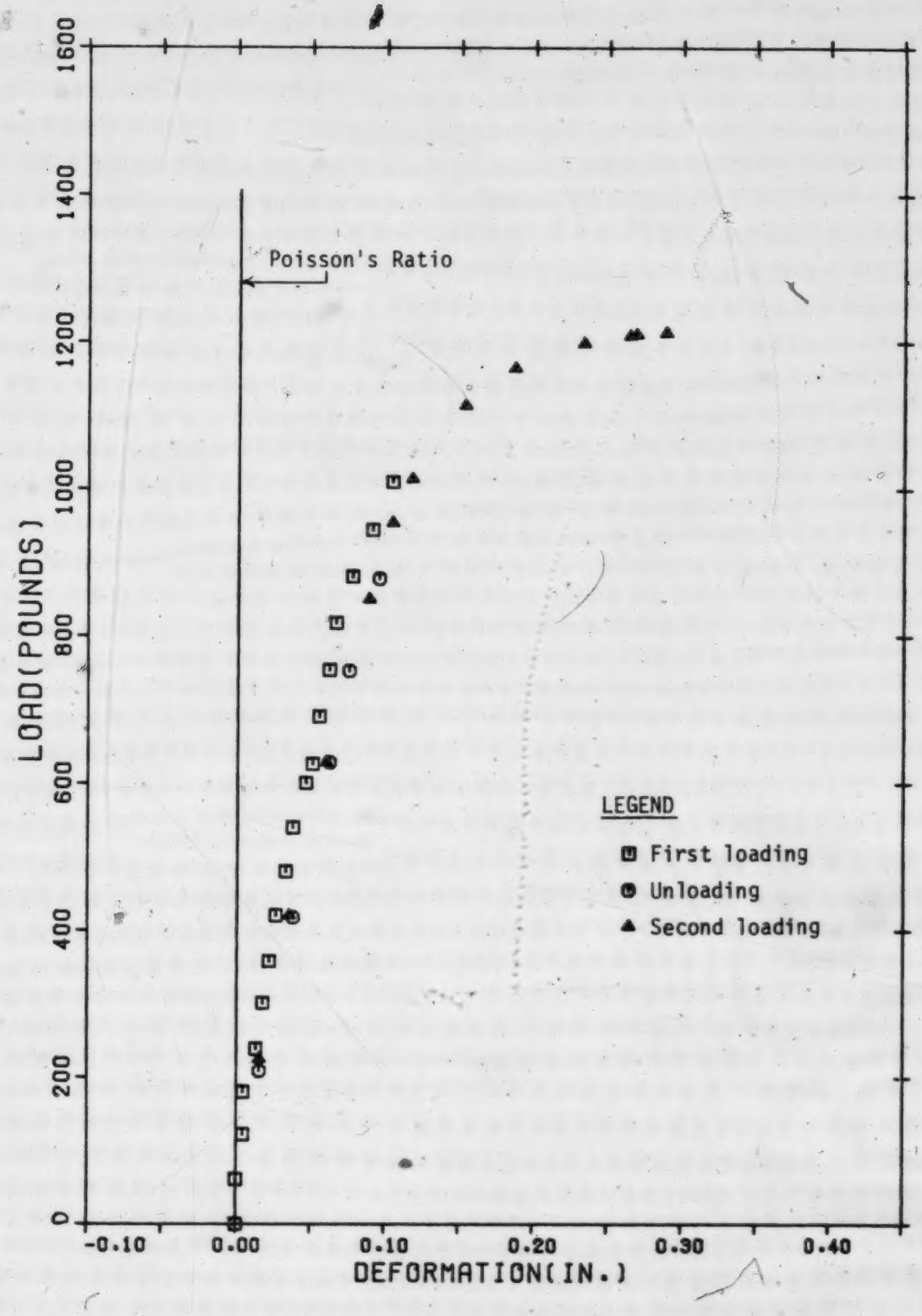


Figure 5.23 Section - Deformation of Member 9T (South), joist CX01

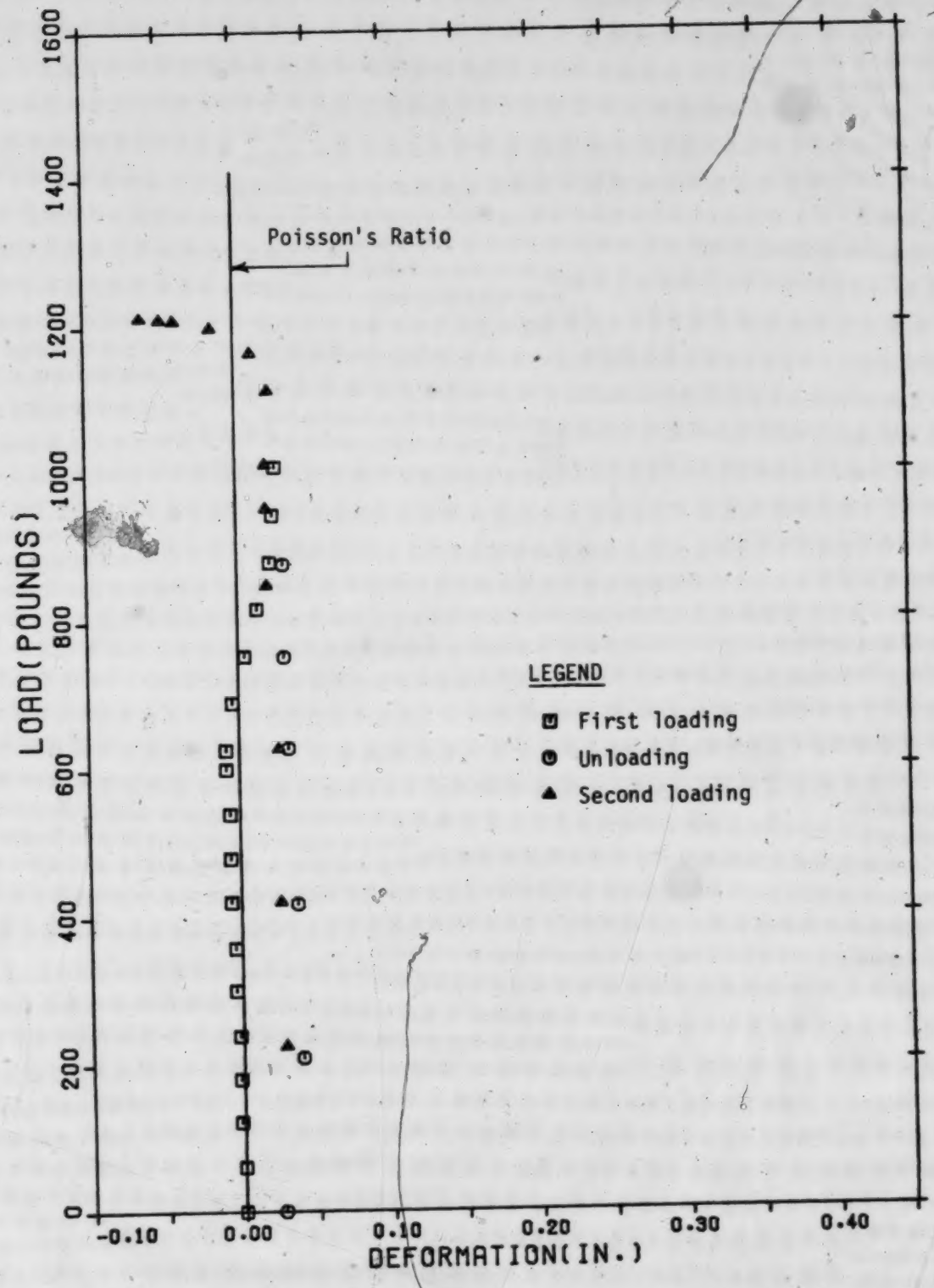


Figure 5.24 Section - Deformation of Member 9T (North), joist CX01

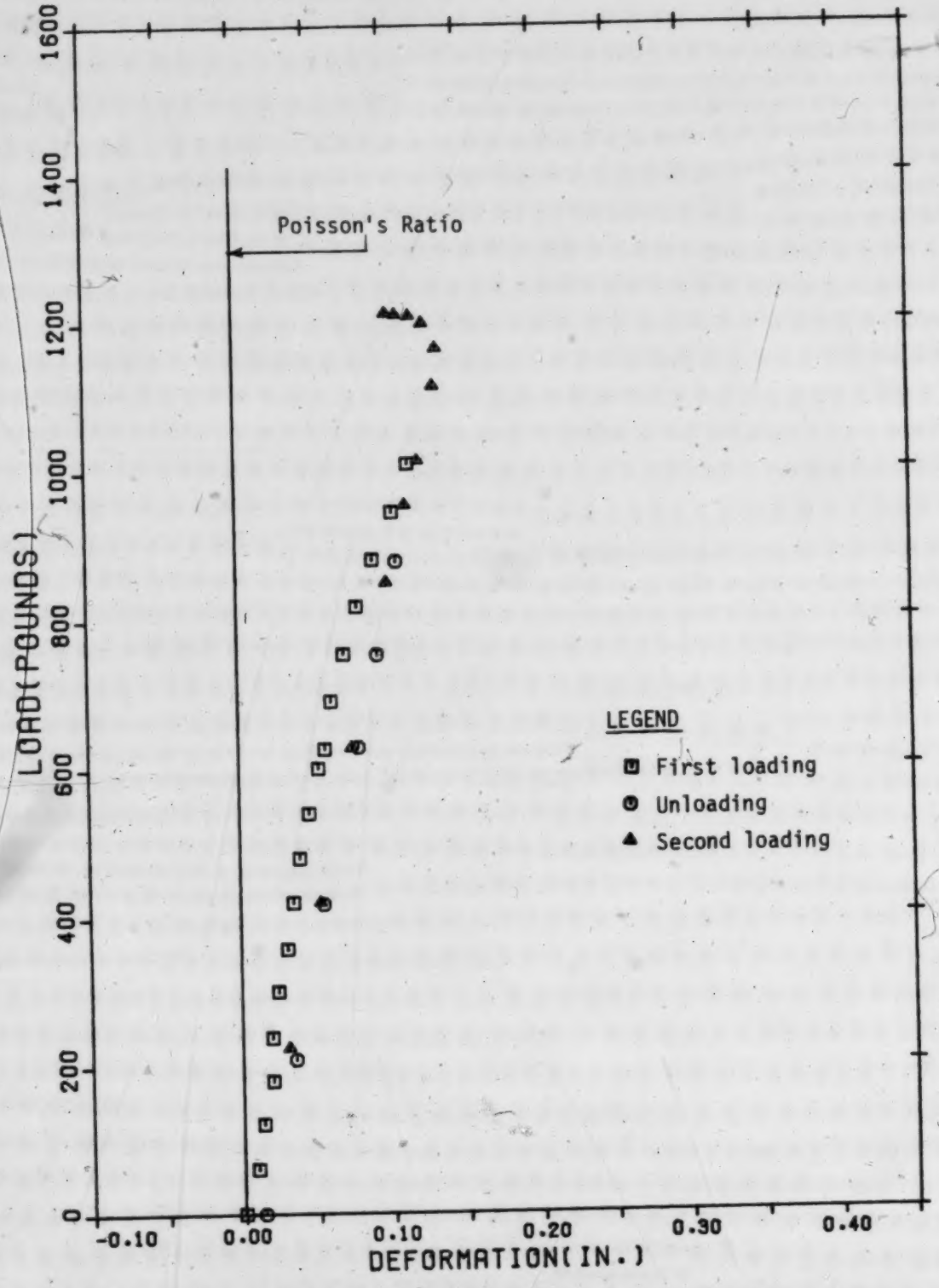


Figure 5.25 Section - Deformation of Member 8T (South), joist CX01

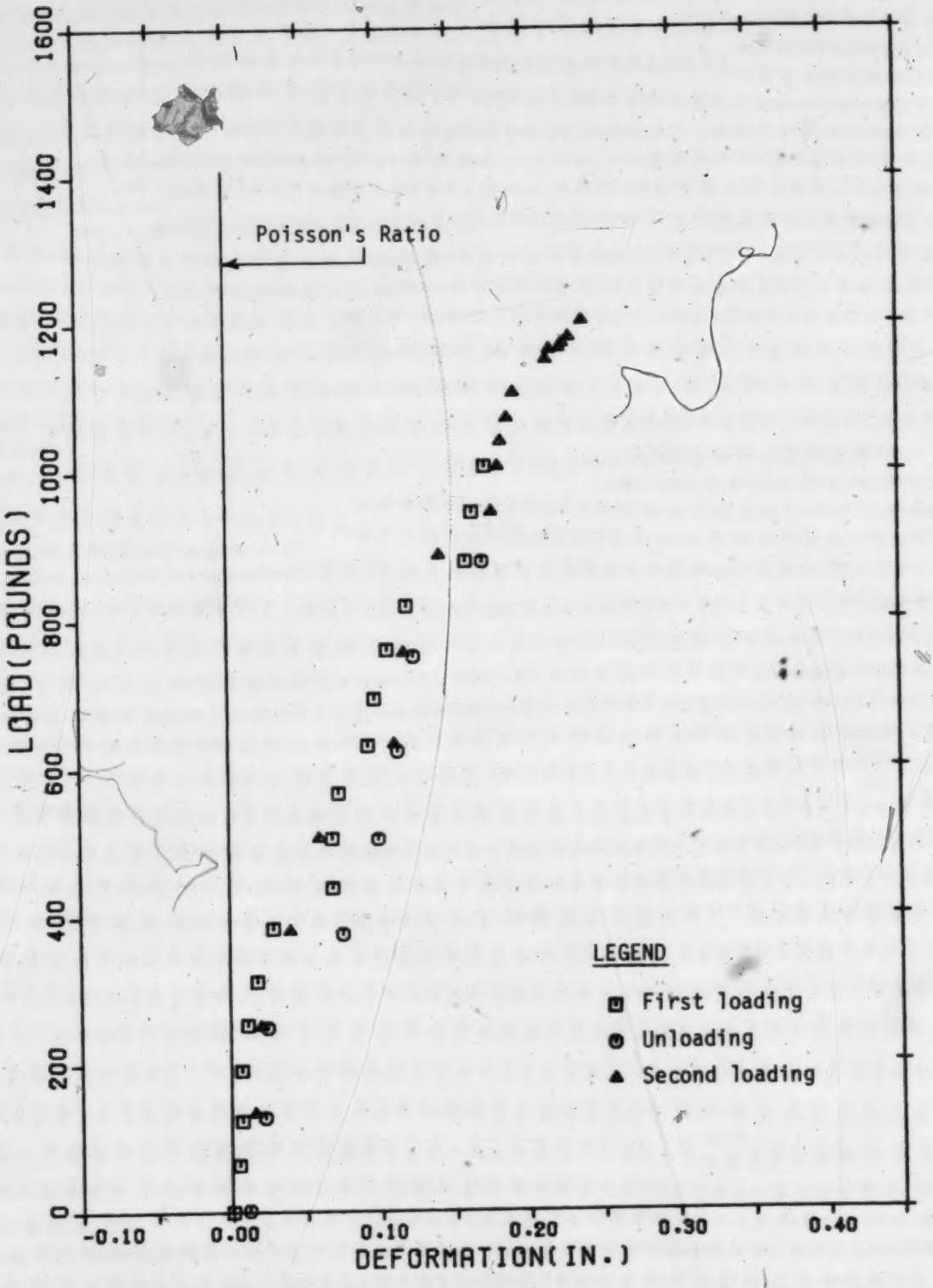


Figure 5.26 Section - Deformation of Member 7T (North), joist CX02

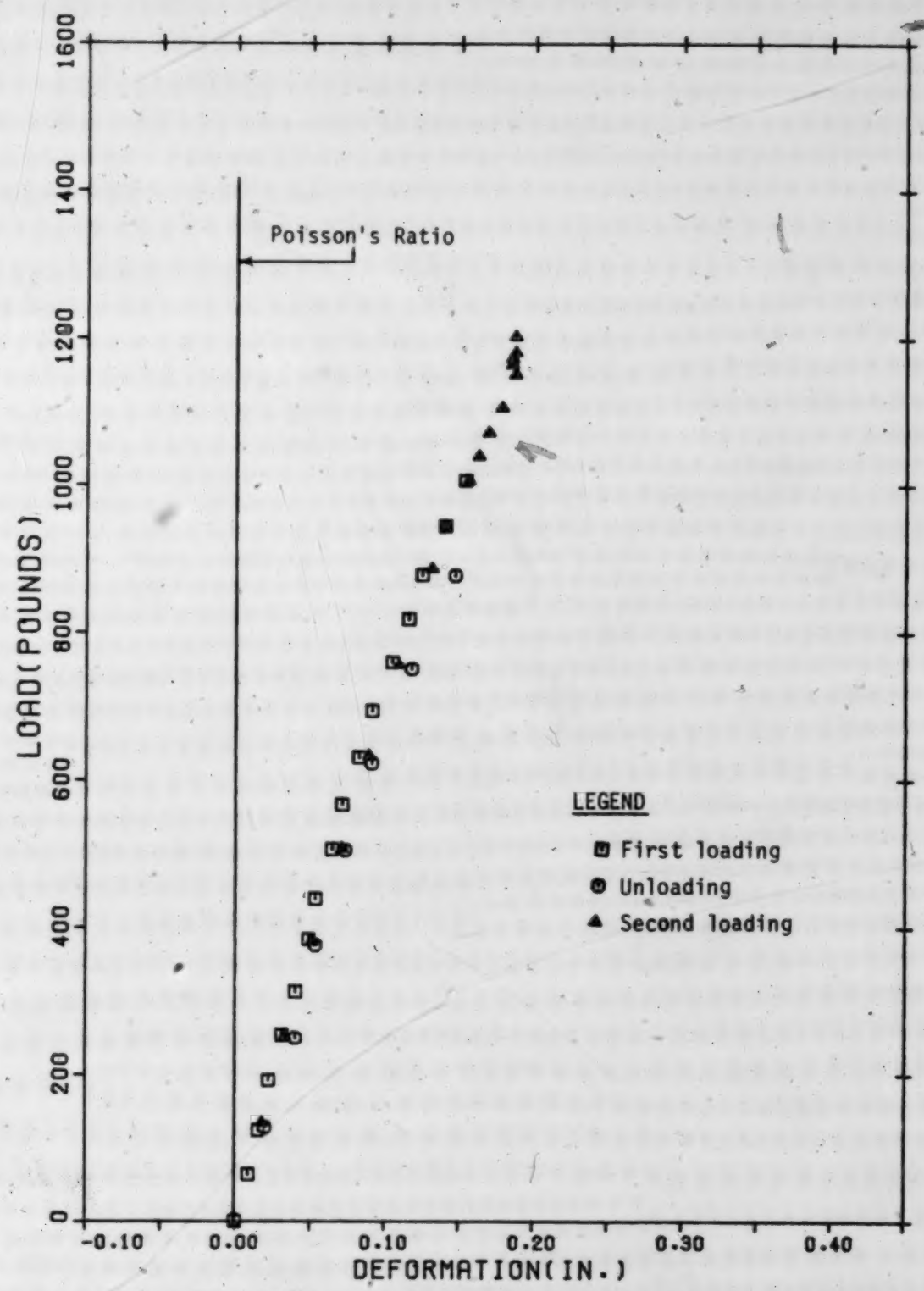


Figure 5.27 Section - Deformation of Member 8T (North), joist CX02

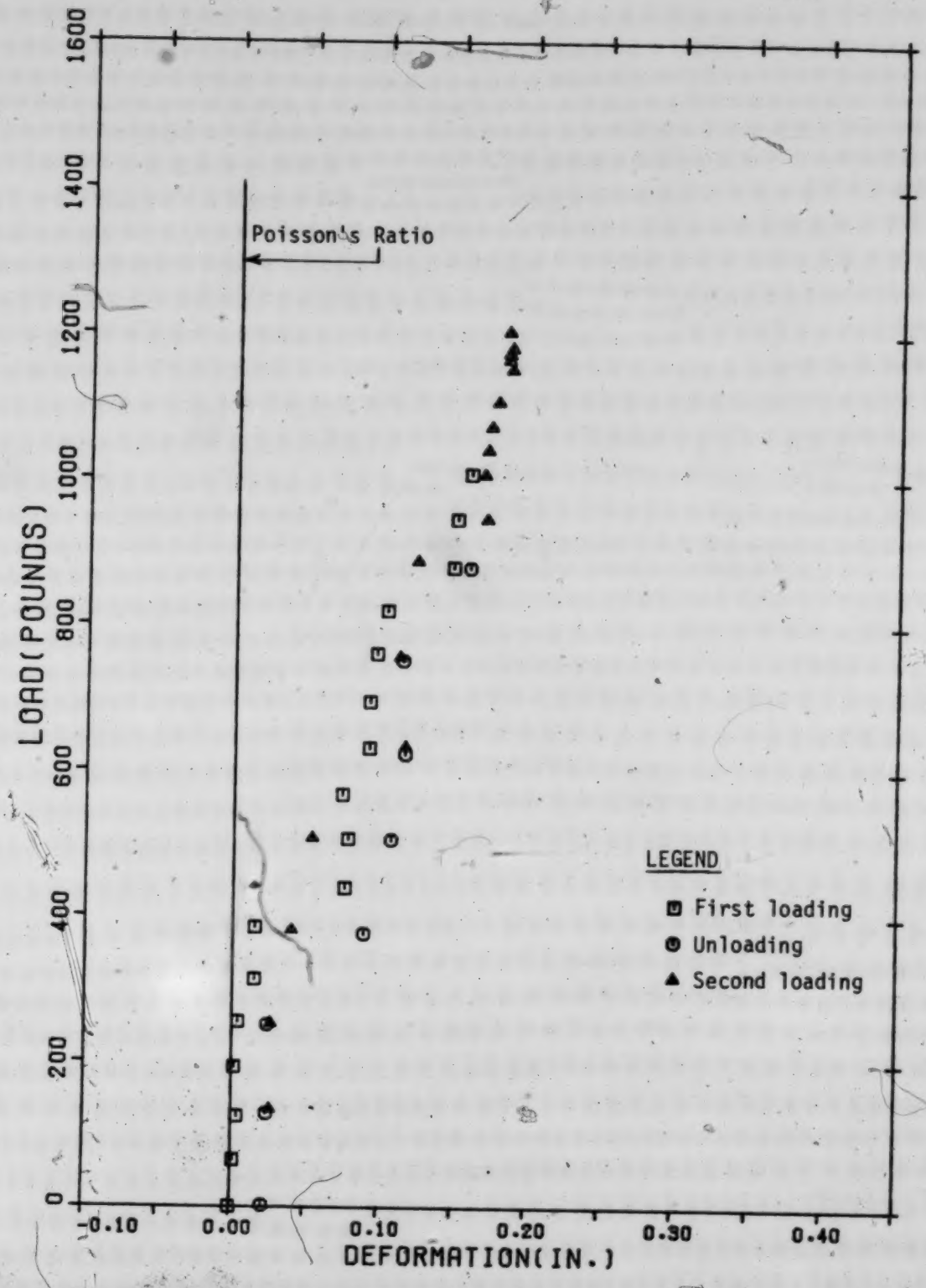


Figure 5.28 Section - Deformation of Member 9T (North), joist CX02

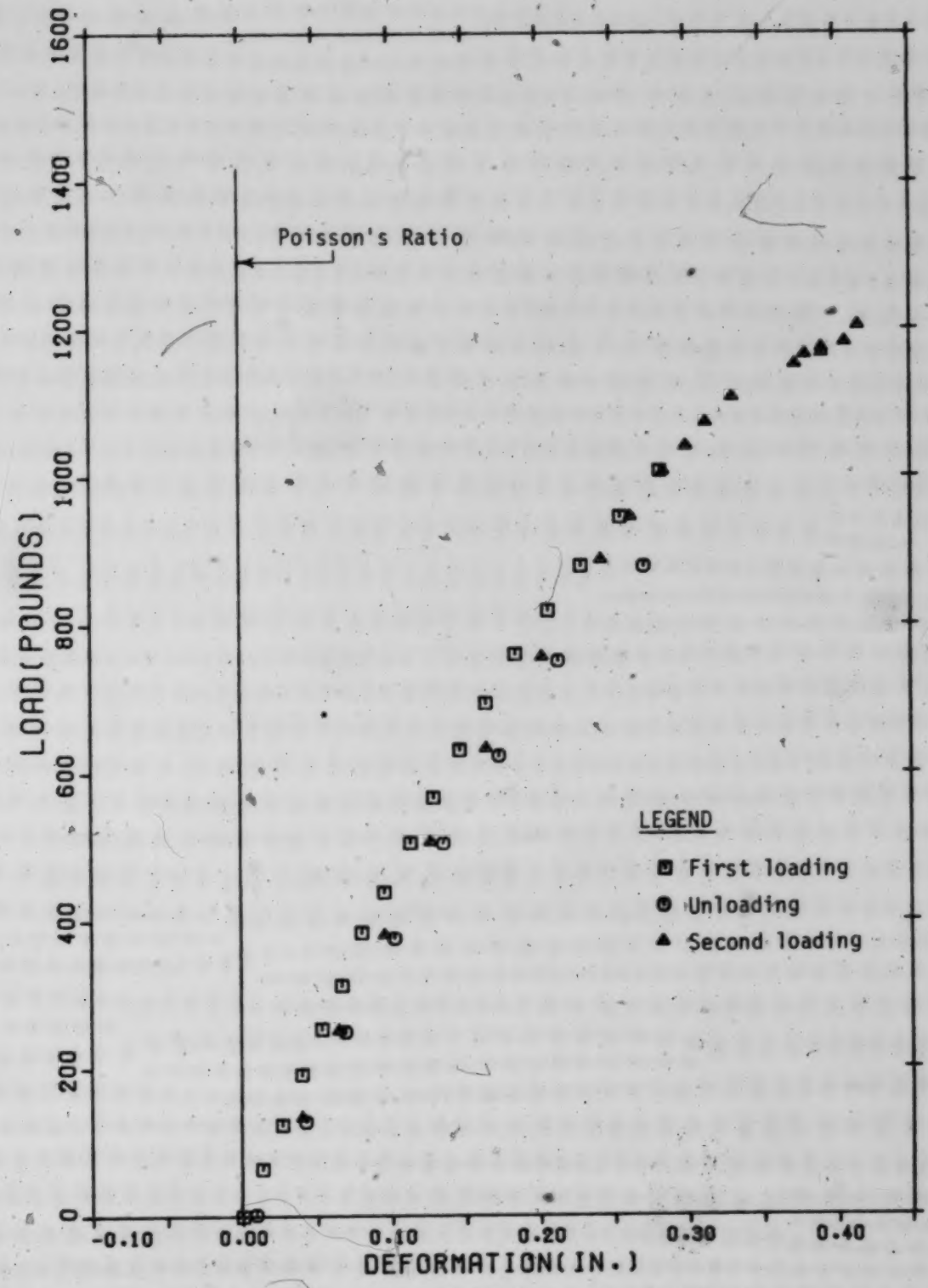


Figure 5.29 Section - Deformation of Member 9T (South), joist CX02

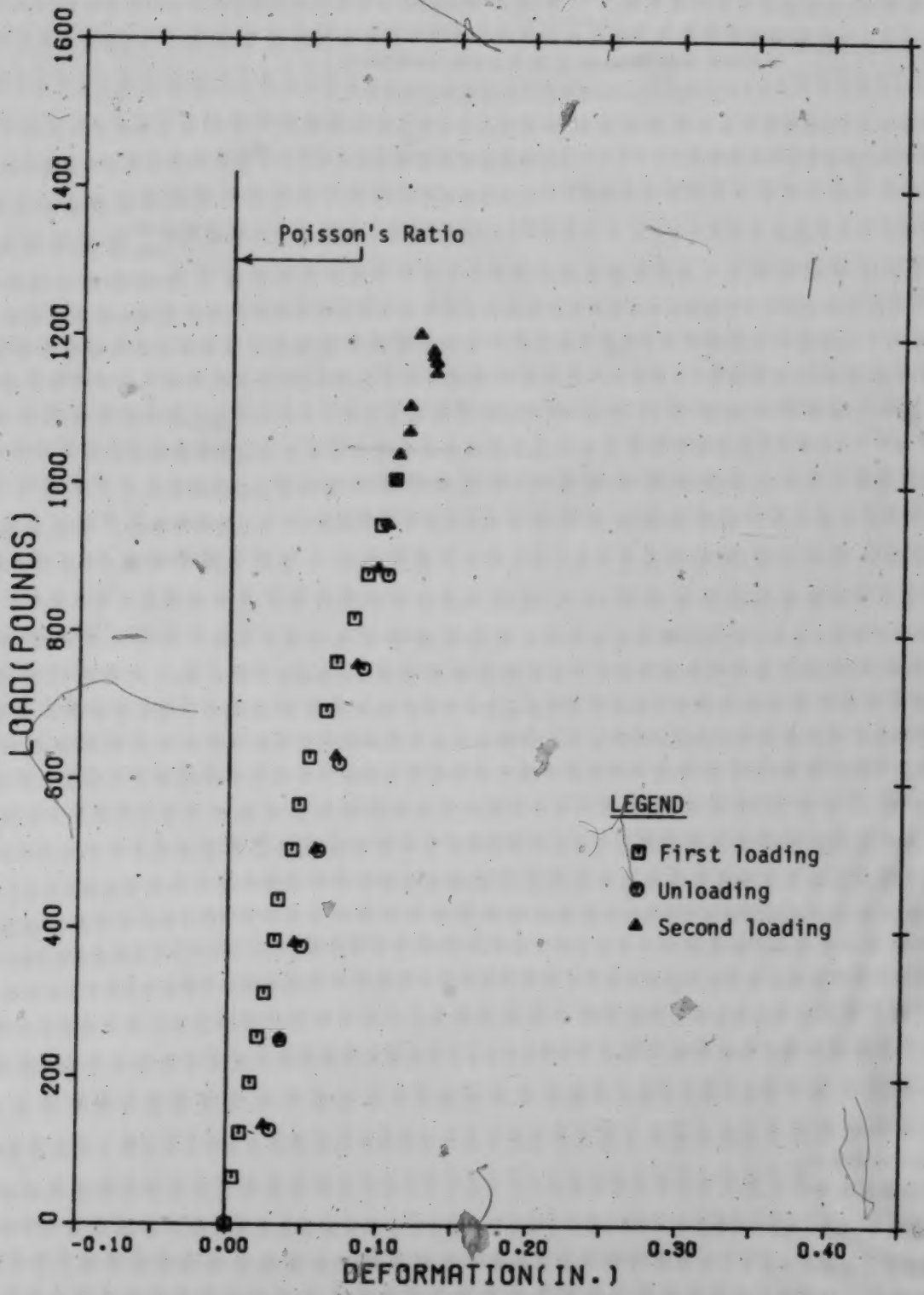


Figure 5.30 Section - Deformation of Member 8T (South), joist CX02

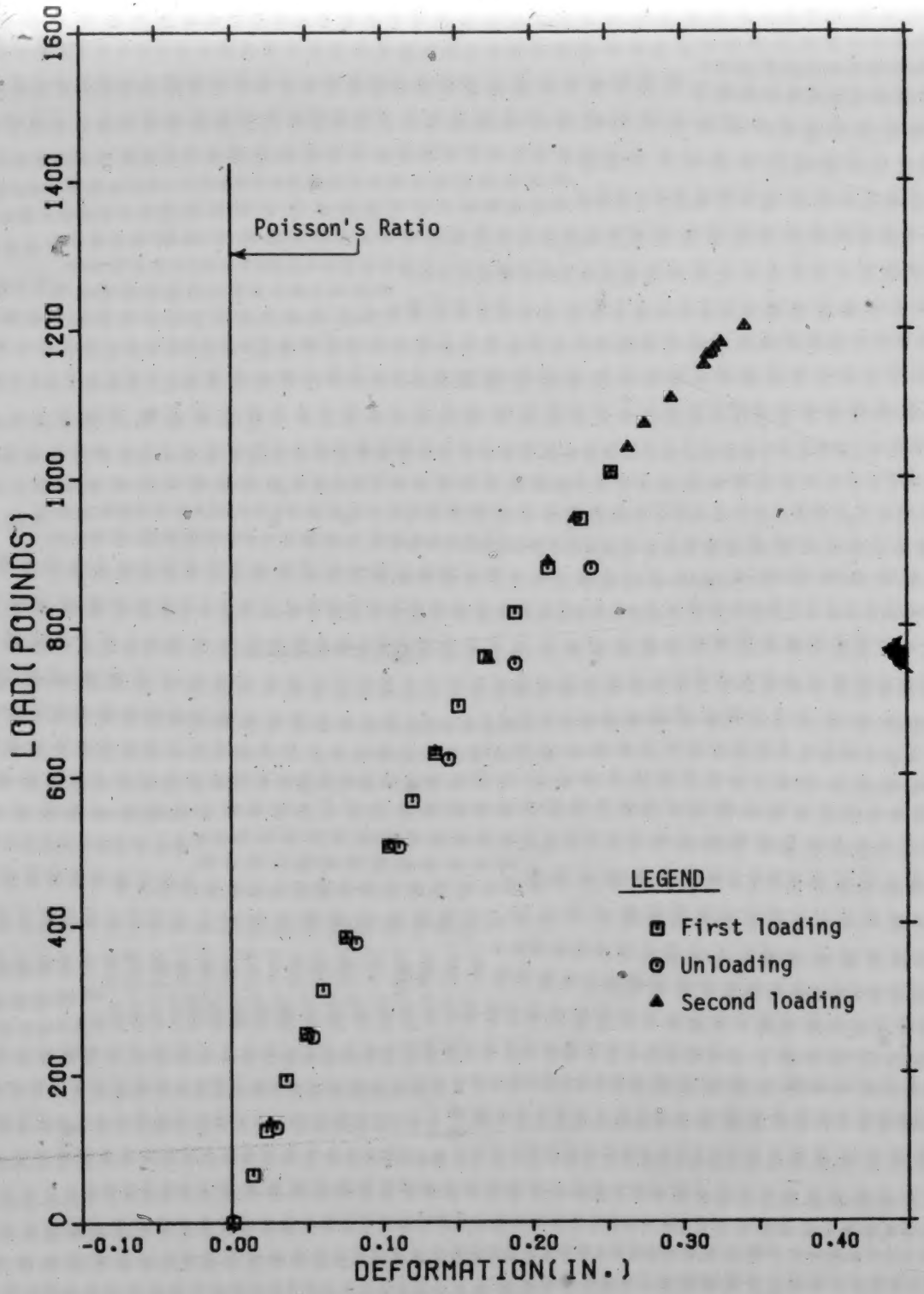


Figure 5.31 Section - Deformation of Member 7T (South), joist CX02

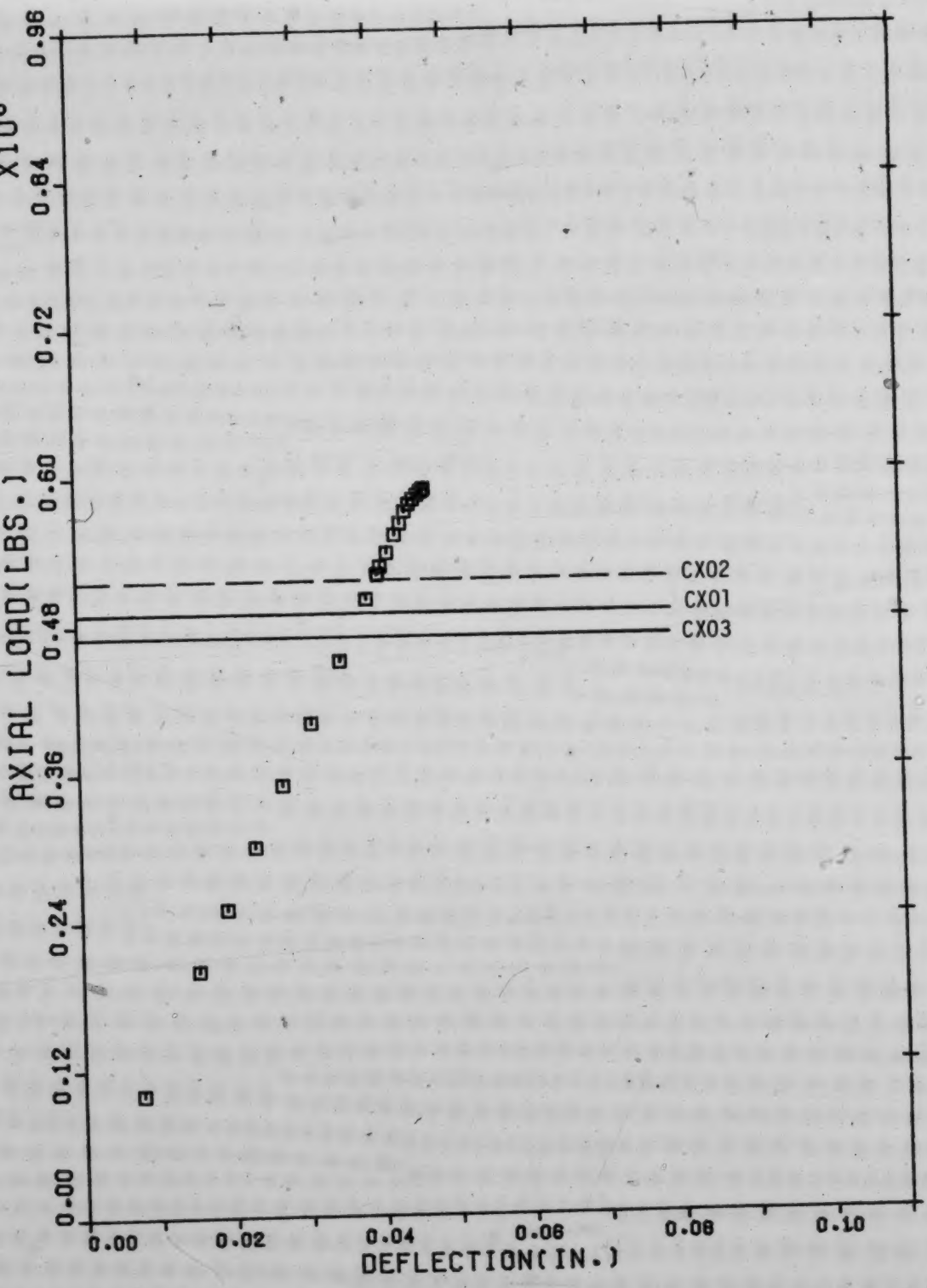


Figure 5.32 Predicted and Measured Buckling Axial Load of Joists CX01, CX02, CX03

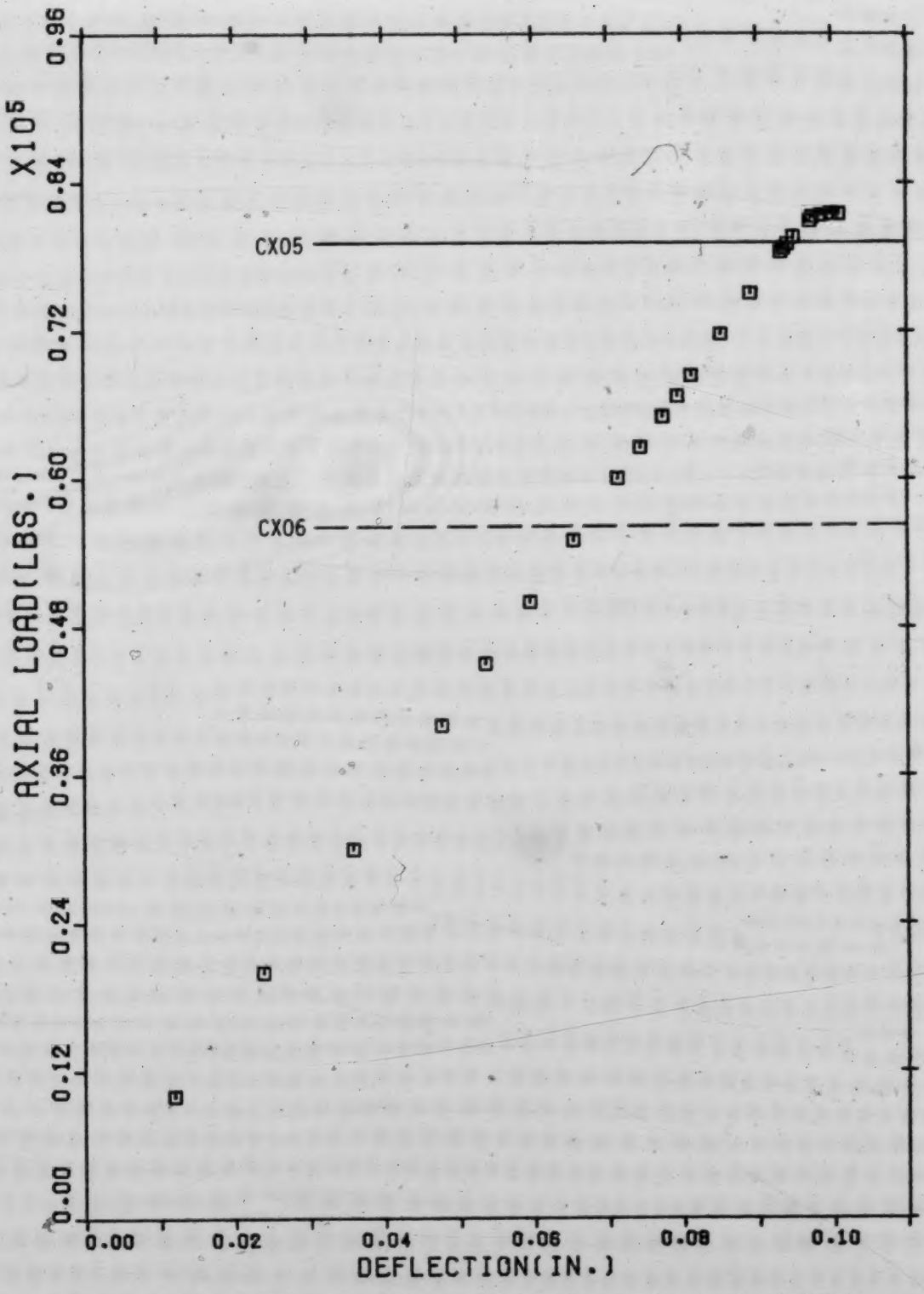


Figure 5.33 Predicted and Measured Buckling Axial Load of Joists CX05, CX06

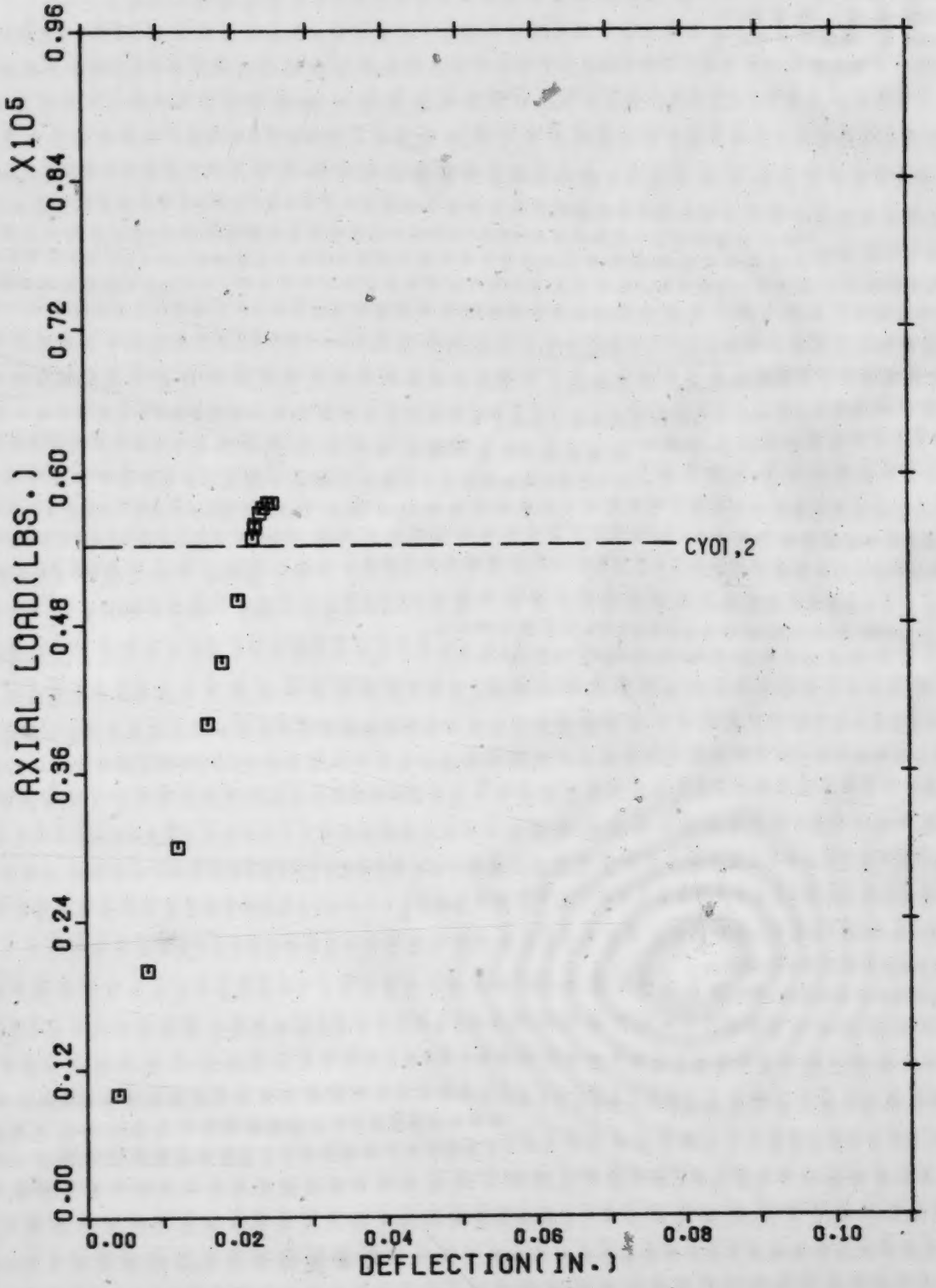


Figure 5.34 Predicted and Measured Buckling Axial Load of Joists CY01, CY02

# CHAPTER 6

# EFFECTS OF JOINT ECCENTRICITY

## 6.1 Introduction

From the comparisons in Chapter 5, it can be concluded that the elastic frame analysis gives a good prediction of the deflections and stresses in the joists for loads up to working load. Thus this method can be used to evaluate the effects of joint eccentricity. It is possible to model the geometry and material properties for a particular series of joists and then to vary the joist eccentricity as the only variable. This was done for the CX(1) series and the results are presented in the following sections.

Due to the similarity of geometry the conclusions are directly applicable to the CX(2) and CY series of joists and in general to the CZ series. Although the numerical values presented were obtained for a specific span to depth ratio and member geometry it is felt that the conclusions drawn are applicable to a wider range of open web steel joists that are similar in construction.

Specifically the effects of joint eccentricity are discussed in relation to the provisions of CSA Standard S16.1(1) with the purpose of evaluating the validity of the limitations on joint eccentricity given in Clause 16.5.11.4. This value of eccentricity is denoted as $e_1$. The value used in the elastic frame analysis is $e_2$.

The maximum eccentricity that can be ignored in the design of joists using CSA Standard S16.1(1) is dependent on the web to chord connection. If the web is continuous, Clause 16.5.11.4(a) stipulates that this eccentricity is the greater of the two distances measured

from the neutral axis of the chord member to the extreme fibres of the chord and if the web is discontinuous, Clause 16.5.11.4(b) stipulates that this eccentricity is the distance measured from the neutral axis to the back (outside face) of the chord member. The standard does not define the distinction between 'continuous' and 'discontinuous' web members. One definition of continuous could be that the web member is physically continuous through the joint having the same geometric properties as in the case of a bent solid rod. A second definition of continuity could be that there is full geometric compatibility of deformations of all members framing into the joint. This definition is used in statically indeterminate structural analysis. A third definition of continuous could be that the web member is physically continuous from panel to panel but that the moment of inertia may not be constant in the vicinity of the joint. This would occur when structural tubing is used for the web members.

When comparing eccentricities with permitted eccentricities in CSA Standard S16.1, below which the effects of joint eccentricity may be neglected the third definition of continuity was used.

The third definition is also the one which is used in practice and based on that definition the web members for joists of the CY type are continuous whereas the web members of the CX and CZ types would be discontinuous since these web members are fabricated as separate members even though complete continuity of deformation is assured because of the fabrication detail.

It can be seen that from the above possible definitions that the terms 'continuous' and 'discontinuous' are not fully descriptive and either a fuller definition as to what factors are required for the web

to be continuous must be given or other more descriptive terms should be devised.

The relation between $e_1$ and $e_2$ is shown in Figure 6.1 and it should be noted that this relation between eccentricities is different for the top and bottom chords. Given a value either of $e_1^B$ or $e_1^T$ a value of $e_2$ can be computed using the given relations and the unknown of either $e_1^B$ or $e_1^T$ can also be computed. For the geometry of the CX(1) series and a value of $e_2$ equal to sixteen inches the web members would become vertical and the joist would degenerate to a Vierendeel Truss.

For any value of $e_2$ the eccentricity $e_1^B$ is larger than the value of $e_1^T$. Thus choosing a value of $e_1^B$ equal to the permitted code value for ignoring eccentricity in design would result in $e_1^T$ being less than the permitted value. Similarly choosing $e_1^T$ at the code value would result in $e_1^B$ being greater than permitted, this is discussed later.

## 6.2 Deflections

A measure of the stiffness of a joist is the deflection at midspan caused by the working load. The ratio of midspan deflection of a joist with increasing joint eccentricity to the midspan deflection of an identical joist with zero joint eccentricity is an indication of the effects of joint eccentricity on the joist stiffness. A plot indicating such a comparison for joists having the geometry corresponding to the CX(1) series is given in Figure 6.2.

For the CX(1) joists the maximum eccentricity, $e_1^B$ given by Clause 16.5.11.4(b) is 0.505 inches. This corresponds to a value of $e_2$ of 0.489 inches and $e_1^T$ of 0.253 inches. For an eccentricity $e_2$ of 0.49 inches the deflection increases by 0.16% from a joist with zero

eccentricity. The maximum permissible eccentricity given by the same clause for $e_1^T$ is 0.42 inches, which corresponds to a value of $e_2$ of 0.798 inches and $e_1^B$ of 0.84 inches, and results in an increase in deflection by 0.25% but the value of $e_1^B$ computed exceeds the value permitted by the CSA Standard.

If the web is considered to be continuous for the CX(1) series Clause 16.5.11.4(a) governs and the maximum eccentricity is $e_1^B$ of 0.72 inches, which corresponds to a value of $e_2$ of 0.689 inches and $e_1^T$ of 0.36 inches, increases the deflection by 0.17%. For a maximum eccentricity $e_1^T$ of 0.79 inches, which corresponds to a value of $e_2$ of 1.438 inches and $e_1^B$ of 1.58 inches, the deflection increases by 2%. Again the value of $e_1^B$ is greater than Clause 16.5.11.4(a) would permit.

Consider the eccentricity $e_1$ is equal to the depth of the chords. For a value of $e_1^B$ of 1.222 inches, $e_2$ equals 1.135 inches and $e_1^T$ equals 0.611 inches, the deflection increases by 1.5%. For a value of $e_1^T$ of 1.212 inches the value of $e_2$ is computed to be 2.105 inches and a value of $e_1^B$ to be 2.424 inches. The increase in deflection due to this eccentricity is 4.5%.

## 6.3 Axial Force

One of the factors which contributes to the critical buckling of a section is the axial force. The ratio of axial force in the midspan member with increasing eccentricity to the axial force in the same member of an identical joist with zero joint eccentricity gives an indication of the joint eccentricity on the critical member. A plot indicating such a comparison is given in Figure 6.3.

For a maximum eccentricity $e_1^B$ given by Clause 16.5.11.4(b) of

0.505 inches ($e_2$ of 0.489 inches) the axial force increases by 0.01% from a joist with zero joint eccentricity. For a value of $e_1^B$ equal to the depth of the chord (1.222 inches), as suggested in Section 6.2, $e_2$ equals 1.135 inches, the axial force increases by 0.02%.

For the end web member 1W, for the same eccentricities, the axial force in the member decreased by 0.5% and 1.5%, respectively. For the web member 3W, for the same eccentricities, the axial force increased by 1.5% and 3.5%, respectively.

## 6.4 Bending Moments

Joint eccentricity has a significant effect on the member end moments. A plot of the ratio of end moments of the midspan member 9T with increasing eccentricity to the bending moment at zero eccentricity, is given in Figures 6.4 and 6.5.

Since the moments are small, for the purpose of discussing the effects of increasing joint eccentricity the magnitude of moments are taken as a ratio of the yield moment, My.

For zero eccentricity the value of the end moment in member 9T (high compressive force member) at end i, that is the joint further from midspan, is -0.033 My while for the other end j, joint closest to midspan is 0.036 My. For an eccentricity $e_1^B$ given by Clause 16.5.11.4(b) of 0.505 inches ($e_2$ of 0.489 inches) the moment at end i decreases to -0.029 My while at end j it increases to 0.045 My. For a value of $e_1^B$ equal to the depth of chord (1.222 inches) as given in Section 6.2, $e_2$ equal to 1.135 inches, for the end i the moment decreases to -0.023 My while at end j it increases to 0.058 My.

For the web member 1W (high tensile force member) for zero

eccentricity the moment at end i, that is the member end framing into the top chord, is -0.4 My. For the end j the corresponding moment is -0.182 My. For the eccentricity $e_1^B$ given by Clause 16.5.11.4(b) of 0.505 the moments at end i and end j increase to -0.431 My and -0.238 My, respectively. If this eccentricity $e_1^B$ is increased to equal the depth of the chord these moments increase to -0.479 My and -0.325 My, respectively.

For zero eccentricity the value of end moment in web member 3W (high compressive force member) at end i, that is the end framing into the top chord, is -0.128 My. At end j the moment is -0.080 My. For the eccentricity $e_1^B$ given by Clause 16.5.11.4(b), the moments at ends i and j increase to -0.456 My and -0.559 My, respectively. If the eccentricity $e_1^B$ is increased to the depth of the chord the moments increase to -0.928 My and -1.24 My respectively.

Thus we see that the end moments in member 3W are extremely sensitive to the joint eccentricity. This sensitivity of the web member to joint eccentricity is very much less for the next compressive web member, 6W.

## 6.5 Discussion of Joint Eccentricity

The effect of joint eccentricity on the stiffness of a joist as measured by the midspan deflection can be ignored for the range of eccentricities likely to be encountered in practice. The increase in the midspan deflection resulting from eccentricities currently permitted by CSA Standards is less than 0.2%. Should the provisions for continuous web members (Clause 16.5.11.4(a)) apply to joists of the type tested the increase would be 0.17%. Indeed permitting joint eccen-

tricities for any web continuity equal to the depth of the chord the deflection increases by only 1.5%. Thus it may be concluded that for joists of this type any reasonable limitation on joint eccentricity will not result in unsatisfactory reduction in joist stiffness.

The failure mode of open web steel joists is frequently by in-plane buckling of one of the compression members. In such cases the effects of joint eccentricity on the failure capacity of a joist can be measured by the effects of the eccentricity in altering the buckling load for a member. This effect can be evaluated by examining the effects of eccentricity on the axial load and end moments. Thus only compression members need be considered.

The axial forces in the chord members are essentially independent of the joint eccentricity and the change in axial forces in web members is due to their change in slope. Again for reasonable eccentricities this effect is sufficiently small that the effects of joint eccentricity can be ignored in joist design.

The most critical chord member is the top chord panel at midspan, member 9T. As discussed in Section 6.4 the maximum end moment due to eccentricities as great as the depth of the chord increased from a value of 0.036 My to 0.058 My. Since this increase is small and both moments are extremely small compared to the moment capacity of the chord and since the axial force is essentially independent of the joint eccentricity it would appear that joint eccentricities as large as the chord depth will have no significant effect on the buckling capacity of the top chord member.

In web member 3W, although the change in axial load due to eccentricities as large as the chord depth are minimal and could be

ignored the end moments induced at the bottom end is greater than the yield moment.

For the eccentricity permitted by the CSA Standard the moment at the top end increases from -0.128 My to -0.456 My and at the bottom end from -0.08 My to -0.559 My. Thus the moments for this member are much more sensitive to eccentricities and increase rapidly.

From the above discussion it would appear that the effects of joint eccentricity cannot be neglected when designing the end compression diagonal and that the current provisions permit large moments to be developed even at working load. This has been substantiated in tests where failure either as a joint mechanism or as buckling of the end compression diagonal has been observed.

It appears that the attempt by the CSA Standards to set a limiting value of joint eccentricity that is applicable to all joints in an open web steel joist is not realistic.

The sensitivity of the joist behaviour to eccentricities at joints located at the ends of the chords is very much greater than for joints located along the chords.

On the basis of this study it would appear that the provisions of Section 16.5.11.4 can be revised so that when stipulating the maximum joint eccentricity that can be ignored in design no distinction need be made between joists having continuous web members and those having discontinuous web members and that, except for those joints at the ends of the chords, the permissible eccentricity can be increased to be equal to the depth of the chord.

For those joints located at the ends of the chords the limitations of Clause 16.5.11.4(b) should apply to both types of joists. For

any joint eccentricity exceeding this amount the designer should do a complete analysis including a computation on the total applied moment at the joint to the resisting capacity of the members framing into that joint.

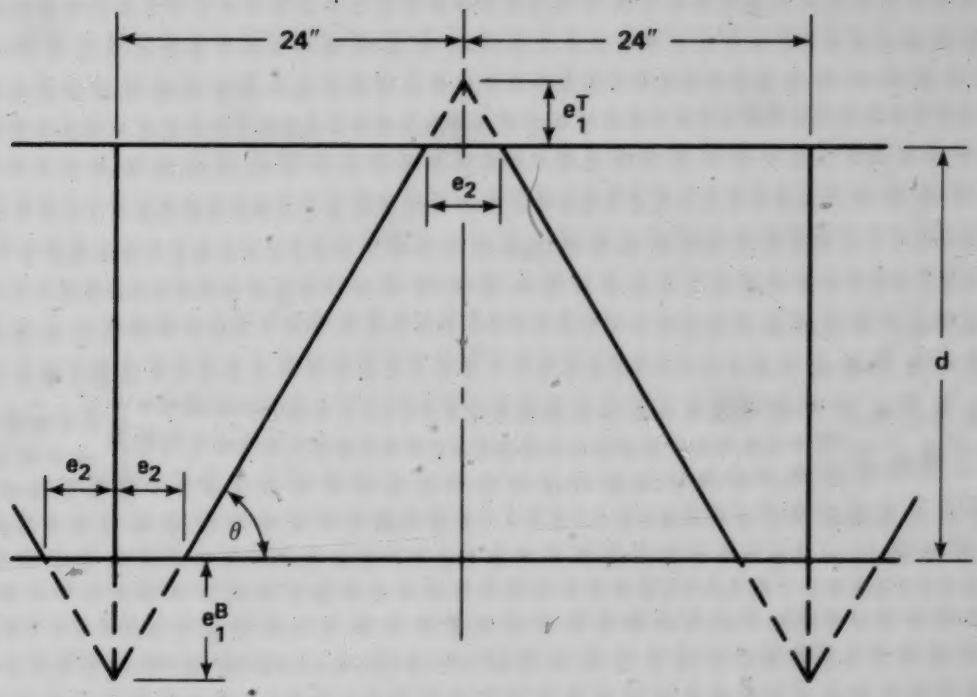


$$e_1^T = \frac{e_2}{2} \tan \theta$$

$$e_1^B = e_2 \tan \theta$$

$$\tan \theta = d/(24-\frac{3}{2}e_2)$$

for d = 24"

$$e_1^B = 2e_1^T = \frac{16e_2}{16-e_2}$$

**Figure 6.1 Calculation of eccentricities at bottom and top joints.**

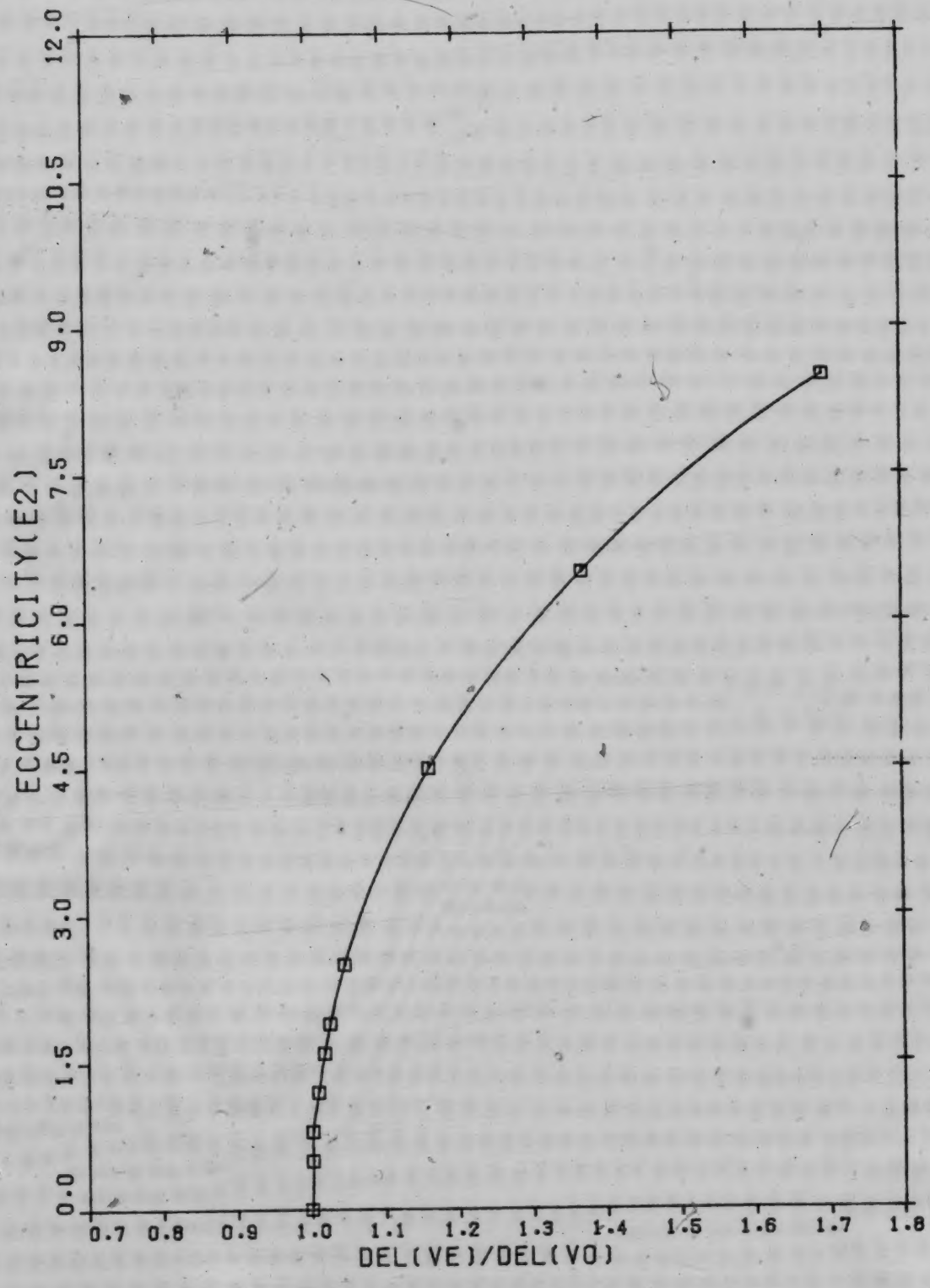


Figure 6.2 Variation of Midspan Deflection With Eccentricity

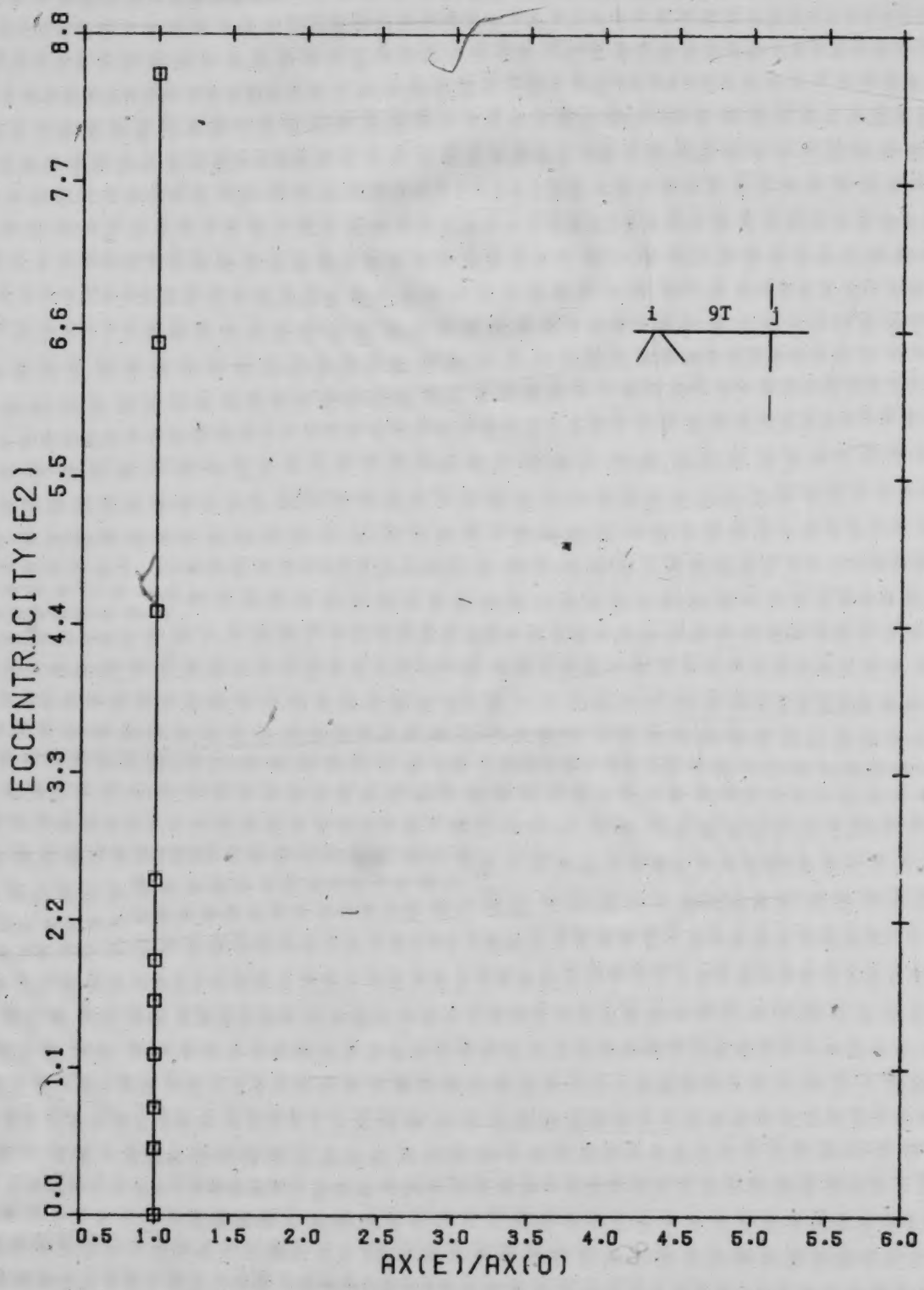


Figure 6.3 Variation of Top Chord Axial Force With Eccentricity

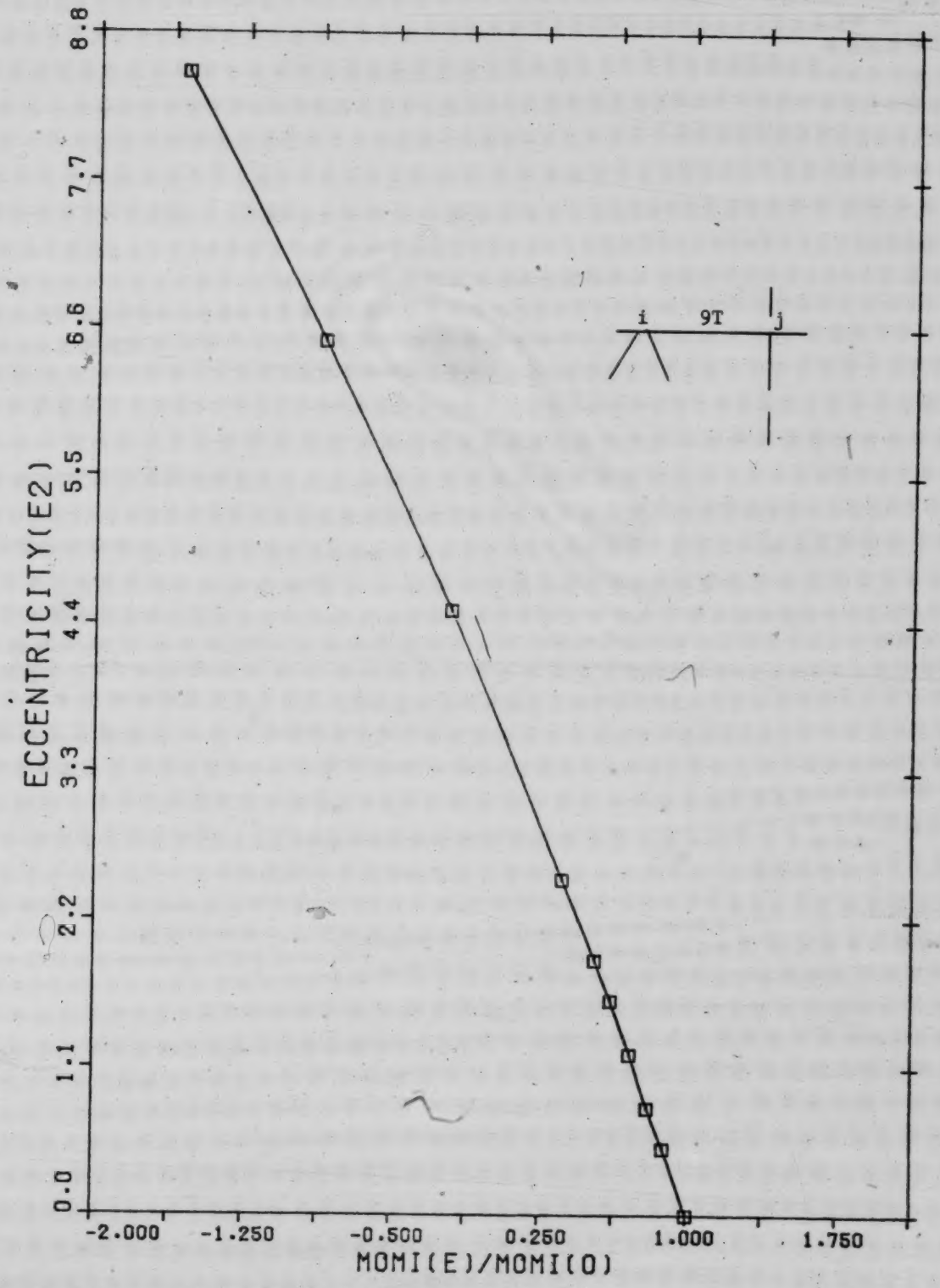


Figure 6.4 Variation of Top Chord Moment, at end i, With Eccentricity

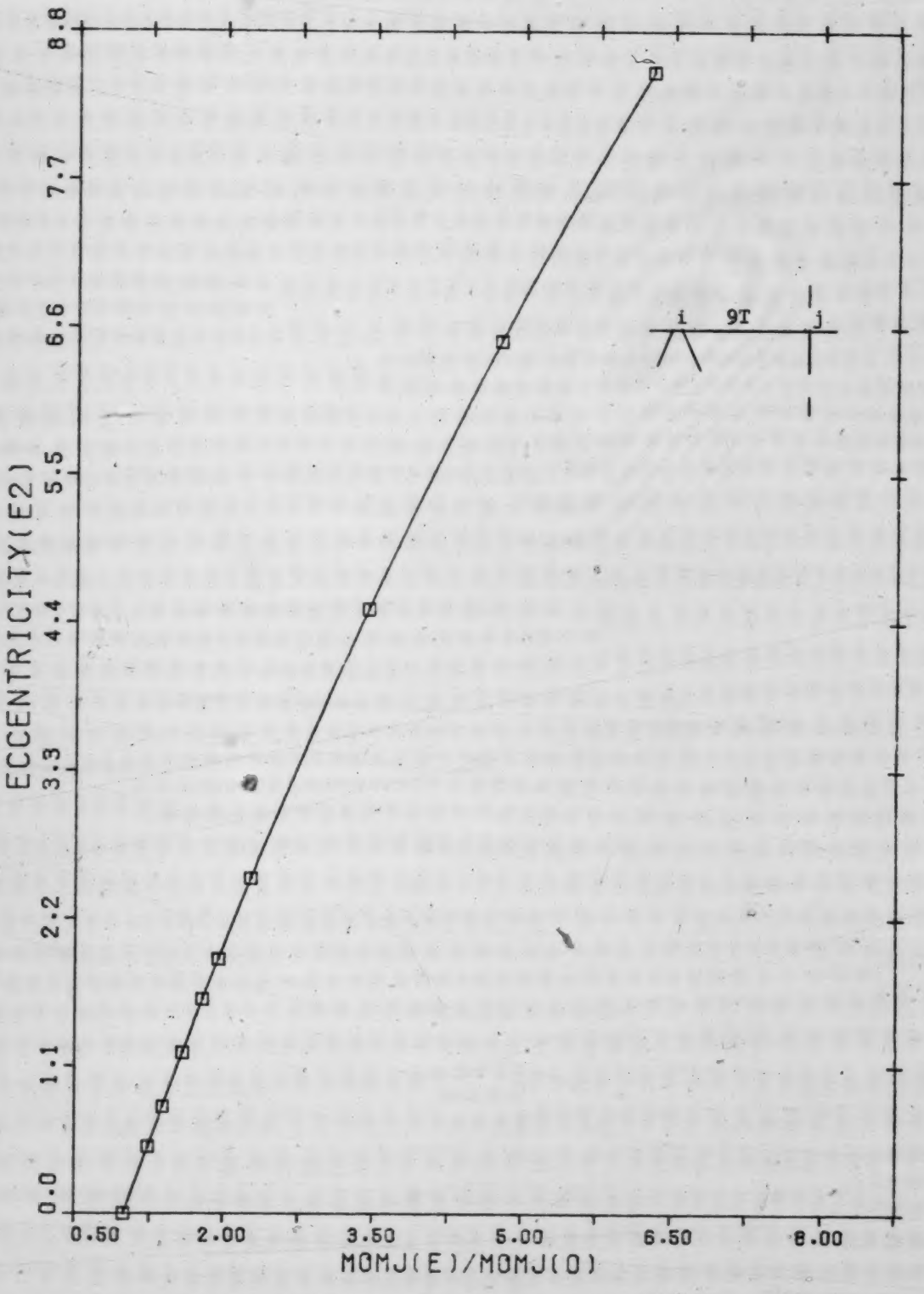


Figure 6.5 Variation of Top Chord Moment, at end j, With Eccentricity

# CHAPTER 7

## SUMMARY AND CONCLUSIONS

To determine the effect of joint eccentricity on the behaviour of open web steel joists a testing program was undertaken. Ten joists having loads, spans and depths representative of typical joists in a light floor framing system were tested to failure. In addition to the joint eccentricities the variables were chord sections and web to chord fabrication details.

Measurements were made of axial forces, bending moments and panel point deflections at selected locations. Each joint was analysed by an elastic frame analysis and the results compared with the measured values. Based on this study the following conclusions can be made:

1. The elastic frame analysis gives an excellent prediction of deflections, axial forces and bending moments in the members of the joist for loads up to the working load.

2. Joint eccentricities have a negligible effect on the deflections and axial forces in the members of the joist.

3. Bending moments in the members are more sensitive to joint eccentricity. However, a distinction between eccentricity at joists along the chords and eccentricity at the joints at the ends of the chords must be made. The effects of eccentricity at joints along the chords has only a small effect on the bending moments and in many cases reduces the bending

moment. Since these changes in moments are very small compared to the bending capacity of the chord they can be neglected in design.

4. Eccentricity at the joints at the end of the top and bottom chord have a significant effect on the moments induced in the members framing into these joints and such eccentricity should be avoided as much as possible. Eccentricities as large as those existing in the test joists could cause moments in the end compression diagonal that exceeded the yield moment for this member at working load.

5. From the analyses made in this study it was not possible to consistently predict the load at which instability would occur in the critical compression members. However joint eccentricity did not appear to have an appreciable effect on the buckling strength of the top chord members.

6. There is no clear definition of the terms 'continuous' and 'discontinuous' web members in the CSA Standard S16.1. From the interpretation of these terms used in this report there did not appear to be any difference in behaviour attributed to joint eccentricity that was affected by whether the web was continuous or discontinuous. For this reason it is recommended that the terms as used in reference to the maximum eccentricity that is permitted such that the effects of joint eccentricity can be neglected in design be deleted and that a

single criteria for all joists be used.

7. For joints along the chords the effects of joint eccentricity of the magnitude expected in practice on the behaviour of the joist are minimal. It is recommended that joint eccentricities may be neglected in design provided that they do not exceed the greater of the two distances measured from the neutral axis of the chord member to the extreme fibres of the chord member for all joists. Further research may include that this limit may be relaxed to include joint eccentricites as large as the depth of the chord for joists with hat section as chords.

8. The behaviour of all joists is sensitive to the amount of joint eccentricity that occurs at the joints at the ends of the top and bottom chords. Eccentricities at these joints can only be neglected in design if the eccentricity does not exceed the distance from the neutral axis to the back (outside face) of the chord member.

## LIST OF REFERENCES


1. CSA Standard S16.1-1974, "Steel Structures for Buildings - Limit States Design", Canadian Standards Association, Rexdale, Ontario, 1974.

2. CSA Standard S136-1974, "Cold Formed Steel Structural Members", Canadian Standards Association, Rexdale, Ontario, 1974.

3. Matiisen, R., "Effect of Joint Eccentricity on Open Web Steel Joists", M.Sc. Thesis, The University of Alberta, 1977, (Research Report sponsored by CSICC).

4. Kennedy, D.J.L. and Rowan, W.H.D., "Behaviour of Compression Chords of Open Web Steel Joists", M.Sc. Thesis, The University of Toronto, 1963, (Research Report sponsored by CSIC).

5. McDonald, W.S., "Inelastic Behaviour of the Compression Chord of Open Web Steel Joists", Ph.D. Thesis, The University of Kansas, 1966.

6. Morris, G.A., Frovich, L.E. and Thiensiripipat, N., "An Experimental Investigation of Flattened-End Tubular Truss Joists", Bulletin STI-74, Department of Civil Engineering, The University of Manitoba, 1974.

7. Ohmart, R.D. and Lenzen, K.H., "Uniform Load Testing of Open Web Steel Joists", M.Sc. Thesis, The University of Kansas, 1961, (Report No. 25, The University of Kansas, 1968).

8. Yu, W.W., "Proceedings of the First Specialty Conference on Cold-Formed Steel Structures", Editor, Department of Civil Engineering, The University of Missouri - Rolla, 1971.

9. Srivastava, B.B.L., "Computation of Inelastic Instability in Steel Joists", M.Sc. Thesis, The University of Alberta, 1976.

10. Epstein, M. and Murray, D.W., "A System of Computer Programs for Large Deformation In-Plane Analysis of Beams", Structural Engineering Report No. 57, Department of Civil Engineering, The University of Alberta, May, 1976.

## APPENDIX A

## CALCULATION OF GEOMETRY

Shown in Figure 2.3 is a typical joint of a joist and the quantities to be measured. Figure 2.4 shows the quantities which can be computed by trigonometry.

$$S1 = x/2 \sin A(I,1),\quad S2 = x/2 \sin A(I,2)$$

where x is the common diameter of the web members.

$$N1 + N2 = D(I,1) + S1 + D(I,2) + S2$$

$$L = G(I) + z - y + w$$

Also $N1 = L(\text{Ctn } A(I,1))$ and $N2 = L(\text{Ctn } A(I,2))$

Hence $L = (N1 + N2)/(\text{Ctn } A(I,1) + \text{Ctn } A(I,2))$

which gives

$$G(I) = \frac{D(I,1) + D(I,2) + S1 + S2}{\text{Ctn } A(I,1) + \text{Ctn } A(I,2)} - z + y - w$$

thereby giving the eccentricity ($e_2$) as

$$H(I,1) = G(I)\ \text{Ctn } A(I,1)$$

and $$H(I,2) = G(I)\ \text{Ctn } A(I,2).$$

## APPENDIX B

## INSTRUMENTATION

The analog signals, which formed the output from the measuring devices, were changed to digital form by a digital voltmeter controlled by a program in the Nova. The format of the equivalent digital signals was a thirteen bit two complement integer numerator (N), plus a gain range index (GRI) of one to thirteen. The readable voltages with any particular gain range was

$$R = \pm (0.0025 * 2 ** (GRI - 1)),$$

but since the gain range selected by the computer resulted in a normalized fraction (except for voltages below 0.00125), a full thirteen bits of significance was usually obtained, or about three to four decimal digits. The smallest voltage change detectable in any gain range (that is, sensitivity) was:

$S = \pm R/4095$, and the voltage was calculated as

$V = N * R/4095.$

For example, if GRI = 13, $R = \pm$ 10.24 volts, $S = \pm$ 0.0025 volts; while if GRI = 1, $R = \pm$ 0.0025 volts, $S = \pm$ 0.0000006 volts.

An interactive Fortran program was used to monitor load and centre line deflection during load application. The raw data was multiplied by the respective conversion factors (strain: 0.318 (in/in)/V, load: 491 kips/V, deflection: 0.639 in/V) to get the loads, strains and deflections at every load increment.